Die approbierte Originalversion dieser Dissertation ist an der Hauptbibliothek der Technischen Universität Wien aufgestellt (http://www.ub.tuwien.ac.at).

The approved original version of this thesis is available at the main library of the Vienna University of Technology (http://www.ub.tuwien.ac.at/englweb/).

Dissertation

Ultrasonically Enhanced Settling: The effects of ultrasonic plane wave fields on suspensions of the yeast *Saccharomyces cerevisiae*

ausgeführt zum Zwecke der Erlangung des akademischen Grades eines Doktors der technischen Wissenschaften unter der Leitung von

a.o.Univ.Prof.Dipl.-Ing.Dr. Martin Gröschl
E134
Institut für Allgemeine Physik

eingereicht an der Technischen Universität Wien

Fakultät für Technische Naturwissenschaften und Informatik

von

Dipl.-Ing. Stefan Radel
Matrikelnummer 8504830
1140 Wien, Felbigergasse 60/10

Wien, am 12.Dezember 2002

To my family, especially Pia and Christiane

CONTENTS

Kurzfassung 4

Abstract 6

Preface 8

Introduction 9

Theory of ultrasonic particle manipulation 14

Materials and Methods 28

M1 Statistical definitions 28

M2 Cultivation and handling of suspended micro-organisms 29

M2.1 Saccharomyces cerevisiae 29
M2.2 Lactobacillus brevis 29

M3 Chemical and microbiological assays 30

M3.1 Measurement of inertial cavitation by a method to pick-up free radicals 30
M3.2 Haemacytometer 30
Image analysis assisted method 30
M3.3 Methylene blue technique 31
M3.4 Ultraviolet-absorption 31
M3.5 Plate counts 32
M3.6 Fluorescent vacuole membrane stain 32
M3.7 Study of cell viability, integrity, ability to reproduce and morphology 33

M4 Polymerisation techniques 34

M4.1 Polyacrylamide 34
M4.2 Agar 34

M5 Evaluation of the acoustic field within a resonator 35

M5.1 Basic concept 35
M5.2 Determination of the effective acoustic quality factor Q_{eff} of a yeast suspension 36
M5.3 In-situ measurement of the admittance spectrum 36

M6 Transmission electron microscopy 37

Results 38

R1 Ultrasonically Enhanced Settling: Effects of process factors on separation efficiency 38

R1.1 Introduction 38
R1.2 Influence of biomass, throughput and true electrical power input on the separation efficiency 41
Flow-through set-up 42
Batch set-up 51
Discussion 52
R1.3 Evaluation of the acoustic field acting within the active volume 55
Discussion 58
R1.4 Selective retention of viable and non-viable yeast cells 60
R1.5 Empirical model of the cell concentration vs. time 61
Discussion 69
R1.6 Conclusion 71

R2 Effects of the state factor ethanol: Turbulence and cell damage 73

R2.1 Introduction 73
R2.2 Breakdown of spatial order/immobilisation in the presence of ethanol 74
The phenomenon 74
Evaluation of the acoustic field in the presence of 12%($^v/_v$) ethanol 77
Effects on the yeast cells 79
Discussion 81
R2.3 Effects on yeast exposed to ultrasound in pressure inter-nodal space 83
Effects on viability, integrity, ability to reproduce and morphology 83
Transmission electron micrographs 86
Discussion 89
R2.4 Acoustic contrast factors of water-rich ethanol mixtures 91
Discussion 95
R2.5 Conclusion 97

R3 Effects of the spatial arrangement: Selective cell immobilisation and alterations of the resonator's acoustic behaviour 99

R3.1 Introduction 99
R3.2 Polymerisation of the host "liquid" during sonication – a novel technique 99
Growth of yeast ultrasonically arranged in gel 103
Discussion 104
R3.3 Size selective effects in a yeast/lactic mixture 104
Discussion 107
R3.4 Alterations of the resonator's electrical admittance due to the arrangement of particles 107
In-situ measurement at operational levels of true electric power input 108
High-precision measurements employing a special resonator 109
Discussion 113
R3.5 Conclusion 113

R4 Examination of damage to yeast cells exposed to plane ultrasonic fields 114

R4.1 Introduction 114
R4.2 Effects on yeast exposed to ultrasound in the pressure nodes of a standing wave field 115
Effects on viability, integrity, ability to reproduce and morphology 115
Logarithmic phase 115
Stationary phase 118
Comparison of fluorescent vacuole membrane staining results 121
Statistical examination of plate counts 122
Transmission electron micrograph 123
Discussion 124
R4.3 Cavitation 125
Discussion 127
R4.4 Effects on yeast sonicated in an experimental resonator 128
Effect of turbulence on cell integrity at different true electrical power inputs 128
Effect of turbulence on cell viability and integrity in the presence of EtOH 129
Effect of turbulence on cell integrity in absence of gas 130
Discussion 132
R4.5 Effects on yeast homogeneously immobilised in a gel-block exposed to an ultrasonic standing wave 133
Discussion 134
R4.6 Effects on yeast exposed to ultrasound in an anechoic system 135
Effects on cell viability and integrity 137
Transmission electron micrographs 138
Discussion 139
R4.7 Conclusion 140

Outlook 142

Acknowledgements 144

Bibliography 145

Curriculum Vitae 154

KURZFASSUNG

Ultraschall-induzierte Sedimentation ist die Folge einer Beschallung von Suspensionen, also in einer Flüssigkeit dispergierter Teilchen, mit stehenden Ultraschallwellen geeigneter Wellenlänge. Das Prinzip basiert auf sogenannten Schallstrahlungskräften, welche Teilchen in bestimmten Regionen des Schallfeldes konzentrieren. Die entstehenden Agglomerate sedimentieren schneller als einzelne Teilchen.

Ziel der vorliegenden Arbeit war es, diese Technik im Hinblick auf ihre Anwendung auf Hefezellen, speziell im Brauereiwesen, zu untersuchen. Demgemäß wurden Suspensionen von Bierhefe verwendet.

Separationseffizienzen von bis zu 99,6% konnten bei der Verwendung eines Separationssystems, welches zur Zellrückhaltung bzw. –filtration bereits kommerziell eingesetzt wird, mit Suspensionen der Hefe *Saccharomyces cerevisiae* erreicht werden.

Durch Analyse der Einflüsse von Prozessparametern, wie dispergierte Biomasse, elektrische Leistung und Volumenstrom, konnte ein Optimierung des Systems erreicht werden. Eine untere Schranke der Zellkonzentration von $5 \cdot 10^6$ Zellen pro Milliliter und eine obere Schranke des Durchflusses von 50 Liter Suspension pro Tag wurden als Grenzen für einen effizienten Betrieb des akustischen Filters identifiziert.

Die Verringerung der effektiven akustischen Güte bei steigender Zellkonzentration wurde untersucht. Ein deutlicher Einfluss auf das Schallfeld im Resonator wurde ab 50 g pro Liter Biomasse festgestellt.

Die zeitliche Entwicklung der Zellkonzentration am Filterausgang nach Einschalten des Ultraschalls konnte mit einem mathematischen Modell beschrieben werden.

Das Endprodukt der Fermentation, Äthanol, wurde als Hindernis hinsichtlich des Einsatzes der Ultraschall-induzierten Sedimentation identifiziert. Die Separationseffizienz fiel bei einer Äthanolkonzentration von 12%($^v/_v$), bedingt durch turbulente Strömungen im Filtersystem, auf null ab. Gleichzeitig erlitten die Zellen morphologische Schäden, über 90% der Zellen wurden bei diesen Experimenten getötet. Dabei wurden keine Hinweise auf transiente Kavitation gefunden.

Die Turbulenzen konnten durch spezielle Eigenschaften von wasserreichen Äthanolmischungen erklärt werden. Der akustische Kontrast zwischen den dispergierten Hefezellen und solchen Mischungen verschwindet. Dies hat den

Zusammenbruch der räumlichen Ordnung der Zellen zur Folge, sie werden nicht mehr in den Druckknoten der stehenden Welle gehalten.

Im normalen Betrieb des akustischen Filters, d.h. wenn diese Ordnung hergestellt war, wurden keine signifikanten Veränderungen der Viabilität der Zellkultur oder ein Auslaufen der Zellen festgestellt. Das Vorhandensein von Äthanol unterhalb der kritischen Konzentration bewirkte unter diesen Bedingungen ebenfalls keine Veränderungen dieser Art. Transmissions-Elektronenmikroskopie zeigte einige nicht-letale Veränderungen der Zellvakuole durch den Einfluss des Ultraschalls.

Die Viabilität der Zellen war nach einer einstündigen Beschallung in einer speziellen, nicht-resonanten Kammer, also in einer laufenden statt in einer stehenden Welle, um 25% verringert. Des Weiteren wurden ein Auslaufen der Zellen und morphologische Veränderungen beobachtet. Diese Ergebnisse legten nahe, dass der Einfluss des Schallfeldes im Bereich außerhalb der Druckknoten für die Schäden verantwortlich war, der genaue Mechanismus konnte nicht geklärt werden.

Eine neue Methode zur detaillierten Untersuchung der räumlichen Anordnung von Teilchen aufgrund der Schallstrahlungskräfte wurde entwickelt. Die Verfestigung von Polymeren wurde während der Beschallung initiiert. Dies bewirkte das „Einfrieren“ der räumlichen Verteilung von Zellen in einem Gel-Block. Dieser wurde im weiteren Verlauf des Experiments zerschnitten und untersucht, es entstanden die ersten mikroskopischen Aufnahmen der inneren Struktur der Agglomerate. Hinweise auf bisher nicht beobachtete Anordnungen der Zellen wurden gefunden.

Die Größenselektivität des Ultraschallfilters wurde verwendet, um die Konzentration von Milchsäurebakterien *Lactobacillus brevis* in einer Hefesuspension zu senken. Dieser Mikroorganismus ist eine verbreitete Verunreinigung im Brauereiwesen. Mit der Gel-Technik konnte gezeigt werden, dass die Selektivität des Ultraschallfilters auf die unterschiedliche räumliche Anordnung der beiden Zelltypen zurückzuführen ist.

Zum ersten Mal wurde der Einfluss der inhomogenen räumlichen Verteilung der Zellen auf das akustischen Verhalten des Resonators gemessen. Die Fixierung im Gel entkoppelt das Schallfeld von den Schallstrahlungskräften, der Vergleich mit gleichmäßig verteilten Teilchen zeigte eine Verringerung der effektiven akustischen Güte der Zellsuspension durch die räumliche Ordnung.

Diese Arbeit wurde zum Teil vom TMR-Programm der Europäischen Kommission, Vertrag Nr. ERBFMRXCT97-0156, EuroUltraSonoSep, unterstützt.

ABSTRACT

Ultrasonically Enhanced Settling is an effect applying to suspensions, i.e. particles dispersed in a liquid, being exposed to ultrasonic standing waves of appropriate wavelength. The principle is based on the fact that due to so-called radiation forces the particles are highly concentrated in certain regions of the sound field, thus building up aggregates that settle more rapidly than single particles.

The object of this study was to exploit this technique in yeast technology especially in brewing. Therefore suspensions of brewer's yeast were investigated.

A separation system based on commercially successfully applied ultrasonic cell retention/filtration of mammalian cells was used and was shown to reach separation efficiencies of up to 99.6% for suspensions of *Saccharomyces cerevisiae*.

Optimisation was achieved based on analysis of the influence on separation efficiency of the process parameters bio-mass load, electrical power input and suspension throughput. Boundary conditions like a minimum cell concentration of $5 \cdot 10^6$ cells/mL and a maximum throughput of 50 L/day were identified for proper filter operation.

The decrease of the effective acoustic quality factor of yeast suspensions when different cell concentrations were used was evaluated. It was shown that this effect influenced the acoustic field within the resonator at a biomass load of 50 g/L.

The development of cell concentration at the filter outlet, from the time the ultrasound was switched on, was successfully described by a mathematical model.

A limitation of applicability of Ultrasonically Enhanced Settling based on the most important fermentation end-product ethanol was identified. The separation efficiency was vanishing when turbulence occurred in the filter chamber in the presence of ethanol at a concentration of 12%($^{v}/_{v}$). Furthermore the cells showed morphological damages in these experiments, over 90% of cells were killed during a sonication of one hour. No evidence of inertial cavitation was found.

The turbulence was found to result from the special behaviour of the speed of sound of water-rich ethanol mixtures. The acoustic contrast between the yeast cells and the host liquid was diminished and thus the spatial ordering that usually keeps

the cells by immobilisation in the pressure nodes of the standing wave was suppressed.

However, at normal operation of the acoustic filter, when the spatial ordering was established, no significant changes of the culture, i.e. decrease of viability or leakage, were detected, the presence of ethanol apart from the critical concentration did not influence this result. Transmission electron microscopy showed some non-lethal changes in the morphology of the cells' vacuoles due to the action of the ultrasound.

The cells' viability was decreased to 25% after one hour when a suspension was exposed to a progressing wave, instead of a standing wave, within a specially designed anechoic sonication system. Additionally, leakage and morphological changes were observed. Results suggested, that the influence of the sound field in the pressure inter-nodal space was responsible for the damages, the exact mechanism could not be elucidated.

A novel technique suitable for very detailed examinations of the spatial arrangement of particles due to acoustic forces was developed. Gelation of polymers was initiated during sonication, therefore the spatial distribution of the cells could be "frozen" within a gel-block, which subsequently was cut and examined. This procedure delivered for the first time light micrographs of the aggregates' inner structures along with evidence of to date unexplained phenomena.

The size selectivity of the ultrasonic filtration system was used to reduce a common contamination in brewing, *Lactobacillus brevis*. This feature could be explained exploiting the novel gel-technique by the different spatial arrangements of yeast and bacteria.

Furthermore the influence of the inhomogeneous spatial arrangement of the cells on the acoustic behaviour of the resonator was successfully measured for the first time. The spatial distribution of the cells was fixed in gel and therefore decoupled from the sound field and its forces. Comparison with gel in which the cells were freely suspended delivered a decrease of the effective acoustic quality factor by the ordering.

The work was supported in part by the European Commission's TMR Programme, Contract No. ERBFMRXCT97-0156, EuroUltraSonoSep.

PREFACE

This thesis came partly into being during EuroUltraSonoSep, an European Commission's Training and Mobility of Researchers (TMR) Programme. This network comprised of university departments and institutes from physics, biosciences and microbiology, two companies developing, manufacturing and selling ultrasonic separation devices and a company-like institute from the field of disposal and environmental technologies. Scientists interested in different topics like scale-up of existing ultrasonically enhanced settling technology, application of the principle in areas as distant as waste-water treatment and medical diagnosis, exploitation in micro-gravity environments, development of new devices and the exploration of new fields of use, collaborated over a period of more than three years. The wide range of expertise and the commitment to work together, share experience, and sometimes the necessity to take a different point of view, created an interdisciplinary environment that was a very fruitful soil for new ideas and approaches.

This circumstances influenced the work presented here written by a physicist educated at the Institute of General Physics at the Vienna University of Technology working in the laboratory of the Department of Industrial Microbiology at the University College of Dublin. As both regimes were present they found their way into this thesis. Especially the fact of the particles dealt with being *living* cells, which might not act/react in the predictive-by-equation way physicists are used to, took a while to be picked up and maybe has not been understood with all its consequences yet.

This has as well influenced the scientist-to-be. The *scientific method* comprises *observation*, *explanation* and *experiment*[1], however in every-day physics the former two use to arrive hand in hand. One concept that emerged from this was to have physical theory deliver hypothesises that were tested experimentally to "interrogate" cells exploiting microbiological methodology. However the procedure did not always lead to explanations as the *causal connection* taken as a basis was unknown. The lesson adopted was that a well established "it is" represents a very valuable stage as the "why" can be too far to reach at the time.

INTRODUCTION

The first description of the concentration of particles suspended in a fluid in the pressure nodal regions[i] of an acoustic standing wave dates back more than a century. Kundt and Lehmann reported the phenomenon when using it for the visualisation of an ultrasonic field[2]. The effect obviously arises from forces acting on the particles when a dispersion is irradiated with ultrasound, the so-called radiation forces. The general source of these forces is the spatial gradient of the sound waves' acoustic pressure. Hence the relation between the sound wavelength and the particle diameter is of great importance, the phenomenon is size-dependent. The direction and strength of the forces is influenced by the compressibility – which itself is a function of the material properties speed of sound and mass density - of each component of the mixture. The coefficient representing this dependency is called acoustic contrast. A more detailed description will follow.

The principle has been shown to work with all combinations of liquid or gaseous carrier fluids and solid, liquid and gaseous "particles"[3,4] – for obvious reasons with the exception of gas-gas systems. Thereby *suspensions* are dispersions of solid particles in liquids, while a liquid-liquid system is called *emulsion*, an important example is oil in water. The nomenclature for gaseous carriers is *smoke* if solid particles are dispersed and *fog* or *mist* when liquid droplets are present in the gas (air). Of the greatest practical importance are *hydrosols*, i.e. dispersions based on water, and *aerosols* with air as the carrier medium.

Most of the applications employing the principle of particle concentration in the nodal regions of a standing wave use a set-up where the cavity of an acoustic resonator contains a suspension. When the volume is irradiated with ultrasound the initially homogeneously distributed particles are driven into the nodal regions of the standing wave field. Solid particles in water travel into the pressure nodes whilst gas bubbles or oil droplets are concentrated in the displacement nodes. The reason for this is the mentioned dependency of the forces on the compressibility, or in other words, the acoustic contrast in water is positive for solids and negative for gases and oil.

[i] In literature sometimes "loop" or "displacement/velocity anti-node" are found to denote the region of vanishing acoustic pressure in a standing wave.

Typically it does not take more than a few seconds until a spatial distribution like in Figure 2 is reached.

The formation of a standing wave in a resonator is shown in Figure 1. A wave is emitted by a sound source, the transducer, in the direction towards a reflector (a). The incoming and reflected waves are both progressing but their superposition is stationary (b), i.e. does not change its location over time and therefore is called a *standing* wave. The amplitude distribution or the *envelope* describes the maximum of displacement or pressure for a given location (c). Under certain boundary conditions - very simplified when an integer number of half-wavelengths fits between the two terminating surfaces transducer and reflector - resonance is observed, the amplitude of the sound field becomes large. If the transducer emits a plane wave, i.e. the locations of equal phase are on a plane in space, the pressure nodes of the resulting standing wave will be planes as well.

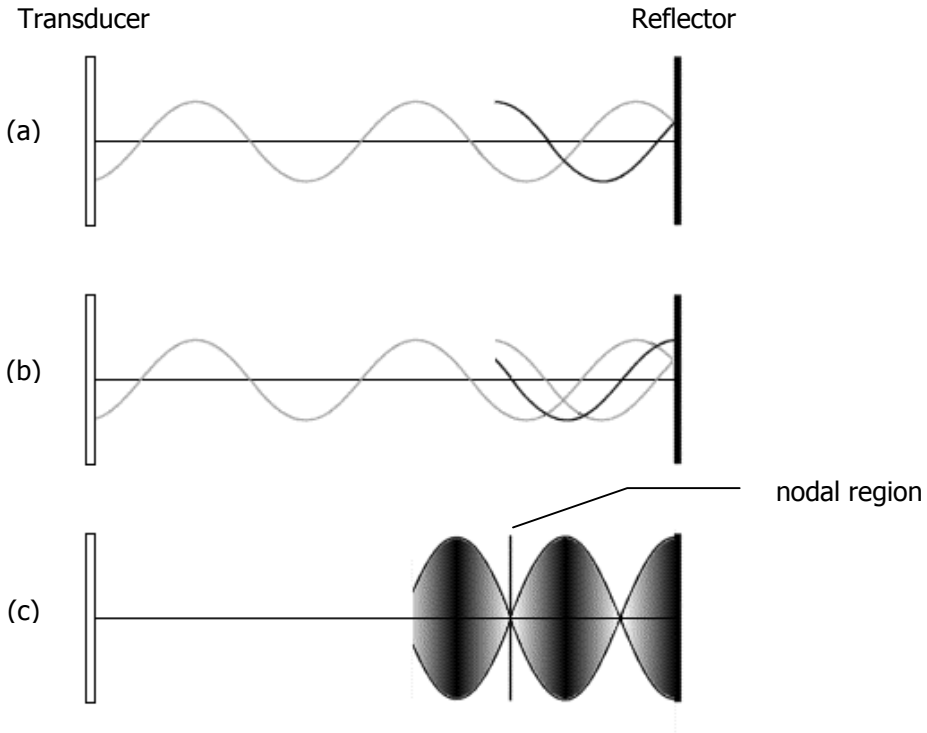

Figure 1 A standing (radiation pressure) wave composed as the superposition of a progressive wave and its reflection (a), the superposition is stationary (b). The amplitude distribution is called envelope (c) .

The line pattern of Figure 2 represents the pressure nodes of the standing wave field, the picture is taken perpendicular to the direction of sound propagation, the parallel planes of concentrated particles are half a wavelength apart.

Recently, the properties of ultrasound standing waves have been used to design retention systems able to immobilise particles in specific regions of the suspension[5,6]. These systems have already proved to perform flow filtration of cell suspensions and are already successfully used in biotechnology[7] and in diagnostic as reliable sample concentration systems[8].

One of the most interesting fields of application of ultrasonic plane wave fields is the micro-manipulation of biological cells. Reports during the last decade showed the exertion of acoustic radiation forces on various cell lines to be gentle and not decreasing viability. Potential applications employing the principle to biological material especially for cell separation and filtration have been identified for animal cells[9,10], hybridoma[11-13], red blood cells[14] and even DNA[15].

Figure 2 Suspended yeast cells concentrated in the pressure nodal planes of a standing ultrasonic wave of 2.2 MHz (horizontal direction of sound propagation).

Another cell system used for a number of studies in the regime of ultrasonic particle manipulation and ultrasonic separation principles was yeast[16-23]. This micro

organism with a diameter in the range of 4-10 μm is of advantage as a biological model for a couple of reasons. Firstly it is of spherical shape and therefore close to the ideal spheres used in the mathematical theory of ultrasonic particle manipulation. Furthermore it is easy to cultivate and save to handle. The particles used in the experiment in Figure 2 were yeast cells of the strain *Saccharomyces cerevisiae*. This particular strain is one of those among the family of yeasts which is attractive for another reason than those just mentioned. *Saccharomyces cerevisiae* is also known as brewer's yeast.

The origins of beer are believed to be in ancient Babylon 8,000 years ago, where it was used for religious purposes. The French chemist Joseph Louis Gay-Lussac found 1810 the reaction equation describing the production of alcohol out of sugar: $C_6H_{12}O_6 \rightarrow 2(CO_2 + C_2H_5OH)$, i.e. the glucose is broken up into two molecules of carbon dioxide and two molecules of ethanol. Later in the 19th century Louis Pasteur (1822-1895) realized that it was the yeast that was carrying out the *fermentation*, i.e. the formation of ethanol, flavour components and carbon dioxide out of the wort, a mixture of barley, malt, hop and water.

The ecological competence of brewing yeast cells is affected by process/environmental stresses such as high osmotic pressure, high sugar and end product concentration[24]. The brewing industry is therefore seeking new methods of improving the stress resistivity of yeast cells. Immobilised cell technology has been shown to increase microbiological cell stress tolerance by the creation of heterogeneously spatially organised microenvironments as protective barriers for the yeast cells[25,26].

The traditional way to remove yeast cells in brewing industry is to exploit the yeast's ability to adhere in clumps under certain conditions. These either settle at the bottom or float at the top of the fermentor or in more sophisticated vessels[27-29]. Preferably flocculation is induced at the end of the fermentation process, the yeast can then be retrieved easily after it has finished its work.

Flocculation is a reversible reaction of a yeast culture to the environment, especially to environmental stresses like physical as temperature or (bio)-chemical as pH changes[30].

Attempts to utilise ultrasound for separation/filtration purposes in brewing have been made earlier, but the technology has been considered to need further

examination[31-33]. However, since then the scale-up of the technology has progressed, perfusion filtering systems capable of 300 L/d and more are in the market (250L BioSep AppliSens, Applikon Dependable Instruments bv, Schiedam, The Netherlands).

Brewing is a money loaded industry today and therefore a promising target for ultrasonic separation systems, however, yeasts are important in other fields of biotechnological environments as well, e.g. for the production of enzymes and proteins in the pharmaceutical industry[34].

The ultrasonic separation technology nowadays is at a stage where applications of practical importance become visible. The main advantages of cell filters based on this technique are the complete absence of moving parts and therefore no filter cakes or filter fouling. The systems can be hot-steam sterilised in-situ, the used materials such as stainless steel and glass are bio-compatible. Furthermore an extensive literature on the theory of the interaction of ultrasonic waves with particles exists, and highly advanced piezoelectric transducers and driving electronics are available.

Therefore this work is focussing on the ultrasonic separation principle applied to hydrosols of yeast with the target to

- examine the existing technology from the point of cell filtration of yeast suspensions

and to

- identify potential applications in brewing and yeast technology.

THEORY OF ULTRASONIC PARTICLE MANIPULATION

The following theoretical introduction is supposed to go into as much detail as seems necessary for the evaluation or explanation of the results presented later. In particular a one-dimensional description in the direction of sound propagation is used for the plane, longitudinal wave fields examined. The overview is guided by the exceptional good presentation given by Gröschl[6].

When a suspension is irradiated with an ultrasonic wave field various forces are exerted on the dispersed particles. The displacement of the liquid over time, i.e. the displacement velocity, results in a hydrodynamic force, however, when averaged over one period of the exciting wave in linear approximation[35] this force is zero.

The explanation for the observed effects was 1934 delivered by King[36]. He integrated the radiation pressure exerted by a plane standing acoustic wave over the surface of a rigid sphere in an ideal, i.e. non-viscous fluid. This derivation taking second order effects from the scattered sound field into consideration led to a non-vanishing time-averaged force displacing the particle. This effect is called the *axial primary radiation force* to express that it is originating from direct (primary) interactions of the particle and the initial sound field in direction of sound propagation (axial).

A description of the axial primary radiation force of a plane standing wave showing good agreement with experimental data was delivered by Yosioka and Kawasima[37] as

$$\langle F_s \rangle = 4\pi \cdot \rho \cdot \hat{\Phi}^2 (ka)^3 K_s(\lambda, \sigma) \sin(2kx) \quad . \qquad \textbf{(1)}$$

Equation **(1)** for the axial primary radiation force F_s of a standing wave - the angle brackets refer to the time-averaging over one period of the cycle - was derived when Kings rigid particle was replaced by a compressible sphere in a host fluid of the mass density ρ. The other symbols in equation **(1)** are the particle's radius *a*, the wave number *k* (which is angular frequency divided by the speed of sound, hence $k = \omega / \upsilon$) and the amplitude $\hat{\Phi}$ of the standing wave field's velocity potential

$$\tilde{\Phi}_s = \hat{\Phi}\left\{e^{i(\omega t - kx)} + e^{i(\omega t + kx)}\right\} \quad . \qquad \textbf{(2)}$$

Equation **(2)** expresses the standing wave as the superposition (compare Figure 1) of an incoming wave and its reflection.

The term sin(2*kx*) in equation **(1)** reflects the half-wavelength pattern of the nodes. The acoustic contrast factor of the standing wave $K_s(\lambda,\sigma)$ describes the strength and, by its sign, the direction of the axial primary radiation force. The acoustic contrast factor K_s is a function of the material properties of the particle and the host liquid

$$K_s(\lambda,\sigma) = \frac{1}{3}\left(\frac{5\lambda - 2}{2\lambda + 1} - \frac{1}{\lambda\sigma^2}\right) \quad , \qquad \textbf{(3)}$$

where $\lambda = \rho_0/\rho$ is the ratio of the mass densities and $\sigma = \upsilon_0/\upsilon = k/k_0$ the ratio of the speeds of sound, the subscript *0* denotes the respective value for the particle. According to this, a solid particle like a cell is driven into the pressure nodes whilst air bubbles or oil droplets are concentrated in the displacement nodes.

The description of the axial primary radiation force in equation **(1)** is valid in the limiting case $ka \ll 1$ and $k_0 a \ll 1$, i.e. the particle must be small compared to the wavelength and $\lambda = O(1)$ which means that the mass densities of the particle and the liquid must be of the same order of magnitude.

For arbitrary sound fields Gor'kov delivered an equation where the radiation force F_G can be expressed as the gradient of a radiation force potential Φ_G, hence

$$\begin{aligned} &\left\langle F_G(x)\right\rangle = -\nabla\left\langle \Phi_G(x)\right\rangle \quad \text{with} \\ &\left\langle \Phi_G(x)\right\rangle = -V\left(\frac{3(\lambda-1)}{2\lambda+1}\left\langle \overline{E}^{kin}(x)\right\rangle - \left(1 - \frac{1}{\lambda\sigma^2}\right)\left\langle \overline{E}^{pot}(x)\right\rangle\right) \quad , \end{aligned} \qquad \textbf{(4)}$$

where V means the particle volume, $\overline{E}^{kin}$ and $\overline{E}^{pot}$ are the kinetic and potential energy densities of the unperturbed sound field respectively[38]. It has to be mentioned, that equation **(4)** is the one-dimensional simplification of Gor'kov's original formula which was defined for the whole three-dimensional space. It is easily shown that for a plane standing wave with the total, kinetic and potential energy densities

$$\left\langle \overline{E}_s(x) \right\rangle = \rho k^2 \hat{\Phi}_s^2 \quad \text{and}$$
$$\left\langle \overline{E}_s^{kin}(x) \right\rangle = \left\langle \overline{E}_s(x) \right\rangle \cdot \sin^2(kx) \quad , \qquad \textbf{(5)}$$
$$\left\langle \overline{E}_s^{pot}(x) \right\rangle = \left\langle \overline{E}_s(x) \right\rangle \cdot \cos^2(kx) \quad ,$$

equation **(4)** leads to equation **(1)**. Again $ka \ll 1$ is necessary for equation **(4)** to hold and the particle radius a must fulfil the additional conditions

$$a \gg \sqrt{\frac{2\mu}{\rho\omega}} \quad \text{and} \quad a \gg \hat{u} \quad , \qquad \textbf{(6)}$$

where μ is the shear viscosity of the host liquid and $\hat{u}$ equals the displacement amplitude of a fluid particle. Equation **(4)** is not valid for sound fields with low gradients of the kinetic and potential energy density[i].

As equation **(4)** allows to examine general situations defined by the energy density distributions the influence of amplitude gradients in directions perpendicular to the sound propagation direction can be assessed. This is an important matter for real resonators as the boundaries of the resonator, uneven amplitude distributions over the surface of the transducer and divergence of the wave rather lead to standing fields like

$$u(x,y,t) = \hat{u}_{dev}(y)\sin(kx)\sin(\omega t) \quad , \qquad \textbf{(7)}$$

with $\hat{u}_{dev}(y)$ describing the deviation, i.e. the non-uniformity of the amplitude in direction y. It has to be emphasized that nevertheless one deals with a *plane* wave, i.e. the phase of the wave is unaffected and therefore the surface of equal phase is flat!

The *transverse primary radiation force* emerging from a situation like this acts in the direction y perpendicular to sound propagation x and can be derived from equations **(4)** and **(7)** as

$$\left\langle F_y(x,y) \right\rangle = \qquad \textbf{(8)}$$
$$\frac{2\pi}{3}\rho\omega^2 a^3 \cdot \hat{u}_{dev}(y)\frac{\mathrm{d}\,\hat{u}_{dev}(y)}{\mathrm{d}\,y} \cdot \left(\frac{3(\lambda-1)}{2\lambda+1}\sin^2(kx) - \left(1 - \frac{1}{\lambda\sigma^2}\right)\cos^2(kx) \right).$$

[i] This is the case for plane progressive waves which will be discussed later.

$F_y(x,y)$ is sometimes as well called Bernoulli force. For a small spherical particle the amplitude distribution in its vicinity can be approximated by

$$\hat{u}_{dev}(y) = \hat{u} + \frac{\hat{u}_y}{a} y \quad , \tag{9}$$

wherein the centre of the particle is assumed at y=0 and $\hat{u} + \hat{u}_y$ is the amplitude at the particle's surface. If this particle is dense, i.e. $\lambda \gg 1$ and its position is in the pressure node where the second term in the brackets of equation **(8)** vanishes the transverse primary radiation force can be written as

$$\langle F_y \rangle = \pi \rho \omega^2 a^2 \hat{u} \hat{u}_y \quad . \tag{10}$$

Equation **(10)**, which was derived by Benes[39] by a different approach, results in a concentration of the particles at regions of maximal amplitude within the pressure nodal planes.

The so-called *secondary radiation forces* are brought about by additional (secondary) sound sources, e.g. an excited particle, and therefore surface as particle-particle interactions. In other words, they describe the effect on one particle in the sound field emitted or scattered by another particle and vice versa. Because of their early investigations in 1871 and 1909, respectively, these forces are sometimes called after König[40] or Bjerknes[41].

Crum delivered in 1971 an expression where the force that would act on a rigid sphere and the contribution due to its compressibility were added[42] yielding the total force on liquid droplets. For a situation where both the distance d between the two particles and their radii a are small in comparison to the wavelength, hence $ka \ll 1$ and $kd \ll 1$, Weiser[43] obtained

$$\langle F_i(x) \rangle = 4\pi a^6 \left(\frac{(\rho_0 - \rho)^2 (3\cos^2\theta - 1)}{6\rho d^4} v^2(x) - \frac{\omega^2 \rho (\beta_0 - \beta)^2}{9 d^2} p^2(x) \right) \quad , \tag{11}$$

for the interaction of two identical compressible spheres in a standing wave field. In equation **(11)** β_0 and β denote the compressibility of the particle and the host

liquid respectively, and θ is the angle between the direction of sound propagation and the line connecting the particle centres. In the special case of the particles being biological cells the effect of this secondary radiation force is a repulsion between the cells that have been brought very close together in a sound field, e.g. in the pressure node of a standing wave. This may lead to a fine structure which was observed by Weiser for red blood cells.

The importance of this is, that cells which are immobilised in a separation system as described are not forced to touch each other or to form dense clumps but to keep a certain distance from each other. Therefore the supply of nutrients and oxygen is ensured as the host liquid is still present around the cells.

It was already reminiscent that in a real resonator the standing wave field might not be comprehensively described by equation **(2)**. Due to the presence of particles, divergence of the wave or absorption in the side walls, but mostly because of the viscosity of the liquid, the acoustical wave field is subjected to losses. This influences lead to an exponential decrease of the amplitude for both the incident and reflected wave while progressing through the cavity of the resonator. This decrease can be accounted for the displacement $\tilde{u}$ like

$$\tilde{u}(x,t) = \hat{u}\left\{e^{-\alpha_{eff}\cdot x} e^{i(\omega t - kx)} + e^{-\alpha_{eff}(2\cdot l - x)} e^{i(\omega t + kx)}\right\} \quad , \qquad \textbf{(12)}$$

where l is the length of the resonator. The effective absorption coefficient α_{eff} of the resonator is the sum of the viscous absorption coefficient α of the liquid alone[44] and α_{oth}, which represents the mentioned additional losses. The viscous absorption coefficient is connected to a quantity called the acoustic material quality factor Q like

$$Q = \frac{k}{2\alpha} \quad \text{for} \quad Q \gg 1 \quad . \qquad \textbf{(13)}$$

The acoustic quality factor is defined as the ratio between the energy stored in the resonator and the dissipated energy per period or power loss. Equation **(13)** can be rewritten expressing an effective acoustic quality factor Q_{eff} by means of the effective absorption coefficient:

$$\frac{k}{2Q_{eff}} = \alpha_{eff} = \alpha + \alpha_{oth} \quad . \tag{14}$$

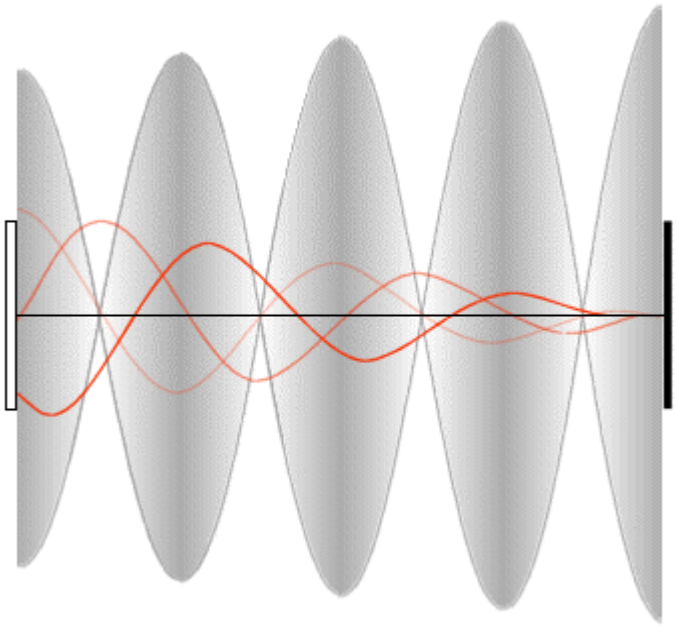

Figure 3 Standing and progressive waves contributing to a quasi-standing wave field. This is a behaviour brought about by sound attenuation.

The consequence of absorption as described by equation **(12)** is an acoustic field called a *quasi-standing* wave, expressing that due to the decrease of the amplitude of the wave while travelling through the resonator the superposition of the incident and reflected waves is not a purely standing wave anymore. The situation can be described mathematically by the superposition of a standing wave and an additionally present progressive wave which moves from the transducer to the reflector. Qualitatively the amplitude of the standing wave is increasing from the transducer reaching its maximum in the vicinity of the reflector. For the progressive wave the exact opposite is true, in that the amplitude has its maximum at the transducer and decreases in direction of the sound propagation. Unlike the standing wave the progressive wave actually vanishes at the reflector[i], Figure 3 shows the circumstances.

[i] This is only true for 100% reflection, which is assumed in this work.

The expression for the axial primary radiation force of the progressive wave[37] is

$$\left\langle F_p \right\rangle = 2\pi \cdot \rho \cdot \hat{\Phi}^2 (ka)^6 K_p(\lambda, \sigma) \quad , \tag{15}$$

with the acoustic contrast factor of the progressive wave K_p

$$K_p(\lambda, \sigma) = \frac{1}{(1+2\lambda)^2}\left[\left(\lambda - \frac{1+2\lambda}{3\lambda\sigma^2}\right)^2 + \frac{2}{9}(1-\lambda)^2\right] \quad . \tag{16}$$

In comparison to the axial primary radiation force of the standing wave in equation **(1)** where one finds the factor $(ka)^3$ equation **(15)** delivers an exponent of six for (*ka*). Together with the limitation $ka \ll 1$, that is necessary for equation **(15)** to hold as well, this means that the axial primary radiation force exerted by a progressive wave is in most cases much weaker than that of a standing wave. However, this will have to be looked into closer later in this work. Figure 4 gives an overview of the various forces exerted on a particle within a separation system as discussed.

The connections between mechanical and electrical properties for piezoelectric structures were assessed among others with electro-acoustic equivalent circuits[45,46] and transfer matrix approaches[47-49]. The separation systems employed in this work were developed applying a one-dimensional transfer matrix model for layered resonators formulated by Nowotny[50]. Typically, resonators for particle manipulation are built up like shown in Figure 5. A piezoelectric ceramic (lead-zirconium titanat, PZT) with two electrodes is glued to a glass carrier. The sound is emitted into one or more liquid layers which are terminated by a reflector.

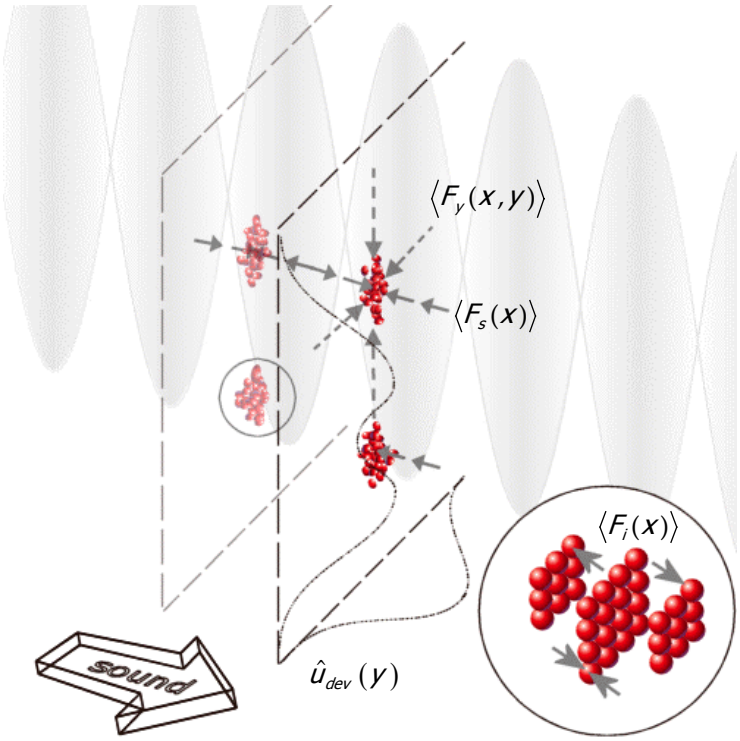

Figure 4 Acoustic radiation forces exerted on a particle in a separation system.

The linear theory of piezoelectricity defines the quantities stress T and dielectric displacement D by the spatial derivatives[i] of displacement u and electric potential φ as

$$T = c\frac{\mathrm{d}u}{\mathrm{d}x} + e\frac{\mathrm{d}\varphi}{\mathrm{d}x} \quad \text{and}$$
$$D = e\frac{\mathrm{d}u}{\mathrm{d}x} - \varepsilon\frac{\mathrm{d}\varphi}{\mathrm{d}x} \quad , \qquad \textbf{(17)}$$

where c, e and ε are the material properties elastic stiffness constant, piezoelectric constant and dielectric constant, respectively. The basic idea of the model is that the connection between the values of $u(l)$, $T(l)$, $\varphi(l)$ and $D(l)$ at the boundary at $x=l$ of a given homogeneous material layer of the thickness l can be described by means of a transfer matrix **M** from the values of $u(0)$, $T(0)$, $\varphi(0)$ and $D(0)$ at the opposite boundary at $x=0$, hence

[i] Due to the restriction to one dimension, tensor and vector quantities here reduce to scalars.

$$\begin{pmatrix} u \\ T \\ \varphi \\ D \end{pmatrix}_{x=l} = \mathbf{M} \begin{pmatrix} u \\ T \\ \varphi \\ D \end{pmatrix}_{x=0} \quad \text{with} \quad \mathbf{M} = \begin{pmatrix} M^{uu} & M^{uT} & M^{u\varphi} & M^{uD} \\ M^{Tu} & M^{TT} & M^{T\varphi} & M^{TD} \\ M^{\varphi u} & M^{\varphi T} & M^{\varphi\varphi} & M^{\varphi D} \\ M^{Du} & M^{DT} & M^{D\varphi} & M^{DD} \end{pmatrix} \quad . \qquad \textbf{(18)}$$

The components of $\mathbf{M}$ depend only on material constants, layer thickness and on the angular frequency ω, the explicit expressions were reported by Nowotny[50]. The whole resonator (compare Figure 5) can subsequently be described by a total transfer matrix $\mathbf{M}_{tot}$ as the product of the transfer matrices of the respective layers

$$\mathbf{M}_{tot} = \mathbf{M}_E \cdot \mathbf{M}_P \cdot \mathbf{M}_E \cdot \mathbf{M}_C \cdot \mathbf{M}_L \cdot \mathbf{M}_R \quad . \qquad \textbf{(19)}$$

With the conditions of vanishing stress and dielectric displacement, i.e. *T=D=0* at the boundaries *x=0* and *x=L* with *L* being the length of the whole structure one gets

$$\begin{pmatrix} u \\ 0 \\ \varphi \\ 0 \end{pmatrix}_{x=L} = \mathbf{M}_{tot} \begin{pmatrix} u \\ 0 \\ \varphi \\ 0 \end{pmatrix}_{x=0} \quad , \qquad \textbf{(20)}$$

and therefore

$$\begin{aligned} 0 &= M^{Tu} \cdot u(0) + M^{T\varphi} \cdot \varphi(0) \quad , \\ 0 &= M^{Du} \cdot u(0) + M^{D\varphi} \cdot \varphi(0) \quad . \end{aligned} \qquad \textbf{(21)}$$

Equations **(21)** deliver a relation between the displacement and the electric potential on the outer electrode of the resonator

$$u(0) = -\left(M^{Tu}\right)^{-1} M^{T\varphi} \cdot \varphi(0) \quad , \qquad \textbf{(22)}$$

and an expression[i] of the electrical admittance Y in dependence of the angular frequency ω. The model is not limited to the physical layers like in Figure 5, but

[i] The reader is again referred to the original work[50] for explicit expressions.

equation **(18)** can be adjusted to the needs of higher resolution in that thinner sub-layers of arbitrary length $l' = x_n - x_{n-1}$ are introduced and computed like

$$\begin{pmatrix} u \\ T \\ \varphi \\ D \end{pmatrix}_{x=x_n} = \mathbf{M}_n \left(x_n - x_{n-1} \right) \begin{pmatrix} u \\ T \\ \varphi \\ D \end{pmatrix}_{x=x_{n-1}} \quad . \tag{23}$$

Therefore it is possible to examine the whole structure starting with appropriate boundary conditions at the outer electrode followed by the stepwise evaluation of the active, piezoelectric layer. Subsequently the primary quantities $u(x)$, $T(x)$, $\varphi(x)$ and $D(x)$ can be calculated over the whole length of the resonator yielding their spatial distribution in discrete steps of the length l'.

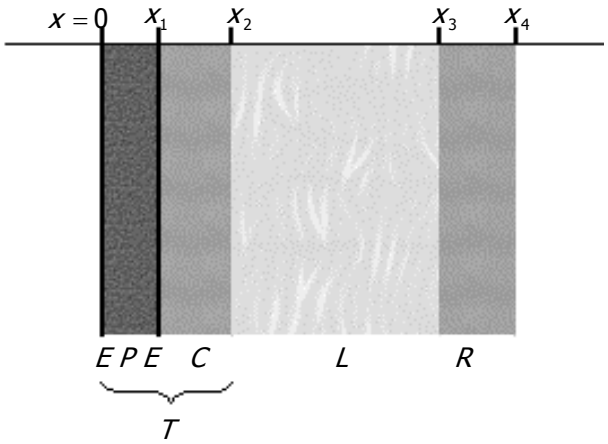

Figure 5 Layered resonator comprising a transducer T, i.e. PZT ceramic P with two electrodes E glued to a glass carrier C, a liquid layer L and a reflector R.

The most elegant way to account for the previously mentioned losses is the use of complex notation in the model. As a starting point Hooke's law

$$T = cS \quad , \tag{24}$$

can be re-written[51] to consider viscoelastic damping in adding a term representing the change of the strain over time which is influenced by the viscosity, hence

$$T = cS + \mu \frac{\partial S}{\partial t} \quad . \tag{25}$$

In the case of harmonic acoustic waves with time dependence $e^{i\omega t}$ one finds the time derivative for any physical property in a multiplication by $i\omega$ and therefore equation **(25)** delivers

$$\tilde{T} = c\tilde{S} + i\omega\mu\tilde{S} = \tilde{c}\tilde{S} \quad \text{with} \quad \tilde{c}=c+i\omega\mu \quad , \tag{26}$$

where $\tilde{c}$ means the complex stiffness constant[i]. Using the definition of the acoustic material quality factor Q

$$Q = \frac{c}{\omega\mu} \quad , \tag{27}$$

the complex stiffness constant can be expressed by

$$\tilde{c} = c\left(1 + i\frac{1}{Q}\right) \quad . \tag{28}$$

Similarly, complex expressions exist for the sound velocity υ and the dielectric constant ε

$$\tilde{\upsilon}=\upsilon\left(1+\mathrm{i}\frac{1}{2Q}\right) \quad \text{for} \quad Q \gg 1 \quad , \qquad \tilde{\varepsilon} = \varepsilon(1 - i\tan\vartheta) \quad , \tag{29}$$

with ϑ being the dielectric loss angle specified by the manufacturer of the piezoelectric ceramic. It already has been shown in equations **(13)** and **(14)** how additional losses can be expressed by using effective material quality factors or absorption coefficients, however, they are frequency dependent and therefore subject of measurements. The advantage of the complex notation is that all calculations can be carried out like before to establish knowledge about the now complex physical quantities $\tilde{u}(x)$, $\tilde{T}(x)$, $\tilde{\varphi}(x)$ and $\tilde{D}(x)$. Therefore an electrical measurement of the complex admittance $\tilde{Y}(\omega)$ at the transducer electrodes enables one to assess the

[i] The tilde (~) is used to mark complex quantities throughout this work.

effective acoustical attenuation within the resonator experimentally regardless of its origin.

The connection of the radiation force potential of equation **(4)** and the theoretical model just presented is made by the acoustic energy density. The Poynting vector for piezoelectric media representing the energy flow density is given by

$$\tilde{\Pi}(x)=\frac{1}{2}\left[-\tilde{v}^{*}(x)\tilde{T}(x)+\tilde{\varphi}(x)\left(i\omega\tilde{D}(x)\right)^{*}\right] \quad \text{with} \quad \tilde{v}(x)=i\omega\cdot\tilde{u}(x). \tag{30}$$

where $\tilde{v}(x)$ is the displacement velocity, the asterisk denotes the complex conjugation. The real part of equation **(30)** is the true energy flow density in [W/m²], the imaginary part delivers peak reactive energy flow density. The true energy flow density of a stationary process is time-averaged and therefore the mean total stored energy density can be expressed as

$$\left\langle \overline{E}(x)\right\rangle =\frac{1}{4}\left[\rho\tilde{v}(x)\tilde{v}^{*}(x)+\Re\left\{\tilde{T}(x)\tilde{S}^{*}(x)-\frac{\mathrm{d}\tilde{\varphi}}{\mathrm{d}x}\tilde{D}^{*}(x)\right\}\right] \quad . \tag{31}$$

The first term of equation **(31)** represents the kinetic energy density, the first spatial derivative of $\tilde{\varphi}(x)$ can be found using equations **(17)**.

In those layers one is interested in when considering particle separation, typically no electrical field is present, hence equation **(31)** can be simplified to

$$\begin{aligned}\left\langle \overline{E}(x)\right\rangle &=\left\langle \overline{E}^{kin}(x)\right\rangle +\left\langle \overline{E}^{pot}(x)\right\rangle \\ &=\frac{1}{4}\left[\rho\tilde{v}(x)\tilde{v}^{*}(x)+\Re\left\{\tilde{T}(x)\tilde{S}^{*}(x)\right\}\right] \quad .\end{aligned} \tag{32}$$

This delivers the mean kinetic and potential energy densities needed for the calculation of the radiation force potential in equations **(4)** and therefore subsequently yields the primary radiation force according to Gork'ov.

As mentioned the quality factor Q is defined as the ratio of stored energy and power loss, hence

$$Q=\omega\frac{\langle E\rangle}{P^{loss}} \quad . \tag{33}$$

Using the power loss density delivered by Poynting's theorem

$$\left\langle \overline{P}^{loss}(x) \right\rangle = \frac{1}{2}\omega \cdot \Im\left\{ \tilde{T}(x)\tilde{S}^{*}(x) - \frac{\mathrm{d}\varphi}{\mathrm{d}x}\tilde{D}^{*}(x) \right\} \quad , \tag{34}$$

one had to integrate over the considered layer *L*, e.g. the liquid layer between $x = x_2$ and $x = x_3$ (compare Figure 5) like

$$\left\langle P_L^{loss} \right\rangle = A\int_{x_2}^{x_3} \overline{P}^{loss}(x)\cdot \mathrm{d}x \quad , \tag{35}$$

where *A* is the cross sectional surface of the resonator perpendicular to the direction of sound propagation. However the total power loss within the layer has to be the difference between the respective values of the true energy flow at the layer boundaries and therefore

$$\left\langle P_L^{loss} \right\rangle = A\left(\Re\left\{ \tilde{\Pi}(x_2) \right\} - \Re\left\{ \tilde{\Pi}(x_3) \right\} \right) \quad , \tag{36}$$

which is an expression easier to evaluate than equation **(35)**. Together with equation **(33)** one finds the total stored energy in the liquid layer in dependence of the acoustic quality factor and the power loss to be

$$\left\langle E_L \right\rangle = \frac{Q_L}{\omega} A\left(\Re\left\{ \tilde{\Pi}(x_2) \right\} - \Re\left\{ \tilde{\Pi}(x_3) \right\} \right) \quad . \tag{37}$$

Finally an important quantity from the practical point of view shall be defined. The only energy source is the electrical driving signal at the transducer electrodes. Therefore the total energy loss per period $\left\langle E_{tot}^{loss} \right\rangle$ multiplied by the oscillation frequency $f = \omega/2\pi$ has to be equal to the true electrical power input P_{el}^{true}. This can be derived from the pointing vector as[i]

$$P_{el}^{true} = \left\langle E_{tot}^{loss} \right\rangle \frac{\omega}{2\pi} = A \cdot \Re\left\{ \tilde{\Pi}(x_0) \right\} \quad . \tag{38}$$

[i] Electrical power quantities are by definition time-averaged.

On the other hand the true electrical power input is defined as a function of the electrical admittance

$$P_{el}^{true} = \frac{1}{2}\hat{U}^2 \cdot \Re\left\{\tilde{Y}\right\} \quad , \tag{39}$$

where $\hat{U}$ is the voltage amplitude at the transducer. The connection between the electrical measurement and the calculated result of the described model as of equation **(30)** is completed by the apparent electrical power input P_{el}^{app} and its electrical definition and the relation to the Poynting vector:

$$P_{el}^{app} = \frac{1}{2}\hat{U}^2 \cdot \left|\tilde{Y}\right| = A \cdot \left|\tilde{\Pi}\left(x_0\right)\right| \quad . \tag{40}$$

MATERIALS AND METHODS

M1 Statistical definitions

The calculation of the standard deviation was performed by

$$s.d. = \sqrt{\frac{\sum_{i=1}^{n}\left(y_i - \overline{y}\right)^2}{n-1}} \quad \text{with} \quad \overline{y} = \frac{1}{n}\sum_{i=1}^{n} y_i \quad , \tag{41}$$

where n is the number of trials, y_i are the measured values and $\overline{y}$ is the mean of the measured values.

The quality of the fit of a model was assessed by the value of the regression coefficient R calculated using

$$R^2 = 1 - \frac{SSE}{SST}$$
$$\text{with} \quad SSE = \sum\left(y_i - \hat{y}_i\right)^2 \quad \text{and} \quad SST = \left(\sum y_i^2\right) - \frac{\left(\sum y_i\right)^2}{n} \quad , \tag{42}$$

where y_i again are the measured values and $\hat{y}_i$ are the values calculated from the model.

Where appropriate the means of a number of trials were compared using the Student's t-distribution. This common method tests a null hypothesis of equal means, i.e. the resulting probability p gives the ratio of all possible populations which actually have equal means. Hence, a value of $P<0.05$ indicates *different* means for a significance level of 95%.

If knowledge existed which of two means was supposed to be higher - for instance because a certain stress was applied longer on living cells - a so-called one-tailed t-test taking just half of the distribution into account was used. The test quantity t for two experiments A and B is given by

$$t = \frac{\left|\overline{y}_A - \overline{y}_B\right|}{\sqrt{\frac{s.d._A^2}{n_A} + \frac{s.d._B^2}{n_B}}} \quad . \tag{43}$$

A subscript “1” or “2” of the given values will indicate a one-tailed or a two-tailed t-test.

M2 Cultivation and handling of suspended micro-organisms

M2.1 *Saccharomyces cerevisiae*

One colony was retrieved from a plate with a loop and seeded in malt extract broth (0.4 g in 40 mL H_2O). This inoculate was left overnight in a 30°C incubator provided with a orbital shaker table (150 rpm). Subsequently, 5 mL of this culture were added to 95 mL of fresh malt extract broth (2 g in 100 mL H_2O) and let grow for 24 hours in the same incubator.

The culture was centrifuged at 3800 rpm in a Sorvall centrifuge for 10 minutes and the precipitate was re-suspended in 100 mL saline (0.9 g NaCl in H_2O) or water. An appropriate volume of 99% ethanol (EtOH) was added to the sample suspension to reach the respective alcohol concentration, when required.

Sample preparation was carried out in a sterile environment.

M2.2 Lactobacillus brevis

A colony was retrieved from a plate using a loop and seeded in MRS broth (Oxoid) followed by 24 hours growth in an incubator at 30°C. Centrifugation and re-suspension were performed in the same manner as for yeast cultures.

M3 Chemical and microbiological assays

M3.1 Measurement of inertial cavitation by a method to pick-up free radicals

The presence of free radicals due to ultrasound treatment was assessed using the method described by Coakley[52]. The basic mixture used was 1.7 g KI, 0.5 mL CCl_4 and 0.15%($^w/_v$) starch on 100 mL of water or 12%($^v/_v$) EtOH-water mixture. To test the reactivity of the iodine-starch mixture 30%($^v/_v$) H_2O_2 was added as external source of free radicals, deep blue colour was detected in each case.

The suspensions for the cavitation tests were pure water and 12%($^v/_v$) EtOH-water respectively, both without and with suspended yeast cells at a concentration of 10^7 cells/mL. Each of the four suspension was sonicated in the separation system at 30 W, 50 W and 70 W for 10 minutes at 2.2 MHz. This treatments were performed one after the other without changing the filling.

Cell debris was expected to influence the optical density measurement and therefore the samples were centrifuged for 10 minutes at 9000 rpm (microfuge, Denver Instruments) to settle the debris. Afterwards the optical density of treated sample and untreated control was measured using a spectrophotometer (UNICAM Heλiosα UV-Visible v2.03) at 565 nm.

M3.2 Haemacytometer

The sample of cell suspension was retrieved and put into a standard haemacytometer. Under a standard light microscope the cells within ten squares - Figure 6 shows two of them – were counted for both sides of the haemacytometer. The mean of both counts multiplied by 25,000 gave the cell concentration in cells/mL.

Image analysis assisted method

Due to the high number of samples for the experiments in chapter R1 the described method was adjusted to allow computer aided counting. A camera connected with the microscope was used to take a picture of two squares of the heamacytometer. Using standard image enhancement methods the picture was

modified (Figure 6) to make it accessible to automatic counting. The number of squares counted and the method of calculations were the same as before.

(a)

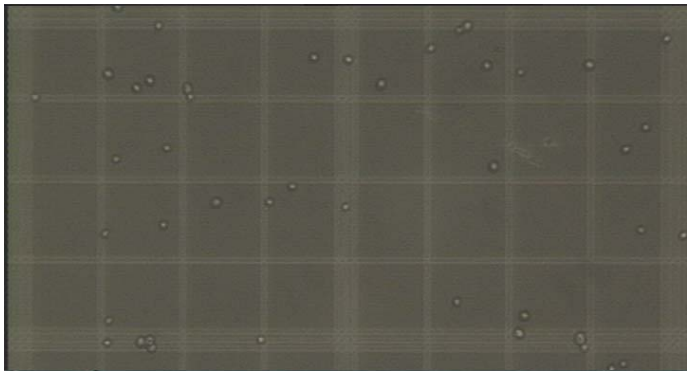

(b)

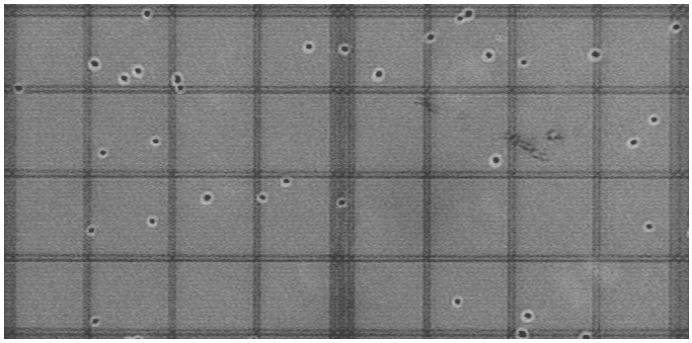

Figure 6 Image prior (a) and after enhancement (b).

M3.3 Methylene blue technique

The sample was diluted with a batch of methylene blue solution. The number of dead cells over the number of total cell population was assessed by haemacytometer method (M3.2). The dye is reduced in a viable cell, non-viable cells therefore appear blue under the microscope. Hence the data of the cell viability are given as percentage

$$Viability = 100\% \cdot \left(1 - \frac{N_{blue}}{N_{total}} \right) \quad . \qquad \textbf{(44)}$$

M3.4 Ultraviolet-absorption

The sample was collected from the resonator after treatment and centrifuged for 10 minutes at 9000 rpm (microfuge, Denver Instruments). The supernatant was then

retrieved with a pipette and put into a quartz cuvette. The optical density was measured at a wavelength of 280 nm with a spectrophotometer (UNICAM Heλiosα UV-Visible v2.03). The system was calibrated with the optical density of water to be zero.

M3.5 Plate counts

The samples were diluted with sterilized physiological saline (0.9%($^{w}/_{v}$) NaCl) until the number of cells in an equivalent of 100 μL was in the range of one hundred. The equivalent was spread with a glass rod on malt extract agar plates (50 g per 1000 mL H_2O). The number of colonies (colony forming units, CFU) growing at 30°C for 5 days provided an index of reproductive ability of the cells after treatment.

M3.6 Fluorescent vacuole membrane stain

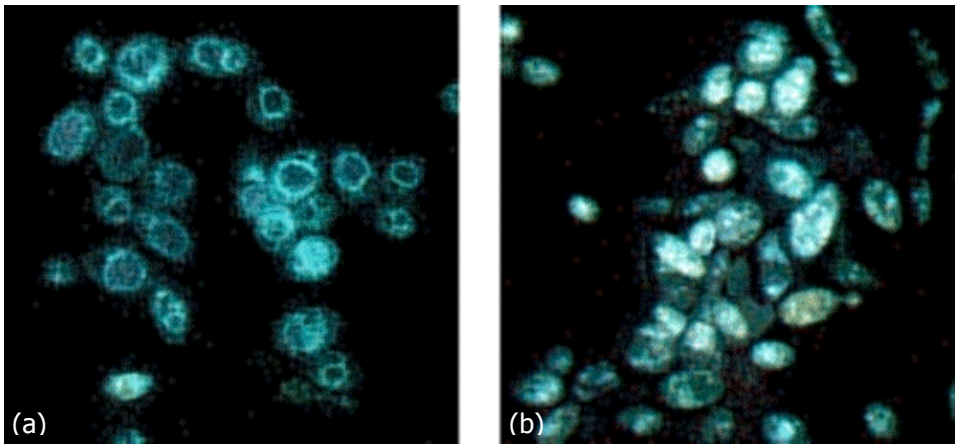

Figure 7 Control (a) and sonicated samples (b) of yeast cells dyed with MDY-64 for the assessment of vacuole membrane integrity. In the control the vacuoles can be identified (darker circles), the surrounding "halo" indicates the cell itself. After sonication the vacuole can not be identified as a discrete structure and dye fills the whole cells. Further stress led to a complete lack of fluorescence indicating loss of dye uptake.

The cells were collected from the resonator chamber after each treatment, centrifuged for 10 minutes at 9000 rpm with a microfuge (Denver Instruments) and re-suspended in 1 mL Hepes pH 7.5 (Sigma) up to approximately $5{\cdot}10^7$ cells/mL. The vacuole membrane was stained using Yeast Vacuole Membrane Marker MDY-64, parcelled from Molecular Probes[53]. 1 μL of 10 mM MDY-64 was added to the cell

suspension and after 3 minutes the cells were centrifuged and the pellet was re-suspended in 1 mL Hepes pH 7.5.

Using a conventional haemacytometer the samples were evaluated under the microscope. Only cells with a visible isolated vacuole were counted to be undamaged. Cells that were fluorescing indifferently and cells that did not show any fluorescence were accounted to be damaged (Figure 7). The result was given as percentage of undamaged cells like the viability in equation **(44)**.

M3.7 Study of cell viability, integrity, ability to reproduce and morphology

Each experiment was conducted with an individually grown (see M2.1) population for treated samples and controls.

Cells were retrieved from the shaker table and spun down after which the growth medium was removed and the cells were re-suspended in distilled water at a concentration around $5 \cdot 10^6$ cells/mL.

For each time-point (15, 30 and 60 minutes) the separation system in batch set-up (see page 40, Figure 9, left hand side) and a similar chamber were filled, but a sound field (2.2 MHz, true electrical power input 24 W) was applied only in the separation system. During irradiation both chambers were thermally connected through the cooling circle, i.e. the output of the cooling circle of the sonicated system was connected to the input of the cooling circle of the sham-treated system to provide both active volumes with the same temperature development. As part of the cells sediment at the bottom of the active volume where no sound field exists the field was switched off every 15 minutes and the suspension was mixed for 30 seconds. The experiments were carried out in triplets, in the study with cells instationary phase the number of experiments was four.

Subsequently the viability of the samples was measured with the methylene blue technique, cell integrity/leakage was assessed with optical density at 280 nm, the number of cells able to replicate on a malt extract agar plate was counted and the vacuole integrity of the cells was examined.

M4 Polymerisation techniques

M4.1 Polyacrylamide

Cells were suspended in a gel mixture containing 30 mL Acrylamide (ProtoGel, National Diagnostic), consisting of 30%($^{w}/_{v}$) Acrylamide; 0.8%($^{w}/_{v}$) Bis-acrylamide), 22.4 mL Tris-HCl buffer at pH 6.8 (Sigma), 16.8 mL H_2O and 0.6 mL Sodium Dodecyl Sulphate 12%($^{w}/_{v}$) (BDH Ltd), achieving a final cell concentration of approximately $6 \cdot 10^7$ cells/mL. The polymerisation process was initiated immediately after the cells reached their final locations within the bands (pressure nodal planes of the sound field), by adding 150 μL of Ammonium Persulfate 10% (Sigma) and 150 μL of TEMET (N,N,N,N-tetramethylethylen-diamine, Sigma). The complete polymerisation of the mixture inside the chamber took up to 1 min at a temperature that was maintained at 35°C by a cooling system.

M4.2 Agar

5%($^{w}/_{v}$) malt extract agar was prepared sterile. Freshly grown yeast cells were re-suspended after the agar had cooled to below 40°C. Freshly grown yeast cells were then suspended and the suspension put into the separation system in batch set-up. Gelation was brought about by further cooling while the ultrasonic field was applied.

M5 Evaluation of the acoustic field within a resonator

M5.1 Basic concept

The one-dimensional model introduced previously[50] can be used to calculate the acousto-electric environment, i.e. the acoustic and electric field quantities of the multilayer resonator used for the separation system. However, to do so one must feed the various material parameters of the resonator's layers into the model. Usually some parameters are given by the manufacturers of the parts of the resonator, e.g. the piezoelectric ceramic, others are not easily to find out or even unknown, like the effective acoustic quality factors of suspensions.

The solution to this is to use the connection in equation **(38)** between the acoustic field within the resonator and the electrical properties accessible at the transducer's electrodes. A highly accurate measurement system yielding appropriate information is available at the Institute of General Physics in Vienna[54]. The measurement system basically consists of a frequency source and a vector voltmeter delivering the real and imaginary parts, the conductance and the susceptance respectively, of the complex admittance in the vicinity of resonance peaks very accurately. The quality factor Q of a resonance can be approximated by

$$Q \cong \frac{f_s}{f_+ - f_-} \quad , \qquad \textbf{(45)}$$

where f_s is the series resonance frequency, i.e. the frequency of the maximum conductance, and f_-, f_+ denote the frequencies of minimum and maximum susceptance respectively.

To assess a resonator two basic steps are performed alternating: first the admittance spectrum over the interesting frequency range is measured and subsequently the model is used to fit this measurement with respect to the resonance frequencies and their quality factors.

The starting point is empty resonator where the admittance spectrum is influenced mainly by the transducer. At the next stage the resonator is filled with a liquid of well known properties, usually pure, distilled water. The following, second fit includes the

influence of the liquid layer and the reflector, material parameters determined before with the empty resonator should not be changed anymore. Finally a liquid or suspension of unknown acoustic properties can be examined: the adjusted parameters of the model when fitting a further measurement of the resonator filled with the liquid in question yield the effective acoustic quality factor and the speed of sound.

M5.2 Determination of the effective acoustic quality factor Q_{eff} of a yeast suspension

As a theoretical derivation or estimation was not practicable[6] the dependency of the effective acoustic quality factor of a yeast suspension on the amount of suspended bio-mass was measured. To reduce the influence of resonator layers other than the liquid layer, a frequency range not including the resonance peaks of the transducer was chosen. In this range the quality factor of the resonances is quite independent of the transducer, i.e. the effective acoustic quality factor of the suspension layer needed for the model calculations can be approximated by the resonance quality factor obtained from the admittance measurement[6].

The electrical admittance spectrum of a resonator comprising a rectangular glass cuvette with a PZT ceramic glued to one wall was measured in the interesting frequency range of 1.8 MHz to 2.8 MHz, empty and for a filling of distilled, degassed water. These data were simulated afterwards based on material parameters from literature for the ceramic, glass and water layers, respectively.

Subsequently, fillings of 1 g/L, 52.5 g/L and 110.9 g/L yeast-water suspensions were used as the liquid layer instead of the pure water. The results of the measurements were simulated as above, except the speed of sound and acoustic quality factor of the suspension have now been varied to fit the measurements.

M5.3 In-situ measurement of the admittance spectrum

The high precision admittance measurement system described above works at negligible power levels. For the measurements at true electrical power input settings in the working range of the Ultrasonically Enhanced Separation (UES) system a different device, the Frequency Power Synthesizer FPS 2540 (Sonosep Technologies, Canada) was used. It was controlled by a computer program delivering the drive voltage and current amplitudes and the electric phase angle. This type of

measurement was not used to be fitted because of limited accuracy. However, the comparison between measurements of different settings (electrical power) or fillings (cell concentration in the suspension) was useful to deliver information about phenomenological changes in the UES system.

M6 Transmission electron microscopy

Yeast cells for electron microscopy were prepared by centrifuging each sample at 3500 rpm for 10 minutes and re-suspended overnight in 2% Glutaraldehyde (Sigma) in 0.1 M phosphate buffer pH 7.4 The suspension was centrifuged to yield a pellet. The pellet was then treated with a solution of 2% osmium tetroxide (OsO_4) for 1 hour. The samples were washed in phosphate buffer and de-hydrated twice with 70% EtOH for 15 minutes each time, then twice with 90% EtOH for 15 minutes each time and finally three times in absolute EtOH for 20 minutes each time. Propylene oxide was then added twice for 10 minutes each time and subsequently replaced by a 50% solution of propylene oxide and epon for 1 hour at 30^0C. The samples were embedded overnight in epon at 60^0C. Ultra-thin sections were stained in 6% uranyl acetate for 20 minutes, and 0.4% lead citrate for 10 minutes and then observed using a transmission electron microscope (Jeol 2000) at 80 kV acceleration voltage.

RESULTS

R1 Ultrasonically Enhanced Settling: Effects of process factors on separation efficiency

R1.1 Introduction

One utilisation of particle manipulation by ultrasonic radiation which has been developed during the last decade up to successful application in industrial environments is the Ultrasonically Enhanced Settling (UES)[5,7,20,23,55-57]. The principle here is it to locally increase the particle concentration by a standing ultrasonic field, which results in loose aggregates stabilised by the ultrasound within certain regions. The terminal sedimentation velocity v_t

$$v_t = {d_p}^2 \cdot \frac{g \cdot \left(\rho_p - \rho_l\right)}{18\mu} \quad . \qquad \textbf{(46)}$$

can be derived from Stokes' law of friction[58]. Equation **(46)** shows v_t to be proportional to the diameter of a settling sphere d_p squared, with a coefficient comprising the product of the gravitational constant g and the buoyancy, i.e. the difference of the mass densities of the particles ρ_p and the liquid ρ_l divided by the liquid's viscosity μ. An increase of d_p therefore leads to an increase of v_t. This subsequently delivers an increase of sediment per time. Thus the build up of aggregates by *ultrasound enhances* the *settling*.

Figure 8 shows the stages of the UES technique: in the beginning the particles are freely distributed in the liquid (a). After the ultrasonic field has built up the axial primary radiation force according to equation **(1)** drives them into nodal planes (b), which appear periodically in the direction of sound propagation. It depends on the acoustic contrast given in equation **(3)** between particle and liquid if this force points towards the pressure nodes or towards the displacement nodes for a given suspension, cells however are driven into the pressure nodes. The transverse primary radiation force further concentrates the particles within these planes (c). This force

perpendicular to the sound propagation direction is a result of an uneven amplitude distribution over the transducer's surface[59]. In case of multi-wavelength resonators as used throughout this work this leads to columns of aggregated particles in the direction of the sound propagation (d). Finally these aggregates settle at the bottom of the vessel (e) due to their increased effective density as described.

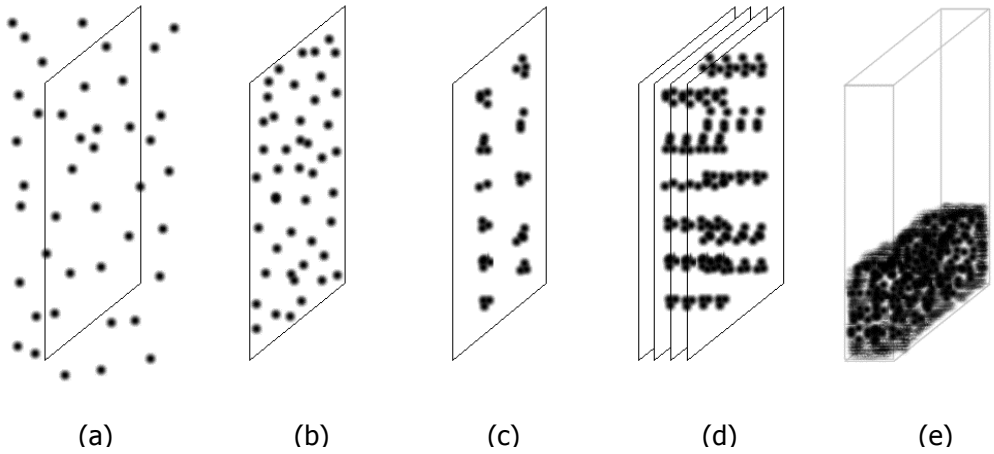

Figure 8 Stages of Ultrasonically Enhanced Settling; homogeneously dispersed particles (a) get accumulated in planes (b) and further concentrated within the planes (c) by the ultrasound, columns are formed in multi-wavelength resonators (d). The aggregates finally settle at the bottom of the vessel (e).

Figure 9 shows the industrial UES system (USSD-05, Anton Paar GmbH, Graz, Austria) used for the following experiments in a batch set-up (left-hand side) and in flow-through mode (right-hand side) on the top of a reservoir holding the suspension, e.g. a bio-reactor. In both cases the ultrasound is emitted by the transducer (Trd) at the left in horizontal direction to the reflector (Ref). Between the transducer and the reflector a cooling volume (C) and the active volume (AV) filled with the suspension are located. The cooling water circulation avoids the transducer to heat the suspension in the active volume.

In case of the flow-through set-up (Figure 9, right-hand side) as used for perfusion filters the clarified liquid is harvested at the top **(out)**. The suspension is pumped into the system from the side at the bottom **(in)** and together with the bottom outlet **(back)** this builds up a re-circulation loop by which the settled particles are immediately fed back into the reservoir. For obvious reasons the sound propagation direction in UES

systems is oriented horizontally as the consequently vertical nodal planes allow an upward streaming of the clarified liquid between the settling aggregates.

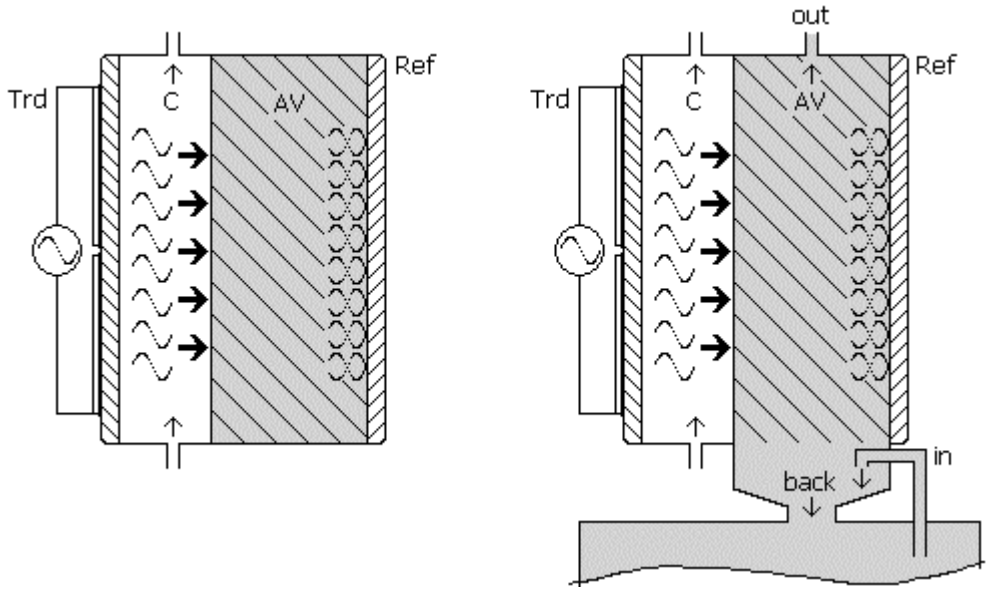

Figure 9 Separation system in batch mode (left) and in flow-through set-up (right) on top of a reservoir, e.g. a bio-reactor. The ultrasound is emitted from the transducer (Trd), passing a cooling volume (C) and the active volume (AV) holding the suspension and finally reflected at a reflector (Ref).

The experiments described in the following were designed to study the UES for the case of yeast/saline suspensions in respect to the influence of process parameters on the separation efficiency, i.e. the ability of the filter to remove particles/cells. Measurements were aiming on the examination of the separation efficiency development after the ultrasound was switched on. The interest was to identify possible potentials but as well limits that the technique has in the regime of yeast technology.

Chapter R1.2 is concerned with measurements of the separation efficiency of UES on varying process parameters[60]. Results for different bio-mass loads and electrical power inputs will be compared for the separation systems in flow-through and batch mode. Additionally for the former the throughput has been varied over the whole working range of the system.

In chapter R1.3 it has been looked at the influence of the amount of suspended cells, the bio-mass load, in connection with the true electrical power input on the ultrasonic field in a more theoretical way. The measured quantity was the acoustic

quality factor of the resonator which carries information about how strongly an ultrasound wave is damped when excited into a yeast/water suspension. This was used to calculate the energy density within the active volume thus delivering information about the influence of cell concentration and power input on the magnitude of the primary radiation force.

It was shown previously that the ultrasonic principle is capable of selectively retaining viable cells more effectively than non-viable[61], i.e. the cell population passing the filter is not of the same viability as the culture in the reservoir or fermentor. This depends on the acoustic properties of the dead versus the living cells. If results like this can be achieved with yeast cells was tested in chapter R1.4.

An empirical model, describing the development, i.e. the decrease, of the cell concentration at the outlet immediately after the ultrasonic field is switched on, will be presented in chapter R1.5.

R1.2 Influence of biomass, throughput and true electrical power input on the separation efficiency

The results of measurements in this chapter will be given as cell concentration *C*, i.e. the actual number of cells per millilitre and/or as separation efficiency (*S.E.*)

$$S.E. = \left(1 - \frac{C_{out}}{C_{in}}\right) \cdot 100\ \% \quad . \qquad \textbf{(47)}$$

The separation efficiency refers to the ability of the respective system or set-up to reduce the concentration of cells of a given suspension. The concentration C_{out} of the sample after treatment, e.g. taken from a given outlet is compared to the concentration C_{in} of the original suspension. The resulting percentage ranges from 0% - meaning no cells were retained - to 100% - all cells have been removed from the liquid. Thus *high* values of *S.E.* indicate a well performing filter, while at the outlet in this case a *low* cell concentration [cells/mL] is measured.

To ensure that all settling effects were induced by the ultrasonic field a non-flocculating type of yeast (Class 1 after Gilliland[62, i]), bakery yeast suspended in

[i] Class 1, the lowest class, indicates yeast that does not flocculate at all, cells do not stick together but are completely dispersed in the medium all the time.

physiological saline was used. This assumption is consistent with sedimentation data for non-flocculating types measured by Brohan[28], where above 90 % of the biomass were reported to have stayed in suspension after 10 minutes.

Three process parameters were varied to assess their effect on the separation efficiency (Figure 10). The cell concentration or bio-mass level and the true electrical power input (t.e.p.i.) of the driving electronics have been set to 0.5 g/L, 5 g/L and 50 g/L and 8 W, 16 W and 24 W respectively. Each of the bio-mass/t.e.p.i. combinations 0.5/8, 5/8, 5/16, 5/24 and 50/24 were carried out at throughputs of 5.6 Litre/day, 20 L/d and 46.2 L/d over the whole working-range of the system of 5 - 50 L/d[56]. Experiments were carried out in duplets.

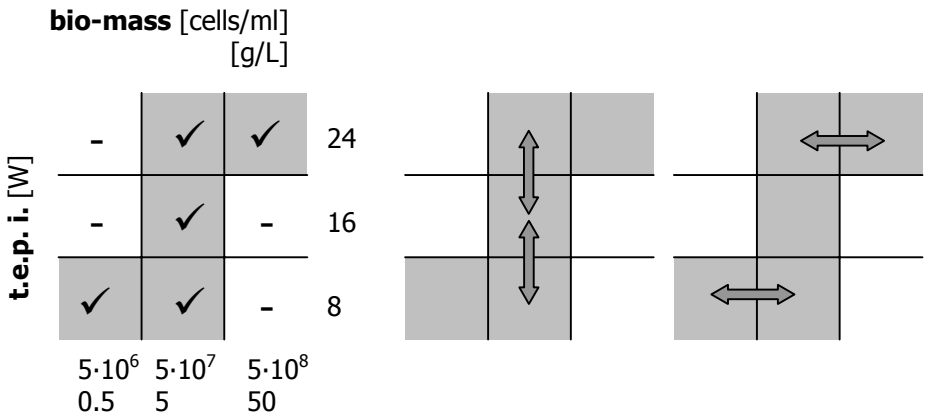

Figure 10 Matrix of performed separation efficiency measurements (left) at varying true electrical power input (t.e.p.i.) and bio-mass level. The following figures will have similar indicators to inform the reader which measurements have been compared according to the arrows in the middle and right hand side figure to asses the influence of t.e.p.i. and bio-mass respectively.

Flow-through set-up

Prior to each run a sample of one millilitre (mL) was taken out of the reservoir bottle. This sample was used to normalise the data, i.e. to reflect 0% separation efficiency, its cell concentration was used as C_{in} in equation **(47)**.

The medium was then fed into the separation system in flow-through set-up (Figure 9, right-hand side) through the inlet at the given throughput. Without stopping the harvest pump, another sample was taken at the outlet when the system was completely filled. Although no acoustic retention of UES system was expected possible settle effects by the influence of gravitation were assessed at this stage. The

measured cell concentration was used as C_{out} in equation **(47)**, the result will be referred to as $S.E._{susp}$ in the following figures.

Immediately afterwards the ultrasound was switched on and further eight samples were taken at the outlet after every nine millilitres or in other words the cell concentrations of the 10th, 20th, ..., 80th millilitre of filtered liquid were examined. The measured values were again used as C_{out} in equation **(47)** resulting in the respective *S.E.* All cell concentrations measurements were performed with a haemacytometer (see M3.1 *Image analysis assisted method*).

The influence of throughput is shown in Figure 11 and Figure 12 for the different bio-mass levels. Figure 11a shows the separation efficiency for 16 W and 5 g/L yeast cells at throughputs of 5.6 L/d, 20 L/d and 46.2 L/d. The values on the x-axis denote the volume that had left the system by the outlet before the respective sample was taken. In all cases a rapid increase of separation efficiency started immediately after the ultrasound had been switched on, though ending at different *S.E.* for different throughputs. The final concentration was reached approximately after 30 mL for 5.6 L/d and after about 50 mL for 20 L/d. If the development was finished for 46.2 L/d at 70 mL was insignificant, however suggested by the data. The highest throughput of 46.2 L/d clearly showed more instability as reflected by the higher standard deviation as of equation **(41)**.

Values of $S.E._{susp}$ as well showed a high standard deviation. No significant differences for different throughputs were detected throughout all of these experiments. Such would have reflected settling effects by natural sedimentation in the separation system, i.e. prior to the influence of the ultrasound.

Figure 11b shows the same set of data for 16 W and 5 g/L biomass load again, but here the elapsed time is the scale of the x-axis[i]. The *chronological* order to reach the maximum separation efficiency was turned around for the different throughputs in respect to the order in Figure 11a. It took 7.7, 3.6 and 2.2 minutes for low, medium and high throughput respectively to reach the final concentration (with the mentioned restriction for 46.2 L/d).

[i] It takes some 21 minutes for 80 ml to be pumped through the system at a rate of 5.6 L/d, therefore the x-axis was cut off at 10 minutes to gain more resolution in the beginning.

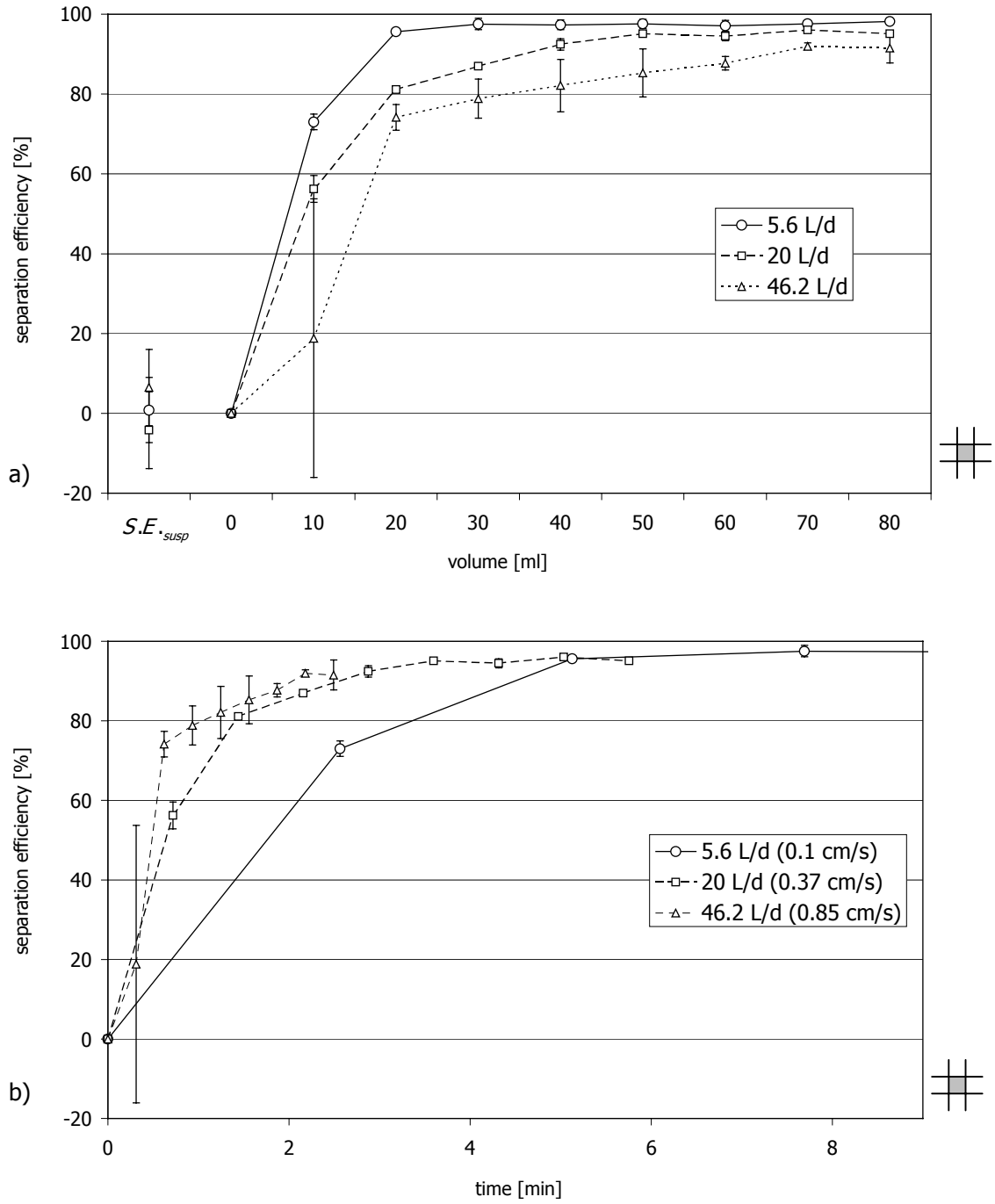

Figure 11 Development of the separation efficiency against volume (a) and vs. time (b) at throughputs 5.6 L/d, 20 L/d and 46.2 L/d. Process parameters true electrical power input and bio-mass level were 16 W and 5 g/L, respectively.

A scale representing the throughputs in another way shall be mentioned: 5.6, 20 L/d and 46.2 L/d translate[i] into 0.1, 0.37 and 0.85 cm/s up-flow speed as shown in the legend of Figure 11b.

For 8 W true electrical power input and a suspension carrying 0.5 g/L yeast cells, results were rather unstable as Figure 12 shows. A very slow increase of *S.E.* after the sound was switched on indicated that the system was used at the limit of its operating range. However some retention yielding a separation efficiency of some 50% was detected for a throughput of 5.6 L/d and due to the acceleration of up-flow stream just 40 % were reached not before 60 mL had left the system for 20 L/d. At 46.2 L/d it was doubtful if any retention took place from the beginning, no significant development could be detected.

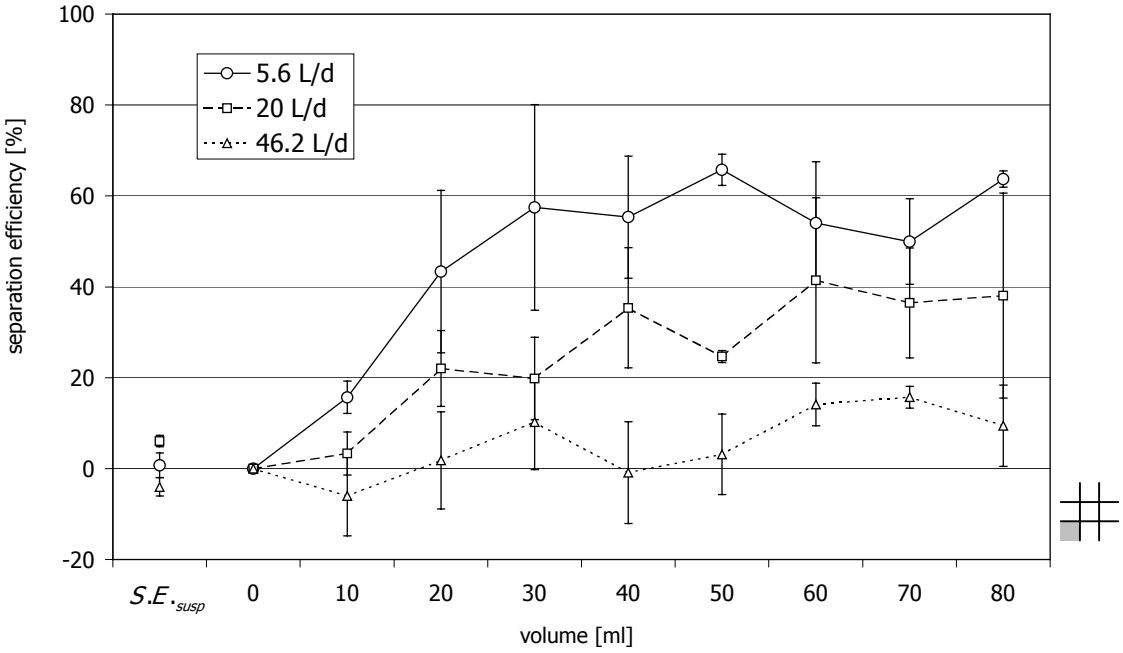

Figure 12 Development of the separation efficiency over volume at throughputs 5.6 L/d, 20 L/d and 46.2 L/d. Process parameters true electrical power input and biomass level were 8 W and 0.5 g/L, respectively.

The highest separation efficiency of all experiments, 99.59 ±s.d. 0.05% was found at 24 W and 50 g/L (see Figure 13) at the end of the low throughput run (5.6 L/d). For this set of process parameters percentages increased rather sharply after the sound was switched on, reaching the region of highest separation efficiency at 30 mL, 40 mL and

[i] According to the cross-section of the system (25 x 25 mm²).

50 mL for 5.6 L/d, 20 L/d and 46.2 L/d throughput respectively. For the high throughput experiment a significant decrease of retained cells was detected at 60 mL and above. This was presumably a result of some aggregates falling down inside the chamber. As these cells partly re-suspend a higher concentration was measured at the outlet as a consequence. Low standard deviations reflected a stable behaviour for low and medium throughput.

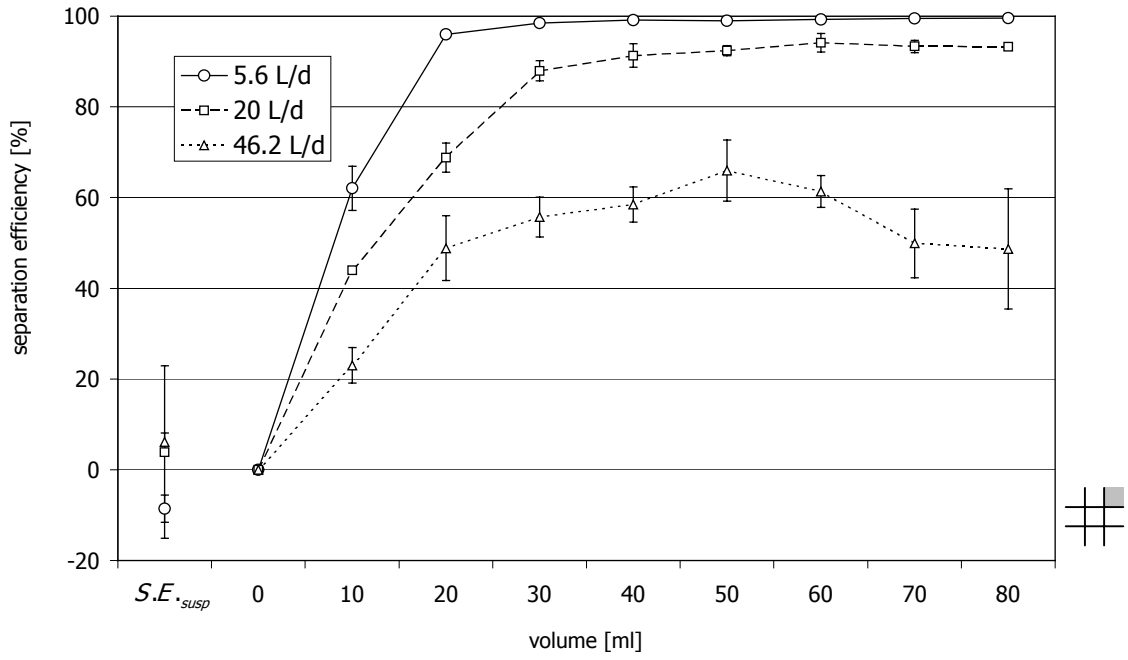

Figure 13 Development of the separation efficiency over volume at throughputs 5.6 L/d, 20 L/d and 46.2 L/d. Process parameters true electrical power input and bio-mass level were 24 W and 50 g/L, respectively.

Results in Figure 14 reflect the influence of the variation of the true electrical power input at low (Figure 14a) and high throughput (Figure 14b). The bio-mass load was 5 g/L.

The use of 16 W showed a steeper slope and a higher final separation efficiency than that of 8 W for 5.6 L/d (Figure 14a), a further increase was not achieved when 24 W were applied, The *S.E.* for 16 W and 24 W were very similar. However as mentioned, this holds only true when the *S.E.* development in respect to the volume pumped through the system was considered, over a time axis as in Figure 11b the final percentage was reached earlier at 24 W.

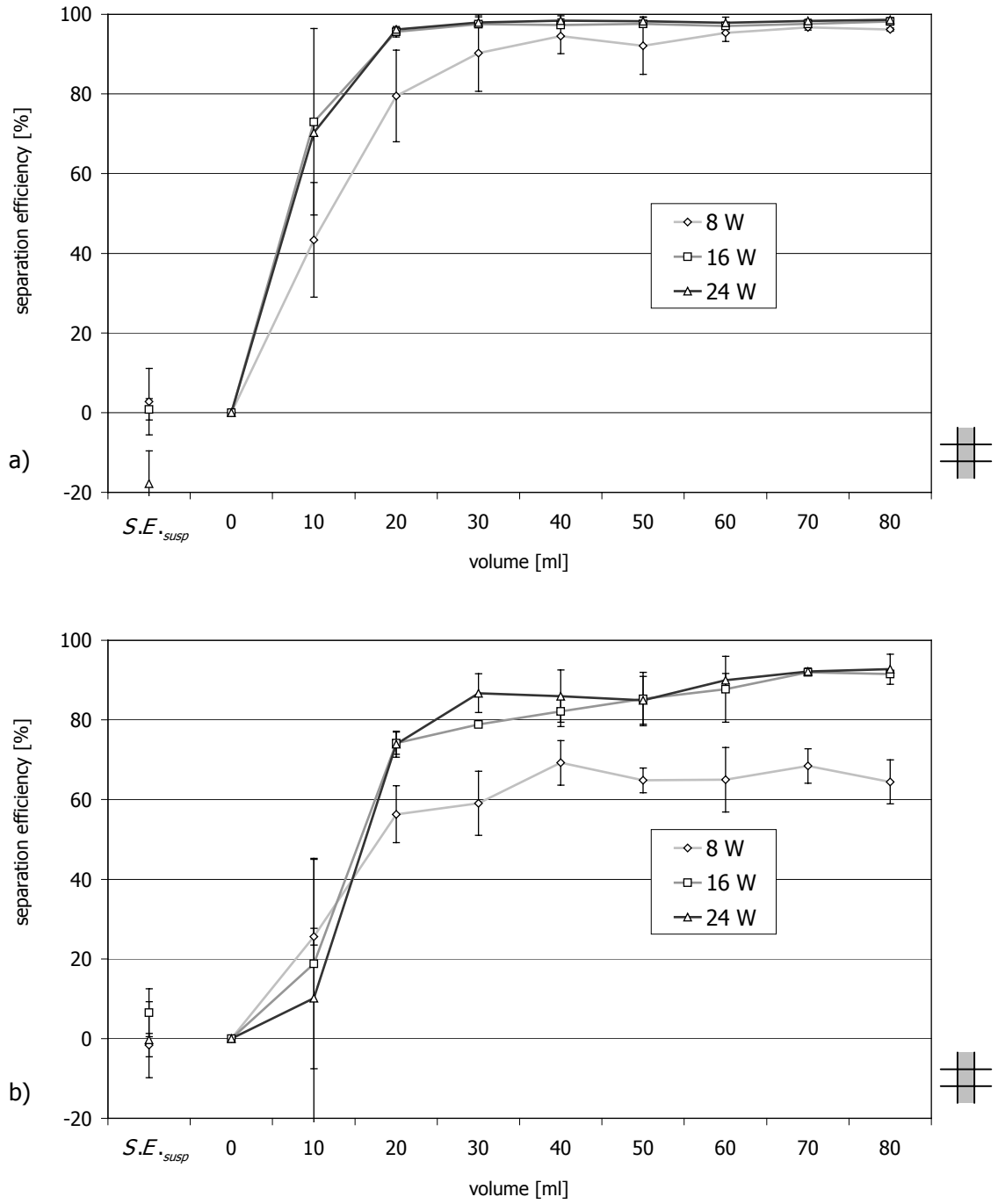

Figure 14 Comparison of the influence of the true electrical power input on the separation efficiency. Settings were 8, 16 and 24 W respectively. The bio-mass level was 5 g/L and throughputs were 5.6 L/d (a) and 46.2 L/d (b). (Data for 16 W repeated from Figure 11a.)

At high throughput of 46.2 L/d the increase of separation efficiency was slower in the beginning (Figure 14b). This led to the crossing of the lines for 8 W, 16 W and 24 W after 15 mL. However the high standard deviation for the 10 mL measurement

prevented this to be a significant result. Throughout all three of those measurements some degree of instability was found, leaving no difference between the final separation efficiencies for 16 W and 24 W.

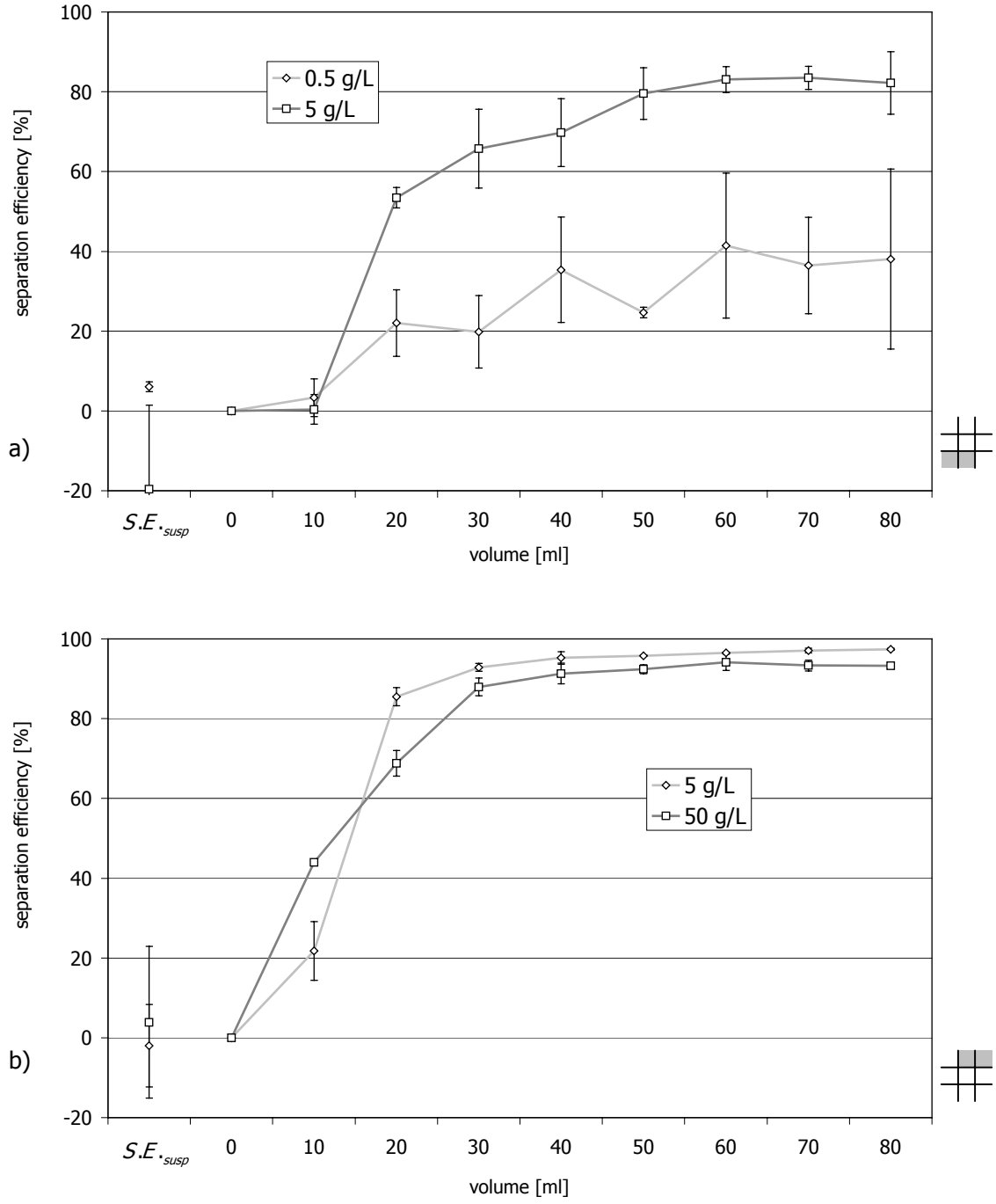

Figure 15 Comparison of the influence of the cell concentration on the separation efficiency. Biomass loads 0.5 g/L and 5 g/L were compared at 8 W t.e.p.i. (a), for 5 g/L and 50 g/L 24 W were used (b). The throughput was 20 L/d. (Data for 0.5 g/L repeated from Figure 12 and for 50 g/L from Figure 13.)

The influences of different bio-mass levels were compared in Figure 15. The use of 0.5 g/L and 5 g/L of yeast in Figure 15a for 8 W true electrical power input and 20 L/d throughput delivered a *S.E.* for the lower solid fraction of below 50 %. Therefore an influence of the suspension's initial cell concentration could be detected in spite of high standard deviations as indicated by the error bars. At the higher bio-mass loads an increase of the *S.E.* was detected after some 20 mL of liquid had left the system.

Figure 15b shows the result for medium and high bio-mass at 24 W true electrical power input and 20 L/d throughput. The lower concentration of cells led to a higher separation efficiency, although the comparison with a bio-mass of 50 g/L revealed a slower development in the beginning of the run.

The maximal *S.E.* detected within all fifteen previously presented measurements are summarised in Table 1. It has to be emphasised that those *S.E.* values refer to the means of the lowest cell concentrations reached during single runs for one set of process parameters, regardless if they were reached after the same amount of liquid had left the system. Therefore these values were not necessarily equal to the highest values of *S.E.* shown in the graphs.

A significant trend of lower *S.E.* caused by increasing throughput for a given set of the process parameters true electrical power and bio-mass was found. The first line of Table 1 shows that 8 W t.e.p.i. resulted in significantly low separation efficiencies for medium and high throughputs for 0.5 g/L biomass.

The picture is similar when 5 g/L were used. However the influence of increased throughput was smaller, i.e. the difference between results measured at the same t.e.p.i. in one row of Table 1 was lower for a higher t.e.p.i. setting. The maximal *S.E.* showed a trend of increased values on higher t.e.p.i. which was not visible due to the standard errors in the graphs (compare Figure 14).

An effect of the higher cell concentration of 50 g/L leading to higher maximal *S.E.* was visible just for 5.6 L/d. At higher throughput of 20 L/d the result for 5 g/L was significantly better. In case of 46.2 L/d throughput at high biomass a remarkable low value around 66 % was found.

The cell concentrations measured at the filter outlet are summarised in Table 2. Here the development within a row of corresponding values showed an increase of cells on increasing throughput. In the case of 24 W applied to a suspension carrying 50 g/L the results were orders of magnitude apart, thus the system was partly beyond

its working range. Equally as well, a tendency of higher true electrical power input retaining more cells was found.

Table 1 Maximum values of the separation efficiency in the flow-through set-up for varying process parameters throughput, bio-mass and true electrical power input. Numbers represent the efficiency maximum in different repetitions, i.e. samples were not necessarily pulled at the same volume.

Separation efficiency maximum, filter set-up [%][a]

bio-mass [g/L]	t.e.p.i. [W][b]	[c]	throughput [L/d]		
			5.6	20	46.2
0.5	8		69.2 $\pm_{s.d.}$ 6.0	41.4 $\pm_{s.d.}$ 18.0	17.5 $\pm_{s.d.}$ 0.1
5	8		97.0 $\pm_{s.d.}$ 0.8	84.6 $\pm_{s.d.}$ 4.4	72.3 $\pm_{s.d.}$ 1.2
	16		98.2 $\pm_{s.d.}$ 0.5	96.0 $\pm_{s.d.}$ 0.2	92.8 $\pm_{s.d.}$ 2.0
	24		98.9 $\pm_{s.d.}$ 0.1	97.5 $\pm_{s.d.}$ 0.1	94.1 $\pm_{s.d.}$ 2.5
50	24		99.6 $\pm_{s.d.}$ 0.1	94.4 $\pm_{s.d.}$ 1.7	66.0 $\pm_{s.d.}$ 6.7

[a] in comparison to original concentration as of **(47)**
[b] true electrical power input
[c] see Figure 10

Comparable sets of the process parameters throughput and t.e.p.i. revealed for different bio-mass levels that the number of cells per millilitre was smaller for 5 g/L than for 50 g/L and as well for 0.5 g/L than for 5 g/L with the exception of 5.6 L/d.

The maximal *S.E.* in Table 1 showed lower standard deviations of not more than 10% - except one where the system was beyond working range - than the cell concentrations in Table 2. As well the selection of the *S.E.* maximum of a set of runs, i.e. without taking into consideration when it was measured within the run, delivered considerable less instability when compared to the error bars in the graphs especially for high throughputs.

Table 2 Lowest values of the cell concentration at the outlet of the flow-through set-up for varying process parameters throughput, bio-mass and true electrical power input. Numbers represent the efficiency maximum in different repetitions, i.e. samples were not necessarily taken at corresponding volumes.

Concentration minimum [10^6 cells/mL], filter set-up

bio-mass [g/L]	t.e.p.i. [W][a]	[b]	throughput [L/d]		
			5.6	20	46.2
0.5	8		1.61 $\pm_{s.d.}$ 0.31	3.04 $\pm_{s.d.}$ 1.18	4.18 $\pm_{s.d.}$ 0.29
5	8		1.46 $\pm_{s.d.}$ 0.40	6.94 $\pm_{s.d.}$ 1.09	15.1 $\pm_{s.d.}$ 0.42
	16		0.84 $\pm_{s.d.}$ 0.19	1.84 $\pm_{s.d.}$ 0.19	3.69 $\pm_{s.d.}$ 0.80
	24		0.49 $\pm_{s.d.}$ 0.06	1.20 $\pm_{s.d.}$ 0.11	2.75 $\pm_{s.d.}$ 0.88
50	24		1.89 $\pm_{s.d.}$ 0.33	25.3 $\pm_{s.d.}$ 1.94	170 $\pm_{s.d.}$ 23.0

[a] true electrical power input
[b] see Figure 10

Batch set-up

The separation system was used in the batch set-up (Figure 9, left-hand side), filled with suspensions of the same three concentrations as for the flow-through set-up and as well the same values of t.e.p.i. were applied. After ten minutes of sonication the concentration of cells within the active volume was measured using a haemacytometer (see M3.2). Sonication duty cycling of 45 seconds "on" and 18 seconds "off" was employed to have the aggregates settle at the bottom of the active volume.

The comparison of the separation efficiencies (Table 3) showed the low-concentration/low-power experiment to deliver a significantly low value of 67%, while all other experiments indicate percentages of above, some far above 90%.

The absolute numbers of cells per volume remaining in suspension revealed a different behaviour. As well some trend in relation to the original bio-mass level and the applied true electrical power input was measured, however a significant difference of the means could only be found for the high-concentration/high-power experiment ($t_2 > 4.8$, $P < 0.04$).

Table 3 Separation efficiency of the UES technique in the batch set-up at varying process parameters (bio-mass level, true electrical power input) after sonication for 10 minutes. A duty-cycle of 45 s sound on and 18 s sound off was used.

Separation efficiency [%][a] and cell concentration [10^6 cells/mL] measured in the active volume of the batch set-up.

bio-mass [g/L]	t.e.p.i. [W][b]	[c]	S.E.	cell concentration
0.5	8		67.0 $\pm_{s.d.}$ 1.0	1.76 $\pm_{s.d.}$ 0.69
5	8		93.4 $\pm_{s.d.}$ 1.6	2.20 $\pm_{s.d.}$ 0.55
	16		95.8 $\pm_{s.d.}$ 1.9	1.99 $\pm_{s.d.}$ 0.92
	24		96.6 $\pm_{s.d.}$ 0.9	1.41 $\pm_{s.d.}$ 0.72
50	24		98.7 $\pm_{s.d.}$ 0.2	5.78 $\pm_{s.d.}$ 0.88

[a] in comparison to original concentration as of **(47)**
[b] true electrical power input
[c] see Figure 10

Discussion

The basic applicability of the ultrasonic separation principle to yeast cells if present as a solid fraction of a suspension was demonstrated. Yeast/water suspensions showed the spatial distribution as predicted[5]. Furthermore it was possible to immobilise the cells, against an up-flowing liquid, to a high extent without influencing their viability. Although the size of yeast (4 – 8 μm) is at the lower end of the systems operating range when applying a frequency of 2.2 MHz, a separation efficiency above 99 % efficiency was possible[20,22].

Recently separation efficiency data measured with a further developed UES system have been published[23]. Although as well yeast/saline suspensions were used the report was aiming on results which could be expected in an industrial environment. For instance duty cycling of the pumps was used instead of the continuously running pump in this work. However very similar trends have been found and the order of magnitude of the measured separation efficiencies was in the same range.

The measurements presented in this chapter delivered a fact which had to be looked at closer. Almost all of the experiments did show a significant increase of the separation efficiency after 10 mL of filtered liquid had left the system by the outlet.

This was surprising as the "dead" volume, i.e. the volume leaving the outlet prior to any influence of the sound field should have been detected, was calculated to be roughly 24 mL (see Figure 16). The likely interpretation was, that the sound field influenced the volume of 14 mL above the edge of the PZT ceramics and therefore just the 10 mL of the tube may be accounted for being the "dead" volume[i]. This might as well be the explanation for the high standard deviations that were measured at the beginning of the runs as at this stage, right after switching on the device, the effect of the ultrasonic field was most sensitive to slight variations.

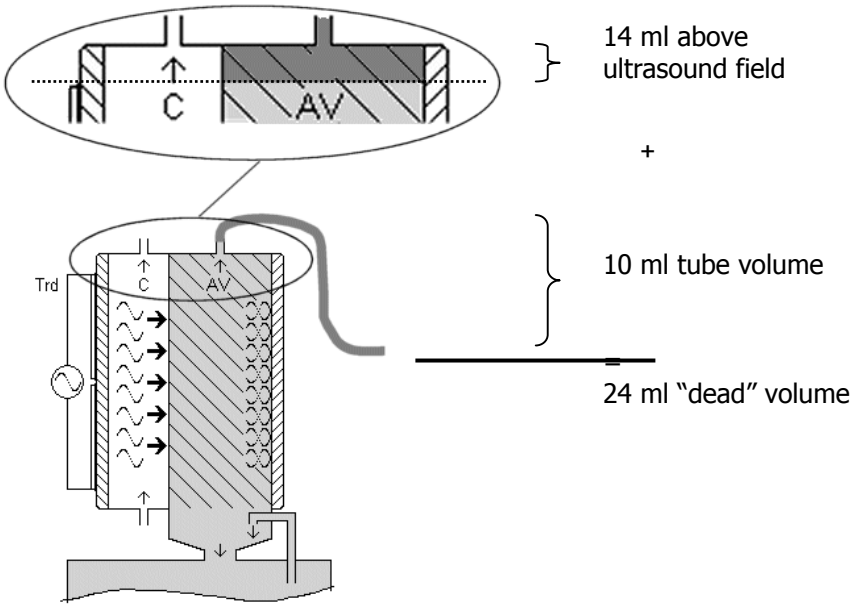

Figure 16 Pulling of samples for assessment of separation efficiency in the beginning of a continuous filtration.

Another point to be explained was the poor separation efficiency (Table 1 first line) at a relatively low bio-mass load of 0.5 g/L. The reason for that was very likely a threshold of cells that have to be present to build up an aggregate large enough to overcome friction and settle efficiently[22,63]. The enhancement achieved by ultrasonic aggregation simply depends on a significant decrease of the surface to volume ratio of the clusters compared to an isolated cell, which was hardly reached at this cell concentration. Therefore, a basic trend was detected in the higher the original solid

[i] This was as well suggested by Schlieren images of the sound field (personal communication M. Gröschl), basically the whole glass-surface of the transducer emitted the ultrasonic wave.

fraction and the true electrical power input were, the more effectively the cells were separated.

This threshold was confirmed by the results in Table 3 of cell concentration measurements within the batch set-up. Although the initial concentrations varied over a range of two orders of magnitude the final values did not differ more than by a factor of three. The explanation is that the amount of cells in the active volume decreases while the aggregates settle until the number of remaining cells is too small to build up aggregates of the needed size.

The increase of cell concentration at the filter outlet for higher bio-mass loads at the same true electrical power input reflects the size distribution of the yeast cells. As the axial primary radiation force as of equation **(1)** is strongly size dependent, there is a higher number of cells too small to be driven into the pressure nodal planes left when the original solid fraction was higher.

The low separation efficiency of 66% (Table 1) for high power/high biomass on the other hand was interpreted as a result of the primary radiation force becoming weaker the farther away from the pressure node the cell is kept. In this case the clusters reached into regions where the draft by the throughput was stronger than the retentive forces of the ultrasonic field, the cells were “washed out”. The system was driven beyond its capacity.

Experiments in the batch and flow through set-up can not directly be compared. The cell concentration within the active volume might not reflect the number of cells leaving the system by the outlet. However a change of order was revealed when the cell concentrations found for the batch experiments in Table 3 were set in relation to flow-through data in Table 2. In all cases the cell concentration measured at the filter outlet during flow-through operation at 5.6 L/d throughput was better than the result from the active volume in batch mode. Hence a certain amount of draft enhances the influence of ultrasound. Furthermore this effect seemed to be more pronounced for higher t.e.p.i. settings, in the case of 16 W and 24 W even the outlet concentration values for 20 L/d were lower than the corresponding results from the batch set-up, however insignificantly.

This influence of the draft might be deduced from two facts: Firstly it was mentioned that for higher bio-mass loads the amount of small cells, on which the radiation forces are weaker, was higher. Secondly the spatial pattern of the transverse

primary radiation force (compare Figure 4 and Figure 8c) is varying in direction of the draft[i]. If a cell now is too small to be moved from its position by the radiation forces, this cell would hold its position in the batch set-up and therefore not settle. In the flow-through set-up however, the vertical drag might transport small cells closer to "hot-spots" with increased transverse radiation force which finally would move them to the location of aggregation.

R1.3 Evaluation of the acoustic field acting within the active volume

It was shown that the separation efficiency was influenced by the biomass load and the true electrical power input. Equations **(5)** show in combination with equations **(4)** the axial primary radiation force to be proportional to the energy density of the ultrasonic field in the active volume. An evaluation of the ultrasonic field with respect to the influence of both parameters was therefore necessary.

The influence of the bio-mass load on the effective acoustic quality factor of a yeast/water suspension on increasing cell concentration was as a pre-requisite for this evaluation as the liquid layer in the active volume is part of the resonator and therefore influencing its overall behaviour. The one-dimensional model of a layered resonator[50] was used subsequently to numerically determine the acoustic field parameters.

The technique of alternating measurement and simulation of the admittance spectrum was performed for a cuvette-resonator (see M5.2). The chosen frequency range is supposed to not include the transducers resonance frequencies as the resonance quality factors then can be assumed to be mainly influenced by the liquid layer. Figure 17 shows the mean of the quality factors of 9 such resonances as measured and simulated. Although the measurements showed some standard deviation, indicated by the error bars, a clear trend of decrease of the mean resonance quality due to an increase of bio-mass level was observed. Additional statistical analysis revealed, that the measurements were significantly different for the two thicker suspensions ($t_1 = 1.95$, $P = 0.035$ for 52.5 g/L and $t_1 = 3.31$, $P = 0.002$ for 110.9 g/L).

[i] The axial primary radiation force does not as the nodal planes are parallel to the drag.

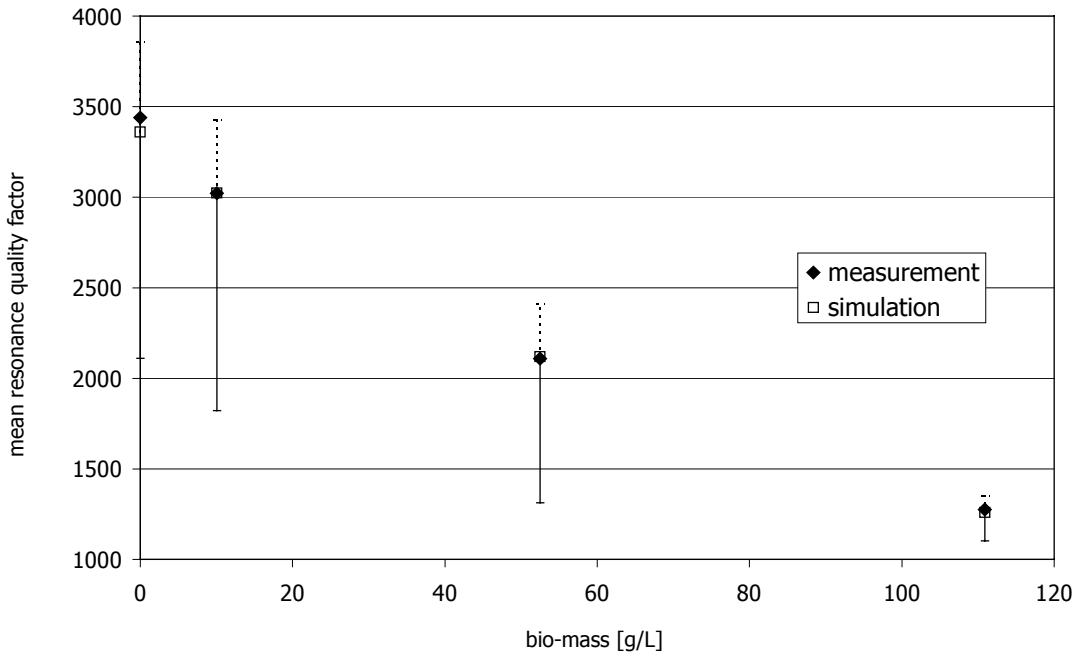

Figure 17 Average of the quality factors of 9 resonances of a glass cuvette-resonator over a range of frequencies not including the transducer's resonances. The resonator was filled with yeast-water suspension of varying bio-mass level.

The averages of the fitted values did for obvious reasons show less standard deviation, however, the agreement with the measurement was very good. The effective acoustic quality factors Q_{eff} for the liquid layer used in the calculations are shown in Table 4. The values are listed together with the effective voltages which have been noted during the experiments described in R1.2.

The presence of 5 g/L bakery yeast did lower the original quality factor of 6000 moderately to 5300, an addition of 50 g/L however led to a considerably decreased value of 3000. Values like this for the acoustic quality factor show the damping to be in the working range of the system[6].

Table 4 Effective voltage used in chapter R1.2 for experiments with suspensions of yeast at different bio-mass levels and effective acoustic quality factors Q_{eff} of the respective suspension used for simulation of the energy density within the active volume (Figure 18).

Effective voltages [V]and effective acoustic quality factors [dimensionless]

bio-mass [g/L]	t.e.p.i. [W][a]	[b]	Voltage	Q_{eff}
0.5	8		20.1 $\pm_{s.d.}$ 1.4	6000
5	8		20.5 $\pm_{s.d.}$ 0.8	5300
	16		29.0 $\pm_{s.d.}$ 1.8	5300
	24		36.7 $\pm_{s.d.}$ 0.8	5300
50	24		40.3 $\pm_{s.d.}$ 2.6	3000

[a] true electrical power input
[b] see Figure 10

The parameters were subsequently fed into the simulation of the layered resonator described in Table 5. From left to right the resonator comprises the transducer, i.e. the PZT ceramic glued to a glass carrier, followed by the cooling and active volumes divided by an acoustic transparent plastic foil. The rightmost layer is a glass reflector terminating the device.

Table 5 Material properties of the layers used for the simulation of the resonator. Additional parameters for the piezoelectric layer were dielectric constant=$9.977 \cdot 10^{-9}$ As/Vm, dielectric loss angel=0.01 and electromechanical coupling factor=0.47.

Material properties for the layers of the resonator used in simulation

Layer	PZT ceramic	glue	carrier (glass)	cooling volume	foil	active volume	reflector (glass)
Thickness [mm]	1.01	0.009	2.690	12.307	0.250	22.240	2.760
Sound speed [m/s]	4460	5600	5700	1580	1485	1520	5600
Mass density [kg/m^3]	7800	1300	2200	998	998	998	2200
Effective acoustic quality factor Q_{eff}	300	35	700	8000	500	see Table 4	700

The resulting energy densities within the different layers of the resonator at the frequency which was used for the experiments (2.194 MHz) in chapter R1.2 are shown in Figure 18. The energy density within the active volume was calculated to be 6.9 J/m³ at a true electrical power input of 8 W. No difference was found for biomass levels of 0.5 and 5 g/L. 16 W t.e.p.i. applied on 5 g/L yeast in water delivered some 13.8 J/m³ into the suspension. The highest power input of 24 W used led to energy densities of 19.7 J/m³ for 50 g/L and 22 J/m for 5 g/L bio-mass load.

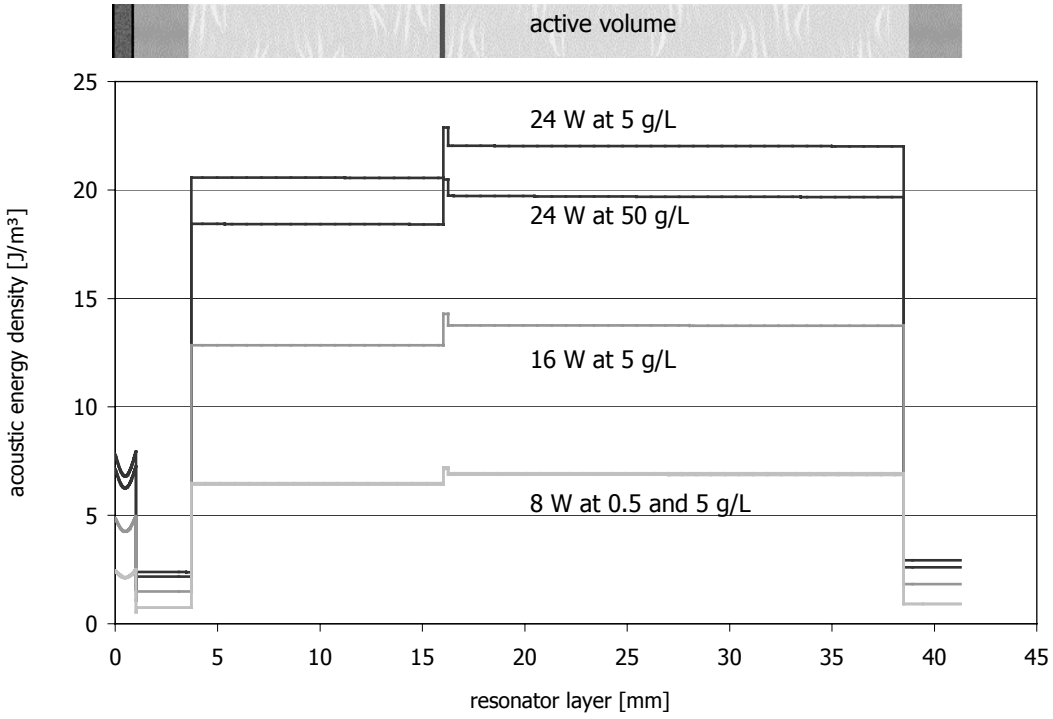

Figure 18 Acoustic energy density in the separation system at different power inputs and bio-mass levels at 2.194 MHz.

Discussion

The energy density is proportional to the true electric power input. This connection was already reflected by the results of the experiments in chapter R1.2. Especially the minimum cell concentrations for both flow-through set-up and batch set-up in Table 2 and Table 3 respectively showed clearly a decrease of cells per volume on an increase of true electrical power input associated with an increase of the acoustic energy density in the suspension layer and thus of the primary radiation force.

According to Figure 18 this means that during the experiments with high bio-mass load, as a consequence of an increasing effective acoustic quality factor of the suspension, the acoustic energy density increased during the run because the cell concentration within the active volume decreased (compare Figure 8e). Figure 19 shows the direct comparison of data measured at 5 g/L and 50 g/L at low throughput of 5.6 L/d. The final *S.E.* was very similar, it was necessary to use log scale for the "reverse" separation efficiency, i.e. the percentage of the cells per millilitre that were found at the outlet to detect the mild difference between the two experiments after 50 mL had left the system.

However the results shown in Figure 15b did not reflect this completely, the *S.E.* was higher for the experiment at 5 g/L than for 50 g/L. This was supposed to be a result of the higher drag force at a throughput of 20 L/d.

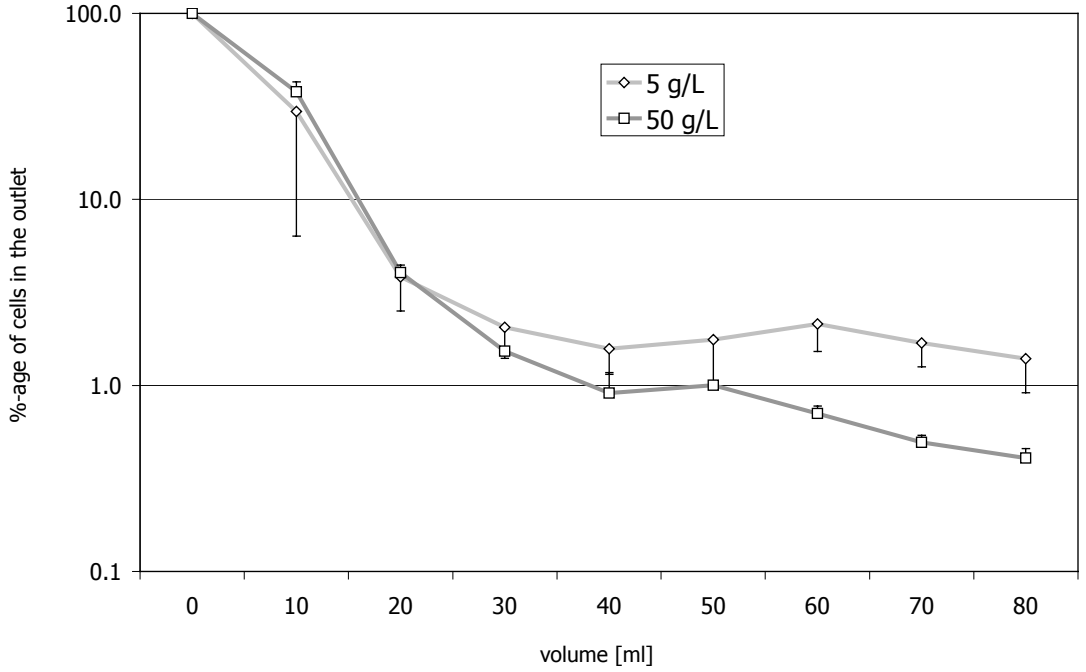

Figure 19 Comparison of 5 g/L and 50 g/L bio-mass load at a throughput of 5.6 L/d and 24 W. Data repeated from Figure 13 and Figure 14a but shown on a logarithmic scale of % cells found in the outlet.

R1.4 Selective retention of viable and non-viable yeast cells

Reports of selectivity of UES in respect to the viability of cells[61] base on the consideration of changes in the acoustic contrast due to the demise of a cell. The following experiment was conducted to clarify if the ultrasonic field would as well retain viable yeast cells more efficiently than non-viable ones.

The separation system in flow-through set-up was used with the inlet closed, as a recycling of the cells by the recycle loop was not desired. Instead the suspension was fed into the back opening (compare Figure 9) to ensure that all cells not kept by the field actually left the system by the top outlet from where the samples were taken.

The resulting percentages of viable cells measured with methylene blue dye (see M3.3) did not deviate from the controls, i.e. the viability of the in-going cells did not differ from the cells that left the system by the outlet. Variations of throughput or bio-mass did not have any effects on the viability of either (Table 6).

Table 6 Methylene blue viability of yeasts after having passed the flow-through set-up directly from back to outlet (Figure 9) for several throughputs and bio-mass levels.

Viability (methylene blue) of yeast in flow-through setup

bio-mass [g/L]	control	throughput [L/d]			
		8.9	18.2	27.4	36.7
0.25	0.96	0.96	0.99	0.98	0.97
1.25	1	1	0.98	0.98	0.96
3.75	0.98	0.98	0.99	0.97	0.97
10	0.99	0.99	0.95	0.98	0.97

Therefore a selective retention of yeast cells corresponding to their viability was not found, non-viable cells obviously do not differ significantly from viable cells in respect to their acoustic material properties.

R1.5 Empirical model of the cell concentration vs. time

The results from chapter R1.2 delivered some information about the influences of the process parameters bio-mass load, throughput and true electrical power input on the base of comparisons in pairs of experiments. However a description beyond that, i.e. a model delivering the separation efficiency in a predictive way based on those process parameters, even to the extent of different particles and suspensions, would be desirable.

A theoretical model based on the picture of two liquids of different mass density and viscosity present in the settler was presented recently[57], the contribution of this work is of more empirical nature.

The graphs shown in Figure 11 to Figure 15 do resemble each other, therefore a mathematical description was attempted. The target was to find an equation which to a high extent describes the separation efficiencies shown earlier. The hope was to conclude the independent parameters of the model out of the process parameters, however this was not accomplished in the end due to an over-parameterisation. Nevertheless an equation was found describing the pattern with high precision and allowing to *calculate* certain properties of the experiments, which delivered additional insights and possibilities of further investigation.

To avoid a loss of information due to normalisation[i] the cell concentration at the outlet versus time instead of separation efficiency versus volume was used here. Furthermore it was found earlier that corresponding samples, i.e. samples taken after the same volume had been pumped through the system, showed higher standard deviations than if properties of a single run were taken into account, e.g. the maximum separation efficiency. Hence the data of single runs weres chosen for this investigation. As a measure for the quality of the fit R^2 as of equation **(42)**, the measure of determination, was used. In equation **(42)**, the cell concentration C at the outlet at time t_i was the measured value, $C(t_i) = y_i$ and therefore calculated data will be given as modelled concentrations $C_{mdl}(t_i) = \hat{y}_i$.

Examination of certain results prohibited the use of a simple biased exponential function $a_0 + a_1 \cdot \exp(-b_1 \cdot t)$. Sets of parameters $\{a_0, a_1, b_1\}$ could not be found to fit the steep decrease of the cell concentration at the outlet in the beginning of the run for all

[i] i.e. division by the initial concentration C_{in} and by the throughput

of the measurements. A solution to this was to add a bell-shaped function $a_2 \cdot \exp\left(-b_2 \cdot (t-c)^2\right)$ yielding

$$C_{mdl}(t) = a_0 + a_1 \cdot e^{-b_1 \cdot t} + a_2 \cdot e^{-b_2 \cdot (t-c)^2} \quad . \tag{48}$$

The three terms of the sum in the non-linear regression equation **(48)** for the modelled concentration C_{mdl} over time t have six independent parameters $\{a_0, a_1, b_1, a_2, b_2, c\}$. The bias a_0 is the cell concentration minimum, $a_1 \cdot \exp(-b_1 \cdot t)$ describes the decrease of the concentration in the beginning of the run. This decrease is additionally influenced by a bell-shaped term represented by $a_2 \cdot \exp\left(-b_2 (t-c)^2\right)$. The parameter c defines the centre of the bell-shape.

Two basic assumptions at time zero reduced the number of free parameters. Firstly the cell concentration $C_{mdl}(0)$ had to be equal to the measured initial cell concentration C_{in}. This led to a formula for a_2:

$$\begin{aligned} &C_{mdl}(0) = C_{in} \quad , \\ &C_{in} = a_0 + a_1 \cdot e^{-b_1 \cdot 0} + a_2 \cdot e^{-b_2 \cdot (0-c)^2} = a_0 + a_1 + a_2 \cdot e^{-b_2 \cdot c^2} \quad , \\ &\rightarrow a_2 = \left(C_{in} - a_0 - a_1\right) \cdot e^{b_2 \cdot c^2} \quad . \end{aligned} \tag{49}$$

The second demand was, as no change of the cell concentration at the outlet was expected before the ultrasound was switched on, that the gradient of $C_{mdl}(t)$ had to be 0 for $t = 0$. This condition led to a dependency of b_1

$$\begin{aligned} &\left.\frac{\partial C_{mdl}}{\partial t}\right|_{t=0} = \dot{C}_{mdl}(0) = 0 \quad , \\ &\dot{C}_{mdl}(t) = -a_1 b_1 \cdot e^{-b_1 \cdot t} - 2a_2 b_2 (t-c) \cdot e^{-b_2 \cdot (t-c)^2} \quad , \\ &\dot{C}_{mdl}(0) = -a_1 b_1 + 2a_2 b_2 c \cdot e^{-b_2 c^2} \quad , \\ &\rightarrow b_1 = \frac{2a_2 b_2 c \cdot e^{-b_2 c^2}}{a_1} \quad . \end{aligned} \tag{50}$$

The use of equations **(49)** and **(50)** in equation **(48)** resulted in the final regression equation

$$C_{mdl}(t) = a_0 + a_1 \cdot e^{-\frac{2b_2 c \cdot (C_{in} - a_0 - a_1)}{a_1} \cdot t} + (C_{in} - a_0 - a_1) \cdot e^{-b_2 \cdot \left((t-c)^2 - c^2\right)} \quad . \qquad \textbf{(51)}$$

Figure 20 shows the exploitation of equation **(51)** for one particular set of data (16 W, 5 g/L, 46.2 L/d). The exponential and the bell-shaped terms are added to the bias a_0 resulting in a fit of high quality $\left(R^2 > 0.96\right)$. It has to be mentioned here, that in cases like this – an increase of cells per millilitre in the beginning of the run - a fitting would not have been possible without the bell-shaped term.

The bell-shaped term was as well suitable for intermediate increases of the concentration like the behaviour between 0.9 and 1.9 minutes in Figure 20. Additional bell-shaped terms (black dashed line) described these very well yielding a significant rise of the quality of the fit $\left(R^2 > 0.999\right)$.

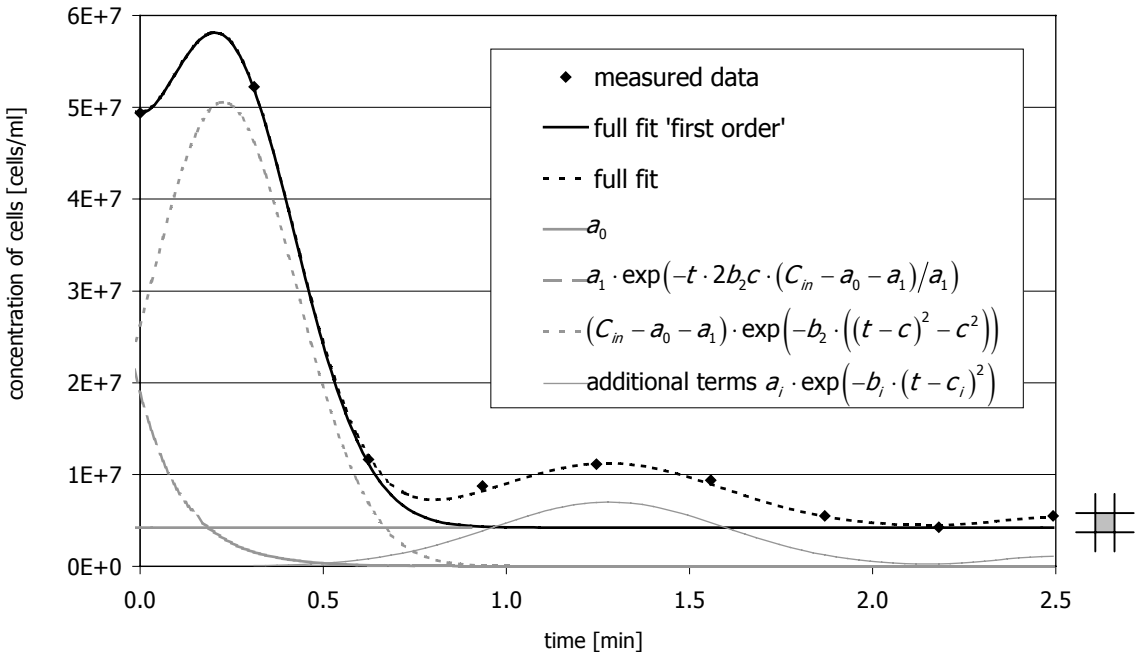

Figure 20 Model of the development of the cell concentration at the outlet over time as of equation (51). A simple biased exponential did not completely describe the data, so the bell-shape was added. For this particular run (16 W, 5 g/L and 46.2 L/d) another bell-shape was added to fit the slight increase starting just before 1 minute.

Although the regression equation **(51)** reflected the behaviour very well the results were not unique. Figure 21 shows three different fits A, B, C for one measurement

(24 W, 5 g/L, 5.6 L/d). The three fits were of comparable high quality $\left(R^2 > 0.999\right)$, however this meant that three different sets of parameters $\{a_0, a_1, b_2, c\}$ were found which could be used to describe the same data. This over-parameterisation prevented the identification of direct relations between the fitting parameters and the process parameters that had been varied during this study. Furthermore this prevented the use of an automatic algorithm based on statistical means optimising R^2, the fitting had to be done by hand.

The values of the parameters $\{a_0, a_1, b_2, c\}$ found for the various results of the experiments are listed in Table 7, Table 8 and Table 9 for throughputs 5.6 L/d, 20 L/d and 46.2 L/d respectively. Only curve fittings with $R^2 > 0.95$ have been accepted. This was not possible for measurements with 0.5 g/L bio-mass and the high-concentration/high-throughput measurement. The parameter $R_{oth}{}^2$ reflected the quality of the fit when additional bell-shaped terms were used to "catch" fluctuations after the main decrease. It was always above 0.99 and mostly greater than 0.999.

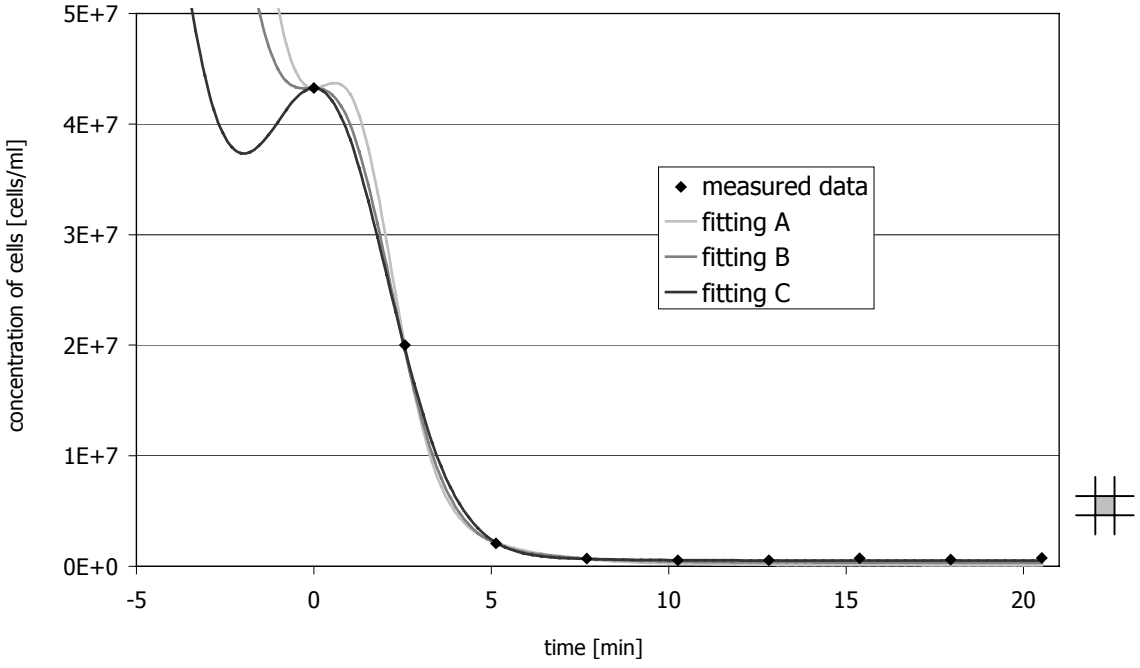

Figure 21 Over-parameterisation; the model allows fittings of the same set of measured data with different sets of parameters. Process parameters of the particular run modelled were 24 W, 5 g/L and 5.6 L/d.

The information reflected by these fitting parameters was subsequently analysed. Using them in the regression equation **(51)** the time t_s of the steepest decrease of the

curve and the times $t_{90\%}$ and $t_{99\%}$ when 90% and 99%, respectively, of the final concentration a_0 was reached were calculated. In a mathematical way this is expressed as

$$\ddot{C}_{mdl}\left(t_s\right)=0 \quad ,$$

$$C_{mdl}\left(t_{90\%}\right)=\left(C_{in}-a_0\right)\cdot\tfrac{90}{100} \quad \text{and} \qquad \textbf{(52)}$$

$$C_{mdl}\left(t_{99\%}\right)=\left(C_{in}-a_0\right)\cdot\tfrac{99}{100} \quad .$$

Table 7 Sets of $\{a_0, a_1, b_2, c\}$ used in **(51)** to model the respective duplicate measurement at a throughput of 5.6 L/d. R^2 denotes the quality of the fit as of **(42)**, $R_{oth}{}^2$ delivers the same quantity in case of additional bell-shaped terms (see Figure 20).

Fitting parameters for measurements with 5.6 L/d throughput.

bio-mass [g/L]	t.e.p.i. [W][a]	[b]	a_0	a_1	b_2	c	R^2	$R_{oth}{}^2$
5	8		$1.1\ 10^6$	$1.6\ 10^7$	0.194	0.68	0.9953	0.9999
			$1.3\ 10^6$	$7.6\ 10^6$	0.052	0.27	0.9876	1.0000
	16		$9.4\ 10^5$	$1.9\ 10^7$	0.352	0.55	0.9990	0.9999
			$2.2\ 10^5$	$1.8\ 10^7$	0.337	0.40	0.9991	1.0000
	24		$4.1\ 10^5$	$1.8\ 10^7$	0.612	0.36	0.9991	1.0000
			$5.2\ 10^5$	$7.6\ 10^6$	0.153	0.37	0.9999	0.9999
50	24		$1.6\ 10^6$	$2.5\ 10^8$	0.388	0.89	0.9998	0.9999
			$2.2\ 10^6$	$2.7\ 10^8$	0.342	1.00	1.0000	1.0000

[a] true electrical power input
[b] see Figure 10

Table 8 Sets of $\{a_0, a_1, b_2, c\}$ used in **(51)** to model the respective duplicate measurement at a throughput of 20 L/d. R^2 denotes the quality of the fit as of **(42)**, $R_{oth}{}^2$ delivers the same quantity in case of additional bell-shaped terms (see Figure 20).

Fitting parameters for measurements with 20 L/d throughput.

bio-mass [g/L]	t.e.p.i. [W][a]	[b]	a_0	a_1	b_2	c	R^2	$R_{oth}{}^2$
5	8		7.1 10^6	2.8 10^7	2.816	0.60	0.9558	0.9976
			6.1 10^6	3.0 10^7	1.700	0.69	0.9835	0.9996
	16		1.8 10^6	3.3 10^7	6.590	0.20	0.9987	1.0000
			1.5 10^6	3.4 10^7	8.100	0.30	0.9978	1.0000
	24		1.1 10^6	2.6 10^7	2.700	0.48	0.9972	0.9991
			1.6 10^6	3.1 10^7	2.500	0.43	0.9998	0.9998
50	24		1.9 10^7	1.9 10^8	2.551	0.26	0.9700	0.9999
			9.2 10^6	2.2 10^8	1.837	0.13	0.9682	0.9996

[a] true electrical power input
[b] see Figure 10

Table 9 Sets of $\{a_0, a_1, b_2, c\}$ used in **(51)** to model the respective duplicate measurement at a throughput of 46.2 L/d. R^2 denotes the quality of the fit as of **(42)**, $R_{oth}{}^2$ delivers the same quantity in case of additional bell-shaped terms (see Figure 20).

Fitting parameters for measurements with 46.2 L/d throughput.

bio-mass [g/L]	t.e.p.i. [W][a]	[b]	a_0	a_1	b_2	c	R^2	$R_{oth}{}^2$
5	8		1.3 10^7	1.2 10^7	6.122	0.03	0.9554	0.9988
			1.4 10^7	1.2 10^7	6.939	0.06	0.851[c]	0.9984
	16		4.2 10^6	1.9 10^7	12.727	0.23	0.9665	0.9997
			2.1 10^6	2.4 10^7	12.524	0.05	0.9818	0.9999
	24		3.1 10^6	3.1 10^7	15.300	0.28	0.9797	0.9997
			1.6 10^6	3.4 10^7	14.184	0.16	0.9944	0.9997

[a] true electrical power input
[b] see Figure 10
[c] although R^2<0.95 was found the measurement could be fitted very well with one additional bell-shaped term

Figure 22 shows the calculated values, the runs were modelled individually and the results as of equation **(52)** subsequently averaged. Graphs a, b, c on the left hand

side reflect the times t_s, $t_{90\%}$ and $t_{99\%}$ respectively elapsed after the ultrasound was switched on. Graphs d, e, f on the right hand side show the corresponding volume that had left the system when the described stages were reached.

The presented calculations have been performed with the fitting coefficients for a bio-mass of 50 g/L as well (Table 10), however the true electrical power input was always 24 W for this cell concentration. In comparison to the data for 5 g/L mild differences were detected in case of a throughput of 20 L/d. The value for t_s was slightly lower, $t_{90\%}$ and $t_{99\%}$ both were higher for the thicker suspension. An exceptional low figure of 0.09 minutes (5.4 seconds) was measured for t_s at 50 g/L bio-mass and 5.6 L/d throughput. Compared to the 5 g/L data this was shorter than the result for 46.2 L/d for the lower bio-mass level, however $t_{90\%}$ and $t_{99\%}$ again were slightly higher for 50 g/L.

Table 10 Sets of $\{a_0, a_1, b_2, c\}$ used in **(51)** to model the respective duplicate measurements at a bio-mass load of 50 g/L. R^2 denotes the quality of the fit as of **(42)**, $R_{oth}{}^2$ delivers the same quantity in case of additional bell-shaped terms (see Figure 20).

Fitting parameters for measurements with 50 g/L at the given throughput and 24 W t.e.p.i.

throughput [L/d]	t_s	$t_{90\%}$ [min]	$t_{99\%}$	V(t_s)	V($t_{90\%}$) [mL]	V($t_{99\%}$)
5.6	0.09	3.83	7.37	0.33	14.94	28.72
20	0.65	1.72	4.18	9.97	23.91	58.03

Table 11 shows the maximum of the separation efficiency calculated from the fitting parameters as a_0/C_{in}. The direct comparison with the measured values in Table 1 confirms the model to describe the measurements very well, however the modelled values tended to be slightly higher than the measured data.

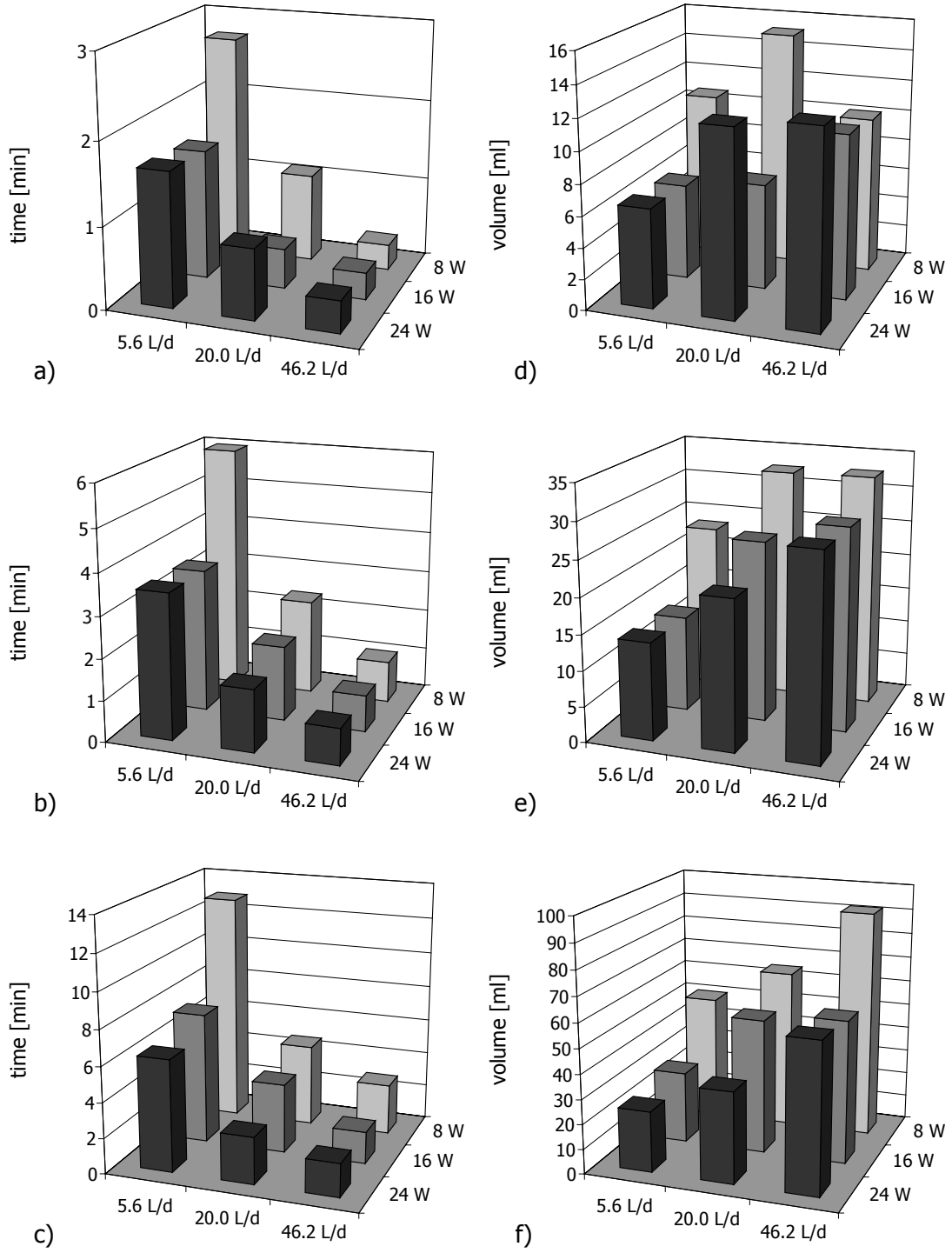

Figure 22 Result of calculations based on the fits. Left hand side graphs (a, b, c) show the times t_s, $t_{90\%}$ and $t_{99\%}$ after which the steepest decrease, 90% and 99%, respectively, of the final concentration were reached according to the fitting of the respective experiments using equation **(51)**. Right hand side graphs (d, e, f) give the volume of suspension that had left the system after the respective time. Bio-mass load was 5 g/L.

Table 11 Maximum values of the S.E. a_0/C_{in} calculated from the modelled data.

Separation efficiency maximum as delivered by the fitting [%][a]					
bio-mass [g/L]	t.e.p.i. [W][b]	[c]	throughput [L/d]		
			5.6	20	46.2
5	8		97.5 $\pm_{s.d.}$ 0.3	85.4 $\pm_{s.d.}$ 3.5	74.9 $\pm_{s.d.}$ 0.3
	16		98.7 $\pm_{s.d.}$ 1.1	96.4 $\pm_{s.d.}$ 0.3	93.8 $\pm_{s.d.}$ 3.3
	24		98.9 $\pm_{s.d.}$ 0.2	97.2 $\pm_{s.d.}$ 0.4	94.9 $\pm_{s.d.}$ 2.8
50	24		99.6 $\pm_{s.d.}$ 0.1	96.7 $\pm_{s.d.}$ 2.3	-

[a] in comparison to original concentration as of **(47)**
[b] true electrical power input
[c] see Figure 10

Discussion

The presented model was found empirically, i.e. the exponential and the bell-shaped terms were chosen for their ability to build up the shape of the measured data. It is however interesting, that the bell-shape could be used to describe the graph of the re-arrangement in the beginning and equally as well the fluctuation observed later during the run. More precisely the right half of the bell-shaped term was important when the cells were driven into the pressure nodes initially, the whole function described a pattern of the cell concentration at the outlet while aggregates where slipping down within the active volume and cells were possibly partly re-suspended. The question is if the mathematical representation actually reflected what happened within the separation system, i.e. if the settling was modelled by the exponential function while the mechanism of re-arrangement/re-suspension of the cells was taken care of by the bell-shape.

Generally the agreement between the data presented in chapter R1.2 and the results delivered by the model confirms the regression equation **(51)** to describe the development very well.

The model reflected the observed trend of quicker decrease of the cell concentration at the outlet for higher true electrical power inputs. This was true up to a certain level, where an increase of electrical power did not improve the result anymore similar to what has been shown before (compare Figure 14).

On the whole, Figure 22 shows a tendency of the trends described in the following to be more pronounced for $t_{90\%}$ and $t_{99\%}$. This is a consequence of t_s - the steepest point of the main decrease by definition - being as well the region most sensitive to variations.

What has been mentioned regarding the use of time and volume on the x-axis (Figure 11) was certainly reflected here as well: to reach a certain stage, e.g. 90% of the final concentration ($t_{90\%}$, compare Figure 22b and e), it took *longer* for lower throughputs but *less* medium left the system by the outlet during this time[i].

Another, somewhat stronger effect was that t_s, $t_{90\%}$ and $t_{99\%}$ were shorter for higher throughputs. The difference between the results was greater for lower settings of the true electrical power input.

Finally Figure 22f delivers an important information regarding the experimental design. For all experiments a stationary state as of 99% of the final cell concentration was reached within the 80 mL that were pumped through the system except for one. The value at 8 W true electrical power input and 46.2 L/d throughput showed that one additional sample had been appropriate until the cell concentration at the outlet would have been stationary.

The presented equations are not the last resort. Additional data, especially in the beginning of the experiment, i.e. after the ultrasound is switched on, would be necessary to finally connect the fitting coefficients with the process parameters. It has to be emphasized, that it was not planned to describe the results mathematically, the motivation to do so was the perception of the similarities between the measured graphs.

However a model enabling one to derive the *S.E.* of this separation system from the process parameters would be of some value. The ability to calculate the behaviour of the cell concentration at the outlet would open opportunities for further optimisation of the duty cycling. The outlet pump and/or the ultrasonic field have to be switched on and off for certain intervals to let the agglomerates settle. This becomes necessary, as a part of the bio-mass can be trapped by the transverse radiation force

[i] This is a property of the system and has nothing to do with the mathematical operation connecting these scales.

and subsequently the virtual mesh of pressure nodes becomes filled up and therefore particles are swept out of the system by the host liquid moving through.

One important value is the time which the ultrasound has to be switched on before the outlet pump is switched on. An equation describing the development versus time in dependence of process parameters would enable one to calculate the time necessary to reach the desired *S.E.*, or cell concentration at the outlet, after which the throughput could be applied at the earliest possible moment.

R1.6 Conclusion

The Ultrasonically Enhanced Settling principle was shown to be basically applicable for the separation/filtration of yeast cells suspended in saline. In particular the following results were found:

- The employed separation system USSD-05 (Anton Paar GmbH, Graz, Austria) delivered separation efficiencies of above 90% over the whole working range of 5 – 50 L/d throughput for bio-mass levels of 5 g/L and up to 20 L/d for 50 g/L.
- A limitation was encountered for low cell concentrations of $5 \cdot 10^6$ cells/mL at a bio-mass load of 0.5 g/L where the number of cells was too low to build up aggregates suitable for enhanced settling.
- The existence of an upper threshold for true electrical power input was identified: the use of 24 W did not improve the separation efficiency in comparison to 16 W at a biomass level of 5 g/L. However when the true electrical power input was increased above that threshold an increase of the applied throughput was possible yielding the same separation efficiency, the maximum separation efficiency was reached earlier.
- Under certain conditions (high cell concentration, low throughput) a separation efficiency of 99.6% was achieved.
- Evaluation of the acoustic energy density within the active volume showed a damping effect of 50 g/L bio-mass level resulting in a decrease of the radiation forces. The separation efficiency however was not decreased for low throughput compared to 5 g/L bio-mass as the higher cell concentration

promoted the enhancement of settling and therefore the effective acoustic quality factor of the suspension layer increased during the run. At a throughput of 20 L/d however, a significantly higher separation efficiency was measured for the lower initial cell concentration at 5 g/L bio-mass.

- The viability of yeast cells at the outlet of the separation system was 96% or above. No selective effects in respect of viability were observed.
- A mathematical model was introduced, the non-linear regression equation of which showed to describe the development of the cell concentration at the outlet versus time elapsed very precisely. However the model explicitly had to be called *descriptive* in opposite to *predictive* as the four fitting parameters used could not be brought into direct relation to the varied process parameters.
- The equation enabled one to calculate certain properties of the system. Among the examples shown was the time it takes until 99% of the final concentration was reached, i.e. no further increase of separation efficiency took place. This result can be valuable for the estimation of optimum values for duty cycling (pumps and sound field operation cycles).

R2 Effects of the state factor ethanol: Turbulence and cell damage

R2.1 Introduction

Ethanol (EtOH) is an important process variable in brewing processes, it represents the end product of the fermentation of sugar by yeast. The final concentration of EtOH in high-gravity[i] brewing is 12%($^{v}/_{v}$). When EtOH was present in the host liquid at this concentration the suspended yeast cells in the acoustic filter showed unexpected behaviour when irradiated with well-controlled ultrasonic plane waves. A breakdown in separation efficiency was evident and turbulence was observed within the separation system. Furthermore cell damage and decreased viability were detected[64].

An overview of the phenomenon along with examinations of the ultrasonic field and measurements of cell viability and cell integrity as of leakage of intracellular material when the turbulence was present will be presented in chapter R2.2.

The results triggered a bigger study about cell viability, integrity, the ability to reproduce and morphology including the employment of transmission electron microscopy. The objective of this study was to further investigate the damage, especially its extent over the duration of sonication. The first part about results obtained with yeast cells exposed to ultrasound in water-rich EtOH mixtures and therefore driven through the pressure inter-nodal space, i.e. regions of non-vanishing acoustic pressure between the pressure nodes, will be the content of chapter R2.3.

The investigations for the cause of the turbulence led to the non-linear behaviour of the material properties speed of sound and mass density over EtOH-concentration when EtOH was mixed with water. This together with the respective properties of the yeast cells delivered acoustic contrast factors which were found to be likely the reason for the turbulent behaviour as shown in chapter R2.4.

[i] The term gravity refers to the primary fermentation products, not to the attraction power of the earth.

R2.2 Breakdown of spatial order/immobilisation in the presence of ethanol

The phenomenon

The ultrasonic separation system in flow-through set-up (Figure 9, right hand side) was filled with yeast cells suspended in a 12%($^{v}/_{v}$) EtOH-water mixture. The original motivation was to assess the separation efficiency in the presence of EtOH for comparison with measurements presented in chapter R1. However the presence of EtOH did alter the behaviour of the suspension in the system completely. The cells did not form planes in the sound pressure nodes which subsequently led to the breakdown of retention and consequently the separation efficiency severely impaired.

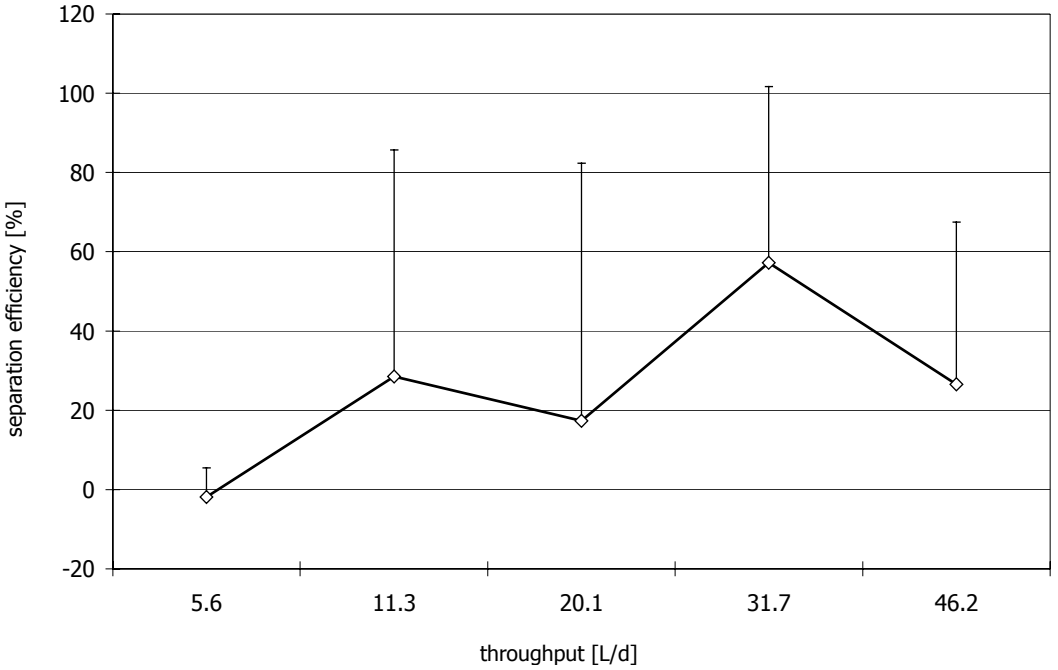

Figure 23 Separation efficiency of yeast suspended in 12%($^{v}/_{v}$) EtOH-water. The high error bars indicate the breakdown of spatial arrangement resulting in complete mixing. Therefore no retention of cells was observed in two thirds of the experiments.

An experiment for the examination of the influence of throughput on separation efficiency delivered the result shown in Figure 23. Each data point represents the mean of three measurements taken at the filter outlet after 40 mL of suspension had left the system. Unlike before, a stable result was not achieved, the error bars indicate the extremely high standard deviation. The reason was that out of the fifteen

measurements in ten cases a spatial distribution as described earlier (Figure 8) did not take place, in the contrary, the cells were turbulently driven through the chamber. As a consequence no clear relation between separation efficiency and throughput could be established.

The detailed data is given in Table 12. Brackets indicate the results of those ten trials where no ultrasonic cell immobilisation was observed. The "separation efficiency" in those cases varies in the range from 6% to –23%, the mean was calculated to be –4.3±10.4%[i]. This value represented complete mixing. However sometimes some separation/retention was observed, but as mentioned highly unstable. The rightmost column gives the corresponding values for yeast suspended in water.

Table 12 Separation efficiency when a 12%(v/v) EtOH-water mixture was used as host liquid (brackets indicate turbulence). The rightmost column gives the means of the same experiments except with water used as a host liquid.

Separation efficiency maximum [%][a], flow-through set-up				
throughput [L/d]	single trials, yeast in 12%(v/v) EtOH			mean, yeast in water
5.6	(-8.3)	(6.1)	(-3.6)	91.7 $\pm_{s.d.}$ 2.6
11.3	(-11.4)	(2.9)	93.9	90.2 $\pm_{s.d.}$ 2.0
20.1	92.3	(-23.1)	(-17.3)	87.0 $\pm_{s.d.}$ 1.8
31.7	87.1	(6.1)	78.4	84.3 $\pm_{s.d.}$ 4.0
46.2	73.8	(0.5)	(5.4)	73.2 $\pm_{s.d.}$ 1.6

[a] in comparison to original concentration as of **(47)**

The further examination of these unexpected results was the target of the following experiments.

A hypothesis was tested that an interaction of the ultrasound with CO_2 inside living cells was the reason for the lack of cell banding in the pressure nodes. For this purpose suspended yeast cells were killed by autoclaving, nevertheless the

[i] Negative values express that due to the turbulence the cell concentration at the outlet at the time of measurement was higher than in the initial suspension.

observations in respect to the ordering effects did not differ from the experiments with living cells.

Consequently, it was assumed, that the presence of EtOH was the reason for the turbulences. Thus an attempt was made to examine the concentration at which the unusual behaviour sets in. Suspensions of yeast were used in the separation system, the EtOH concentration was increased in steps until the separation efficiency showed a significant decrease indicating the breakdown of the spatial order. Figure 24 shows the results of trials with yeast cells in water (triangles) where turbulence was not observed until the concentration of EtOH reached 8%($^{v}/_{v}$). When physiological saline was used as host liquid (circles) an influence of EtOH was not detected until the concentration had reached 15%($^{v}/_{v}$). However, as the EtOH content was increased in steps of 1%($^{v}/_{v}$), it could be established that the lack of spatial ordering is a sudden process "hitting" in rather than gradually decreasing the separation efficiency. The third trial (squares) in Figure 24 showed that one is dealing with a reversible process. A suspension of yeast and water was used, the breakdown was observed first at 9%($^{v}/_{v}$). Subsequently the EtOH concentration was decreased again to 8%($^{v}/_{v}$) by adding water. At this concentration the proper arrangement of the cells was re-established.

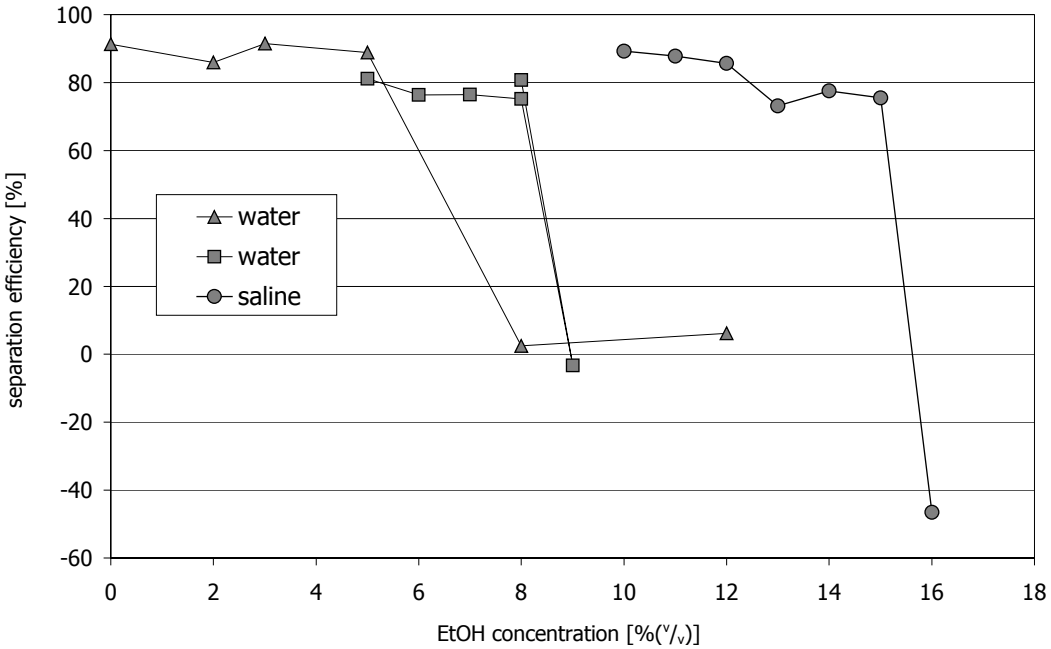

Figure 24 Evaluation of the EtOH concentration at which the spatial arrangement of yeast cells breaks down. Suspensions of yeast cells in water (triangles, squares and 0.9%($^{w}/_{v}$) NaCl (circles) were used.

Evaluation of the acoustic field in the presence of 12%($^{v}/_{v}$) ethanol

The experiments showing the breakdown of separation efficiency gave rise to the question if a standing acoustic wave was present in the filter chamber when water-EtOH mixtures of certain concentrations were used as host liquids. Therefore the true electrical power input of the separation system with fillings of water and 12%($^{v}/_{v}$) EtOH-water, respectively, was recorded at frequencies between 1.9 MHz and 2.1 MHz at a constant drive voltage level of 21 V (M5.3).

Losses within the excited resonator are compensated for by the true electrical power input as of equation **(38)**. The high amplitudes of the acoustic field at resonance result in high acoustic losses. Therefore a true electrical power input *spectrum*, i.e. the measurement of the true electrical power input over a range of frequencies, yields information about the occurrence of acoustic resonance by delivering high values (peaks) of true electrical power input[i] at certain frequencies (so-called series resonance frequencies). Resonance in turn is the state in which the reflected wave is *in phase* with the incoming wave emitted by the transducer thus contributing constructively to the wave field, the wave "fits" between the two acoustical mirrors (compare Figure 1). As a standing wave is the general result of the superposition of an incoming wave and its reflection, resonance does conclusively proof the existence of a (quasi-)standing wave field[ii].

The measurement result clearly showed resonance peaks of about 18 W (Figure 25), no significant difference between the two liquids was detected. A standing wave was therefore presenting both cases. Furthermore, the unchanged width of the resonance peaks suggested that as well the ratio of standing and progressive waves was not affected, hence one could assume that no major differences between the acoustic fields in pure water and the water-rich EtOH mixture existed.

[i] This is valid for an impressed, i.e. load independent, drive voltage level supplied by the amplifier.

[ii] The state of resonance is always associated with a pure standing (ideal case, no losses) or quasi-standing (lossy case) wave. However, the existence of a (quasi-)standing wave is not at all restricted to resonant situations.

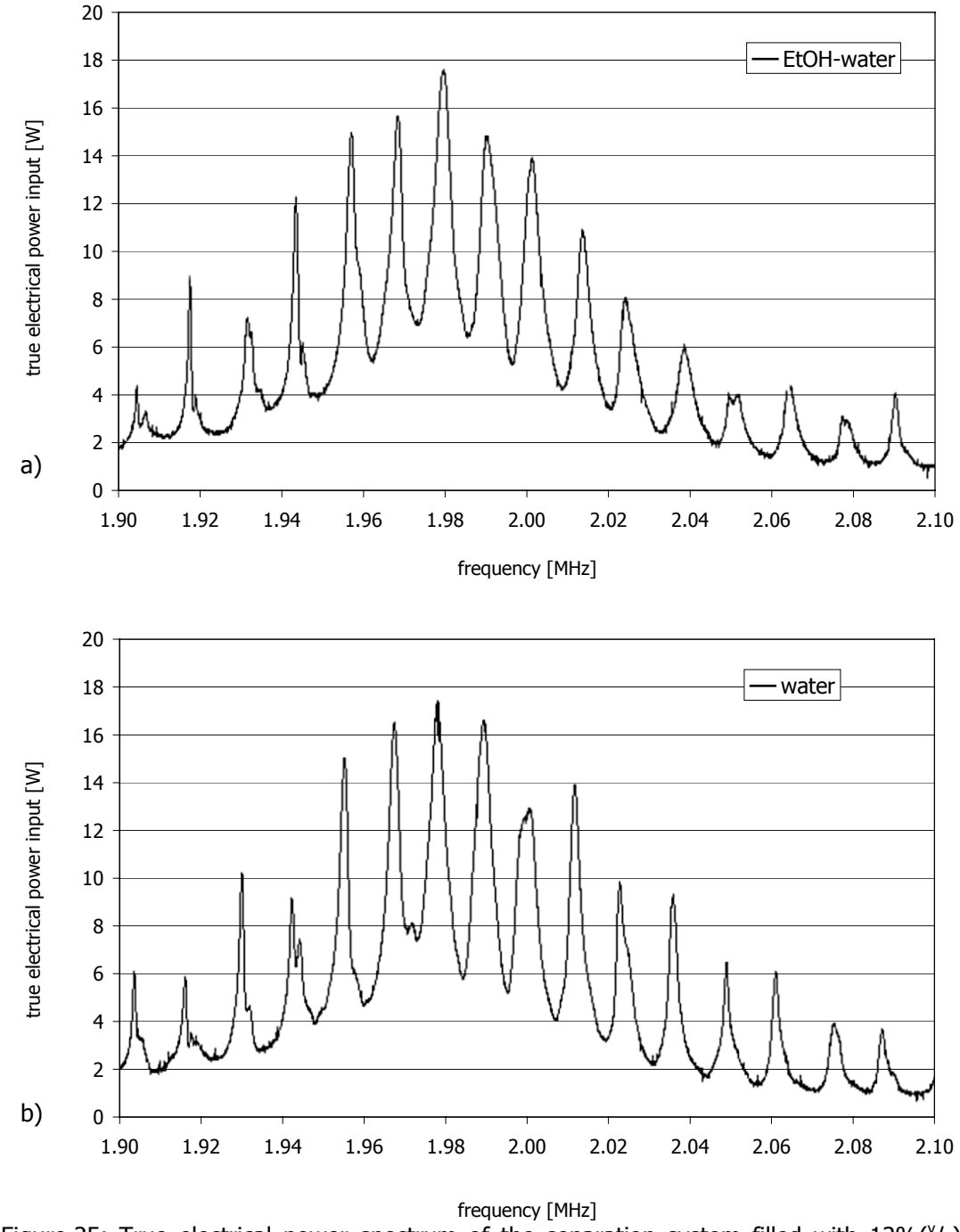

Figure 25: True electrical power spectrum of the separation system filled with 12%($^{v}/_{v}$) EtOH-water (a) and pure water (b). No significant differences were detected, hence standing waves of comparable quality existed in both cases.

The experiment was carried out with yeast cells present in an EtOH-water mixture at the threshold of 8%($^{v}/_{v}$) EtOH (see Figure 24) as well. The measured power spectra showed a significant increase of the resonance peak widths on higher settings of the impressed drive voltage level. In Figure 26 the respective setting of the amplifier were

10 V, 18 V and 28 V. Clearly the spectrum did loose structure caused by the overlapping of the peaks at higher levels of true electrical power input. This behaviour is typical for a decrease of the acoustic quality factor as of equation **(33)** which in turn was an indication for an energy consuming process. In correspondence with the turbulent movement of the suspended cells observed in the resonator chamber, the reason of the energy loss of the acoustic field was easily identified: part of the acoustic energy was transformed into the kinetic energy of the moving particles. In consistence with the observations Figure 26 shows furthermore, that the velocity of the cells turbulently driven through the separation system increased with an increase of electrical input power, resonance peaks were wider for higher settings.

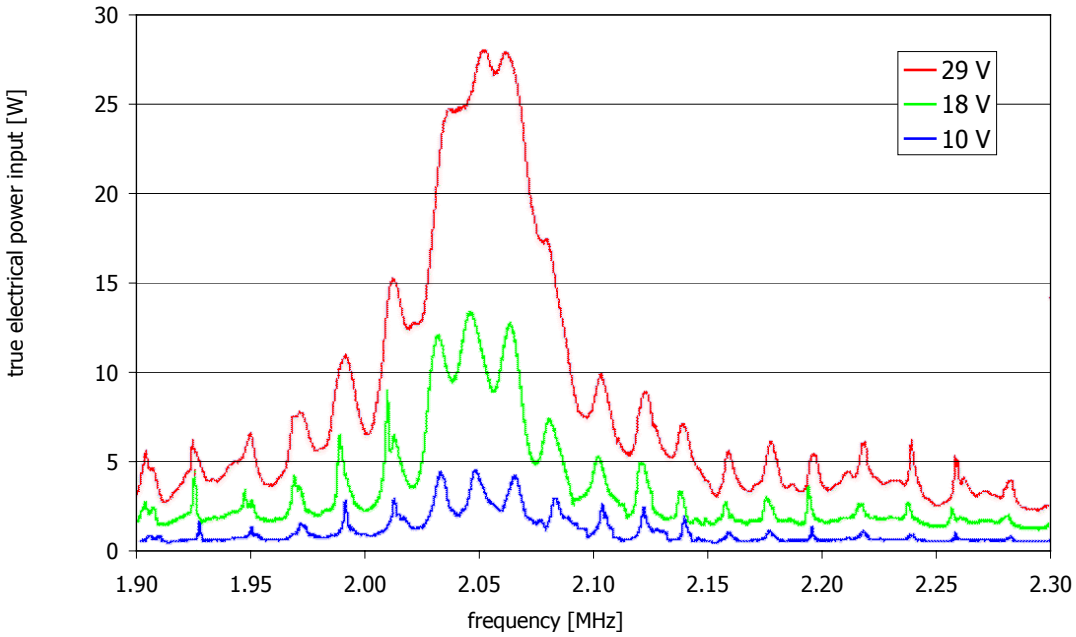

Figure 26: Power spectra of the separation system filled with yeast (approximately $5 \cdot 10^6$ cells/mL) suspended in 8%(v/v) water-ETOH at impressed (load independent) drive voltage settings were 10 V (blue), 18 V (green) and 29 V (red). A decrease of the acoustic quality factor with increasing true electric power input was detected.

Effects on the yeast cells

Yeast cells were suspended in a 12%($^v/_v$) EtOH-water mixture and sonicated in the separation system in batch set-up (Figure 9, left-hand side) at 14 W input power. During the whole experiment the lack of spatial arrangement of the cells as described

in the last chapter was observed. Samples were taken out of the chamber from the beginning to half an hour every 5 minutes and afterwards at one hour and two hours.

The examination of sonicated yeast cells revealed a tremendous decrease of viability according to methylene blue counts (M3.3) in comparison to the control samples which were from the same suspension but not exposed to ultrasound. The fraction of viable cells in the sonicated samples was decreasing from some 80% in the beginning to less than 20% after two hours as Figure 27 shows. After 30 minutes already more than half of the cells were counted blue under the microscope. It has to be mentioned that the viability of the control at 25 and 30 minutes was not measured.

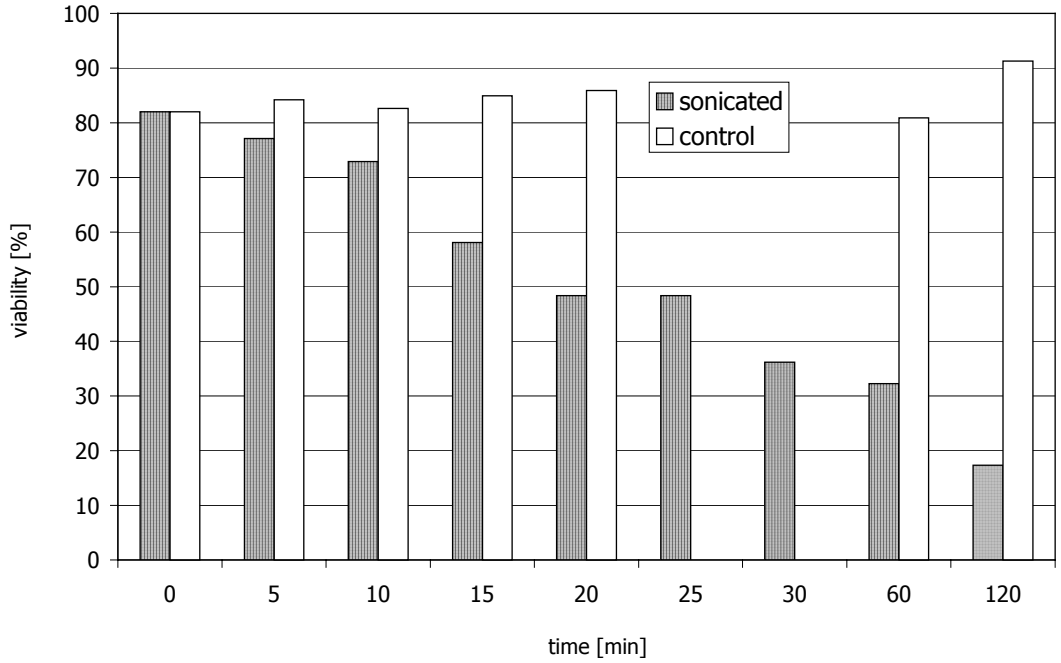

Figure 27 Viability according to methylene blue counts over sonication time of yeast (approximately $5 \cdot 10^6$ cells/mL) suspended in 12%($^{v}/_{v}$) EtOH-water. The cells were driven turbulently through the separation system in batch set-up.

The release of intracellular material was assessed for the same samples by the optical density (O.D.) for ultraviolet light (UV) which is influenced by protein in the liquid (see chapter M3.4). The results in Figure 28 show the increase of UV O.D. with sonication time indicating leakage of the cells. The corresponding measurement of control samples did not show any changes over two hours.

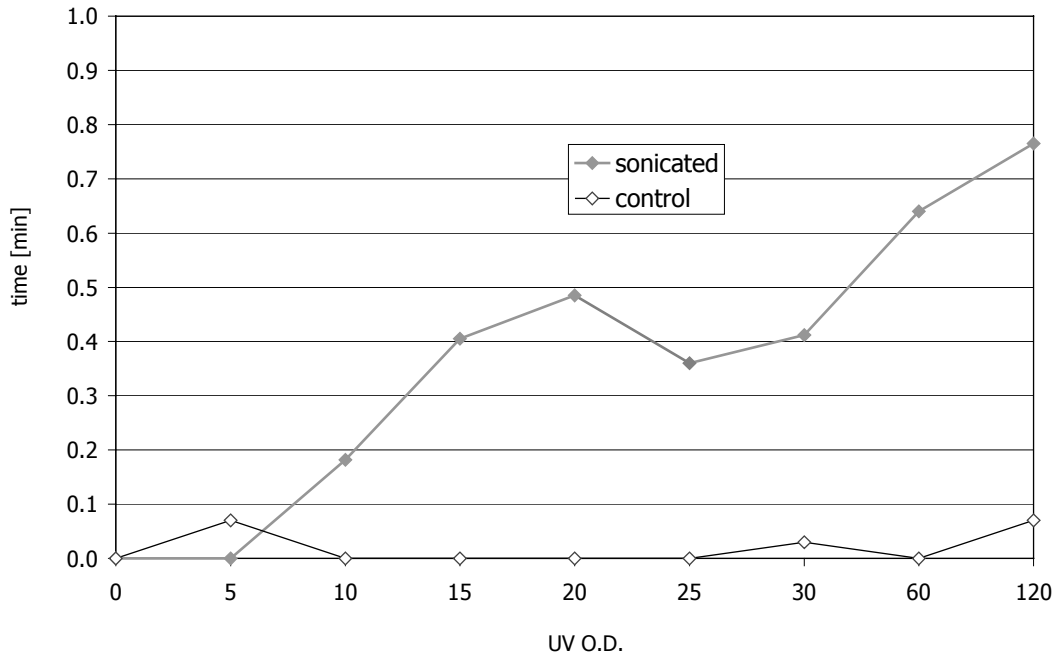

Figure 28 Measurement of intracellular material in the supernatant of yeast (approximately $5 \cdot 10^6$ cells/mL) in 12%($^{v}/_{v}$) EtOH-saline by ultraviolet O.D. over time during sonication at 14 W t.e.p.i.

Discussion

These observations were puzzling and unexpected, although the phenomenon was mentioned in personal communication (A. Oudshoorn). Two aspects or questions could be isolated in the results:

Firstly, no explanation was at hand for the turbulent behaviour of the particles in the sonication chamber. The UES is a technique applied in industry and to the knowledge of the author no reports of problems establishing the spatial distribution with solid particles or biological cells existed. Also it was shown that the lack of spatial distribution (i.e. the fact that the cells are driven through all areas of the sound field), in a water-rich EtOH mixture caused a breakdown of filtration/retention. The used separation system was optimised to deliver well known and well controlled wave fields, hence a "fail" like observed needed further examination. To exclude the possibility that the turbulent behaviour was the result of damping or distortion the existence of a standing wave field was proven by measuring the true electrical power input spectrum of the acoustic resonator. This result has been achieved at power levels in the range of normal operation. Thus no indication was found that non-linear

effects[65] distorted the ultrasonic field[66]. Such effects would have been e.g. the formation of micelle structures[67-69]. However some anomalies if water-EtOH mixtures in relation to their speed of sound and other acoustical properties over the concentration of EtOH[70,71] will be further examined in chapter R2.4.

Secondly, the described decrease of cell viability and increase of intracellular material in the supernatant had not been observed before. Many studies have shown that there is no loss of cell viability when cells are subjected to ultrasonic standing wave fields in acoustic cell retention systems. Unlike the results presented here these systems had proven to manipulate more delicate cells than yeast, e.g. animal hybridoma without causing any harm[9]. In a report about scale-up tests[10] the viability was measured at 90% after 950 hours of continuous ultrasonic filtration on top of a fermentor. Therefore it was assumed that the acoustic radiation forces exerted on the particles push them very gently into the pressure nodes.

Ethanol has known effects like relaxation of the membrane and an increase of permeability of the cell wall, however according to both viability testing methods no significant effects due to the exposure of yeast to EtOH alone were detected: neither did the un-sonicated controls deliver increased optical density of UV-light nor did the methylene viability measurement of the controls reflect the presence of EtOH.

The environment between the pressure nodes, the pressure inter-nodal space differs from where the cells reside in the normal non-homogeneous distribution within UES systems (compare Figure 8). In opposite to the pressure nodes, where pressure vanishes by definition, in the inter-nodal space the cells are exposed to the high amplitudes of the acoustic pressure of the ultrasonic standing wave. However, at normal operating conditions of the UES system the inter-nodal space is usually populated by cells for a very short period[i] only.

[i] Usually it takes less than a second until the primary radiation force has moved particles into the pressure nodal planes.

R2.3 Effects on yeast exposed to ultrasound in pressure inter-nodal space

The observed decrease of viability and the increase of protein in the suspension were interpreted as possible cell damage or decrease in cell integrity. Therefore a study in the changes of the viability, integrity, ability to reproduce and morphology (M3.7) of yeast populations after they were exposed to ultrasound in the separation system was conducted. In this chapter the results of experiments with suspensions of freshly grown yeast in 12%($^{v}/_{v}$) EtOH-water sonicated at a power input of 24 W will be presented. The sonication took place in the separation system in batch set-up, it was taken care that the cells where driven through the pressure inter-nodal space for the duration of the experiments.

The target was to further examine the decreased viability and integrity as shown in R2.2.. Hence new methods were additionally exploited to connect the measured changes of cell viability and protein content of the host liquid with the cells' ability to *replicate* and a more sophisticated method was used to assess the internal integrity of the population. Furthermore transmission electron microscopy (TEM) was employed to further examine the alterations to the yeast cells' morphology when exposed to ultrasound without ultrasonically induced spatial arrangement in the acoustic pressure nodes.

To assess the reproducibility samples were plated out on growth medium after sonication and the number of colony forming units (CFU) was counted (see chapter M3.5). Following the observation that damage to the cells occurred, fluorescent vacuole membrane staining (see chapter M3.6) was used. The vacuole is a large, spherical compartment with a thin membrane within the yeast cell. The fluorescent vacuole staining method deliveres information about the spread of an alteration of the internal structure of the cell.

Effects on viability, integrity, ability to reproduce and morphology

The viability of cells exposed to turbulences in the water-EtOH mixture was decreased confirming the previous results. Methylene blue staining showed that over 90% of the cells became non-viable during the first 15 minutes of sonication(see Figure

29). The controls showed no significant decrease in viability due to the exposure to EtOH without sonication.

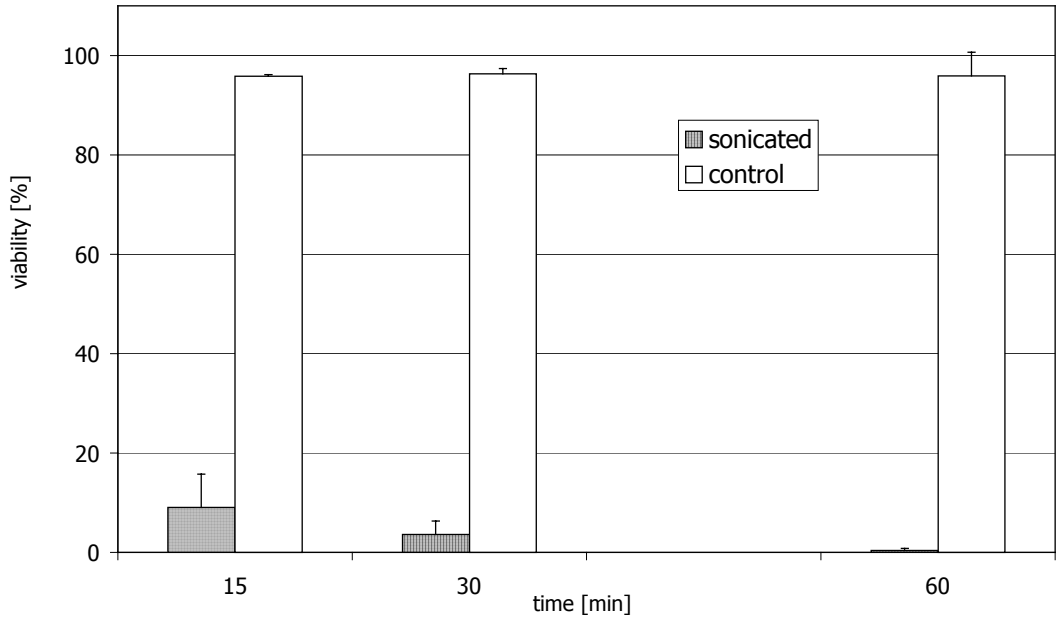

Figure 29 Viability measured by methylene blue counts. Data acquired after 15, 30 and 60 minutes of yeast cells suspended in a 12%($^{v}/_{v}$) EtOH-water mixture sonicated at 24 W. The cells were driven turbulently through the separation system in batch set-up.

In correspondence, the UV O.D. results (Figure 30) delivered an increase of intracellular material in the supernatant, while the controls, un-sonicated samples out of a thermally connected dummy separation system, did not show any response to the presence of EtOH in the suspension. The level of intracellular material increased over the duration of sonication.

The viable plate counts as shown in Figure 31 indicated that after 15 minutes over 90% of the cells were dead, although the controls too indicated in this case some decrease of the ability of the cells to reproduce when exposed to EtOH alone. Due to the low numbers of CFUs a time-dose response could not significantly be established, however a trend of a decrease over duration of sonication was detected.

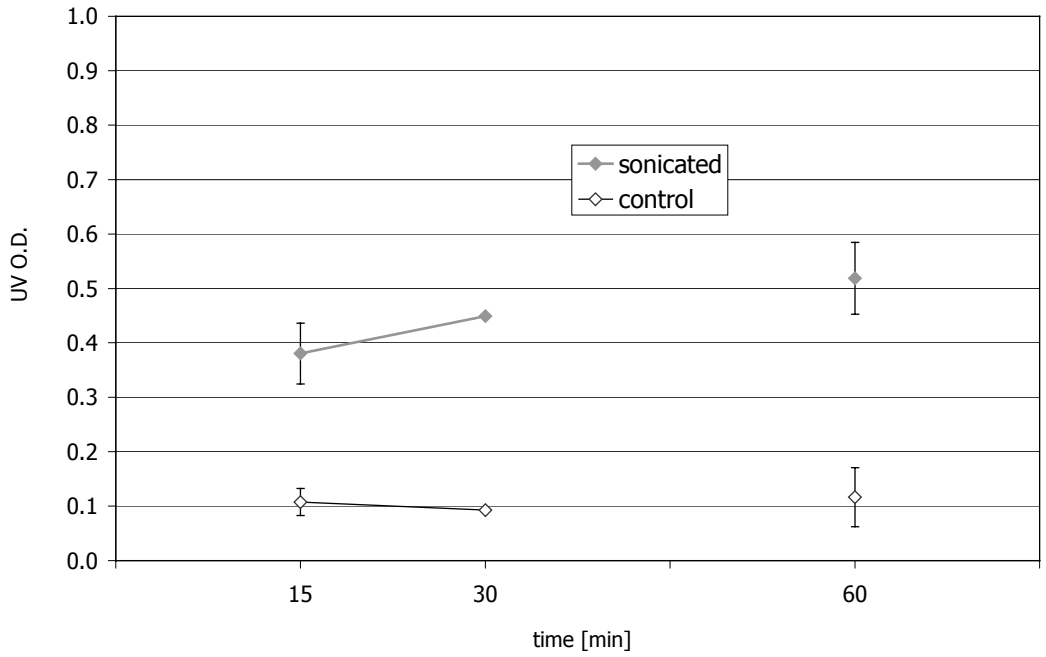

Figure 30 Measurement of intracellular material in the supernatant by the optical density (O.D.) of ultraviolet light (280 nm). Data acquired after 15, 30 and 60 minutes of yeast cells suspended in a 12%($^{v}/_{v}$) EtOH-water mixture sonicated at 24 W. The cells were driven turbulently through the separation system in batch setup.

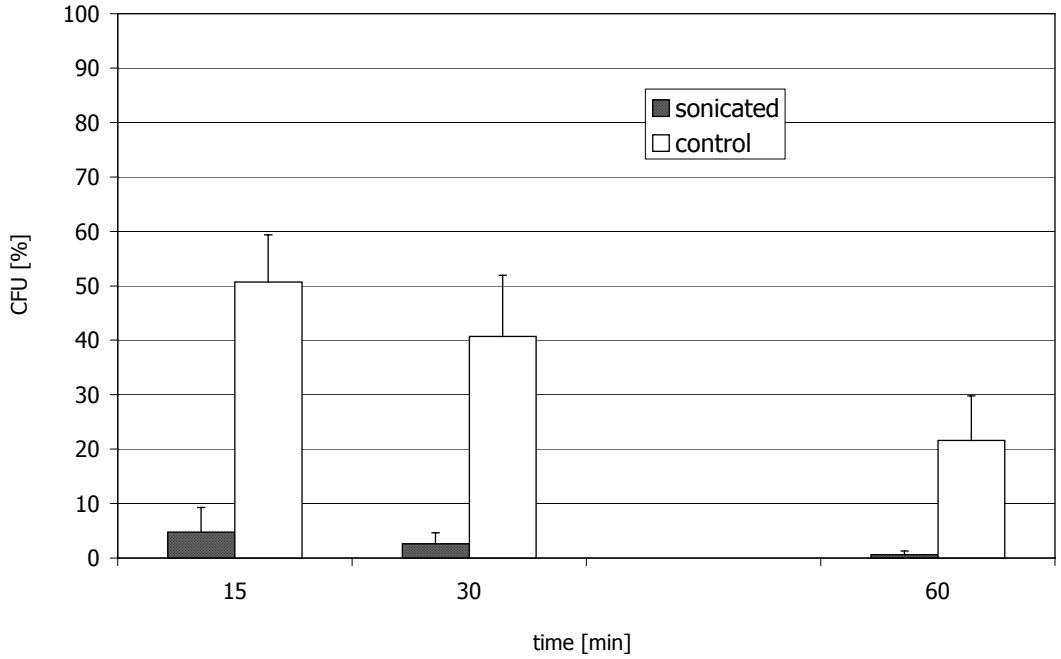

Figure 31 The cells' ability to reproduce as of viable plate counts, result given in percentage CFU. Data acquired after 15, 30 and 60 minutes of yeast cells suspended in a 12%($^{v}/_{v}$) EtOH-water mixture sonicated at 24 W. The cells were driven turbulently through the separation system in batch set-up.

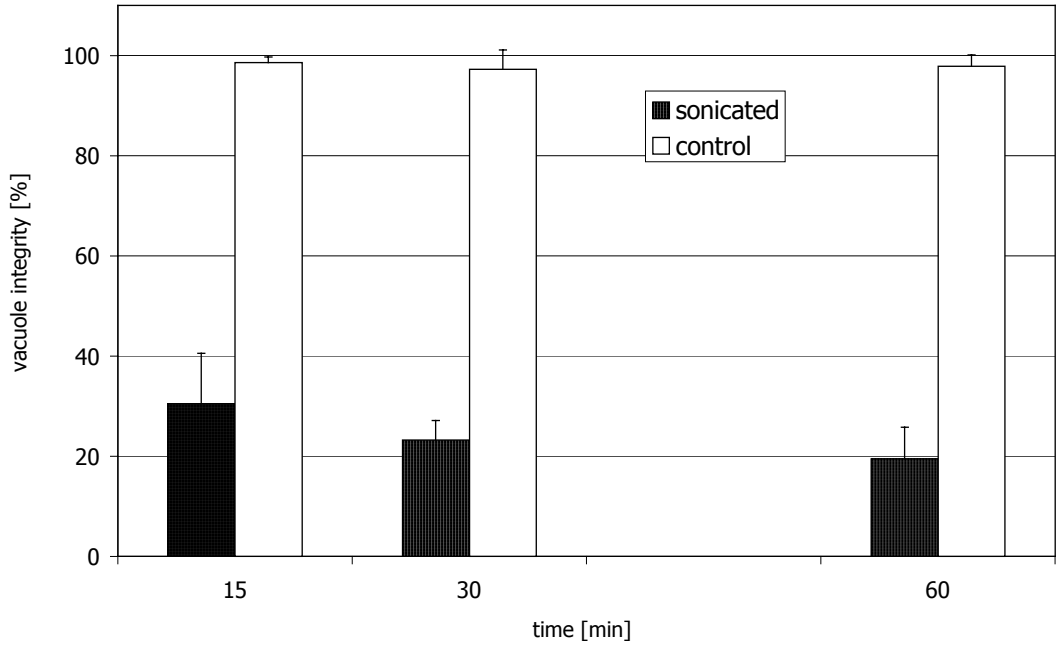

Figure 32 Fluorescent vacuole membrane dye counts to asses the internal integrity of the cells. Data acquired after 15, 30 and 60 minutes of yeast cells suspended in a 12%($^{v}/_{v}$) EtOH-water mixture sonicated at 24 W. The cells were driven turbulently through the separation system in batch set-up.

The fraction of cells showing the very specific alteration of integrity delivered by the fluorescent vacuole membrane staining (see Figure 32) was above 70% after ultrasonic treatment for 15 minutes. Again a trend of an increase over the duration of the experiment was suggested by the data, however insignificant due to the overlapping of moderate standard deviations. The controls did not display any decrease in vacuole integrity over the period of one hour.

Transmission electron micrographs

For the transmission electron microscopy (TEM) study (see chapter M6) freshly grown yeast cells were suspended in a 12%($^{v}/_{v}$) EtOH-water mixture and sonicated in the batch set-up (Figure 9 left-hand side, page 40). The described breakdown of spatial ordering by the ultrasonic field (true electrical power input 14 W) caused that the cells were present in the pressure inter-nodal space for the duration of the experiment of half an hour.

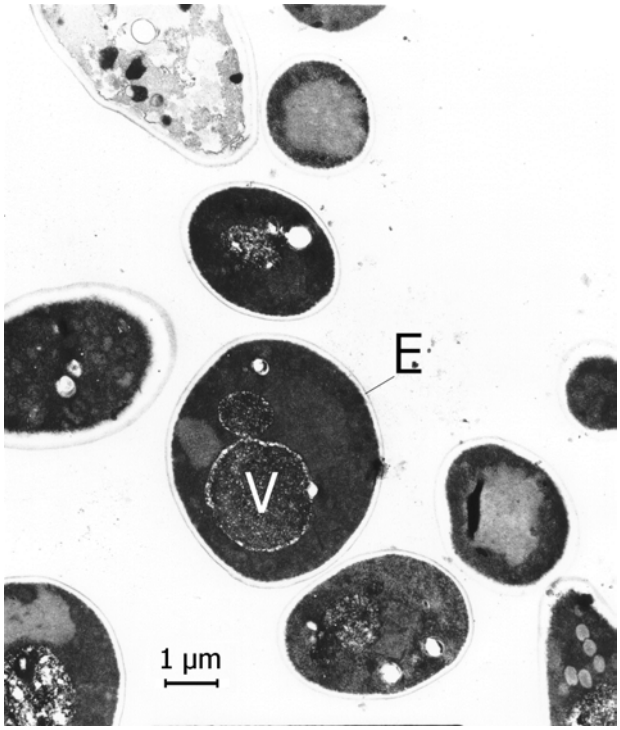

Figure 33 Transmission electron micrograph of non-treated yeast cells. A typical yeast cell shows the large vacuole (V) and other intracellular organelles. The cell envelope (E) consisting of the cell wall and the cell membrane is also visible.

The internal structure of yeast is dominated by one ore more large vacuoles (V) clearly identifiable in the un-sonicated control in Figure 33. The spherical cell is delimited by the cell envelope (E). This is comprising the cell wall, in case of yeast reinforced by a calcium cage, and the cell membrane responsible for the exchange of substances with the environment.

The mere presence of EtOH in the host liquid did not cause alterations of the yeast's morphology. The TEM of cells after having been exposed to 12%($^{v}/_{v}$) EtOH-water for half an hour (Figure 34) did show the vacuole intact and no changes in the cells' envelope.

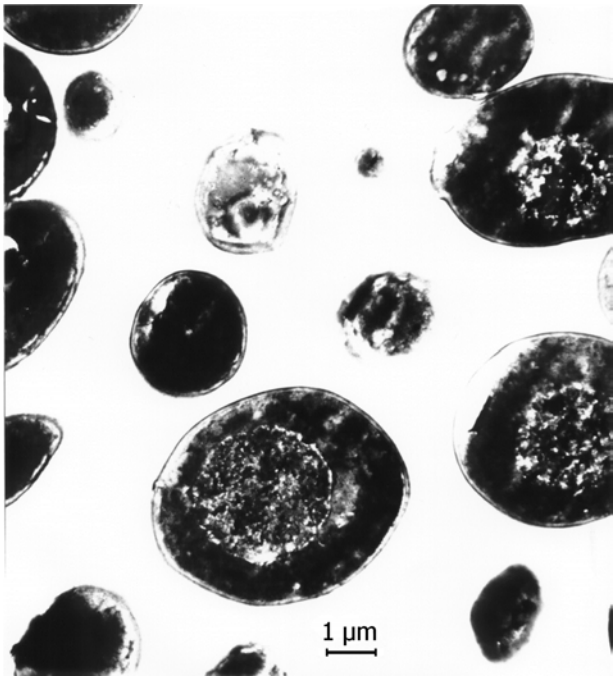

Figure 34 Transmission electron micrograph of yeast in presence of 12%($^{v}/_{v}$) EtOH. This un-sonicated control did not show changes in the morphology due to the different host liquid.

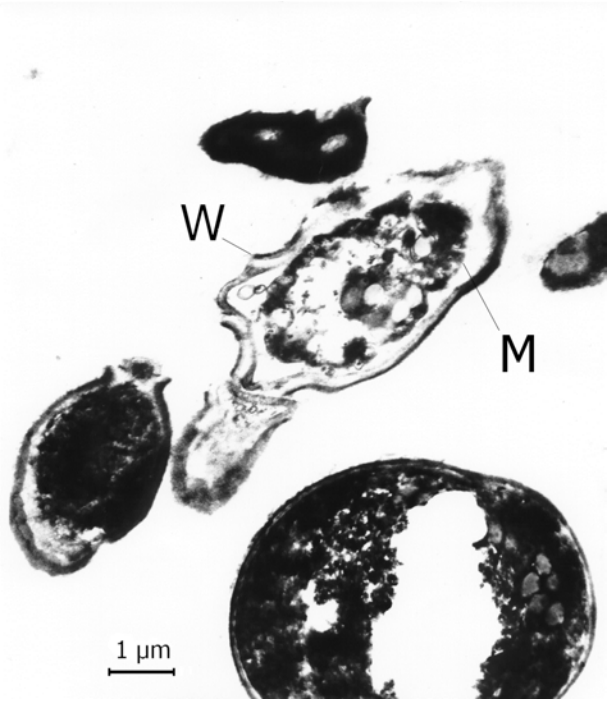

Figure 35 Transmission electron micrograph of yeast cells sonicated in presence of 12%($^{v}/_{v}$) EtOH. The cell envelope appears damaged with the cell wall (W) detached by the cell membrane (M). Damage of the vacuole is also visible.

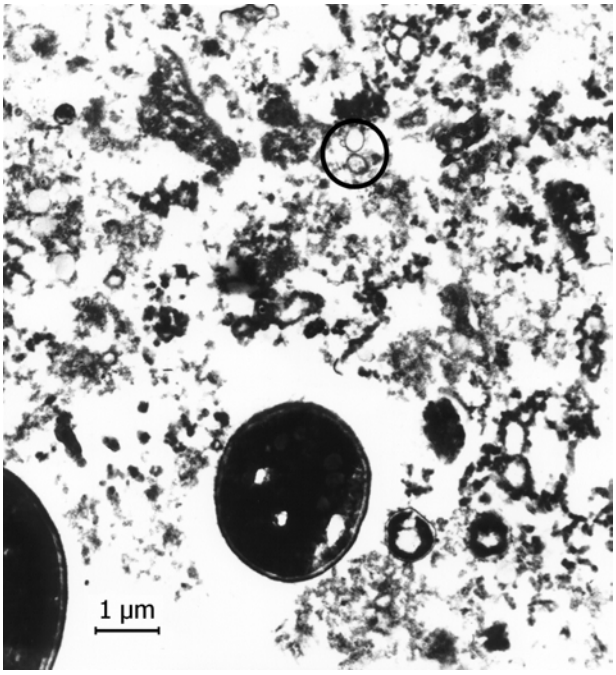

Figure 36 Transmission electron micrograph of yeast cells sonicated in presence of 12%($^{v}/_{v}$) EtOH. Intracellular contents and organelles are visible (circle) in the extracellular matrix, indicating extensive cell damage.

TEM of the sample additionally sonicated however revealed a significantly different picture. Figure 35 documents the presence of a severe damage in the cell envelope due to the breakdown of the spatial cell ordering in the acoustic field. The cell walls (W) and membranes looked detached and the inner structures of the cells were altered, the vacuoles could not be identified in the electron microscope images.

Furthermore intracellular components were found in the extracellular matrix after sonication in the water-EtOH mixture (Figure 36). The identification of organelles (circle) in the supernatant was possible.

Discussion

The refined examinations of the nature of yeast cell damages due to the combined action of EtOH and ultrasound gave valuable new insights to the physical effects experienced by cells in the ultrasonic field. The decrease in viability of yeast and the leakage as measured by the level of intracellular material in the supernatant as already observed in previous experiments when cells were sonicated in 12%($^{v}/_{v}$) EtOH-water were confirmed and the alterations resulting from sonication were identified as a significant damage to the vacuole and the cell envelope.

Confirmation was achieved that the exposure to ultrasound was the reason for the cell damage by using controls that had not been subjected to ultrasound. For all experiments except the viable plate counts no significant influence due to the presence of EtOH alone was measured.

A tremendous decrease of viability was detected when the cells were exposed to ultrasound in 12%($^{v}/_{v}$) EtOH-water and therefore driven turbulently through the resonator chamber. This decrease was furthermore heavily influenced by the applied power input as the fraction of non-blue cells was significantly lower for 24 W than for 14 W (compare Figure 29 and Figure 27).

For yeast suspended in a 12%($^{v}/_{v}$) EtOH-water mixture it was shown that the ability of cells to reproduce was impaired to a greater extent when the suspension was sonicated, compared to the effect of EtOH alone[72,73]. In addition these measurements indicated that the decrease of the ability of the cells to reproduce when subjected to 12%($^{v}/_{v}$) EtOH without ultrasound was not associated to any damage to the vacuoles or membranes. The number of cells with damaged vacuoles was lower than that for non-viable and non-replicating cells. This indicated that the observed alteration in morphology was not caused by a physiologic reaction of the cells.

Transmission electron microscopy delivered an insight to the type of damage. It was confirmed, that the increase of the optical density (O.D.) for UV-light arise from material from inside the cells. The identification of organelles in the supernatant however suggested that the cells were opened or burst during the ultrasonic treatment rather than more or less voluntarily released their ingredients.

The observed changes of viability, the intracellular material in the supernatant and the alterations of the cell envelope and inner structure were interpreted as mechanical damage caused by the ultrasonic treatment in combined action with EtOH. Furthermore it could be concluded that physical damage brought about by the sonication was responsible for the decrease in viability and affected the ability of the yeast to reproduce. In agreement with previous reports[74,75] these findings were supporting a suggestion for an explanation of the described damage based on the assumption that the damage is directly related to the pressure impact on the cells. Due to the presence of EtOH the cells were driven turbulently through the acoustic standing wave rather than kept in the pressure nodes as usual and thus exposed to the pressure amplitude. The question whether the direct influence of the pressure on the

cell, or another effect caused by a secondary mechanism, for instance, the degree of cavitation in the pressure antinodes, is responsible for the observed effect, will be dealt with in chapter R3.

R2.4 Acoustic contrast factors of water-rich ethanol mixtures

The breakdown of the spatial ordering of yeast cells in the separation system in presence of EtOH needed further investigation[76]. The observed phenomenon of turbulence was similar to the effect of the acoustic radiation pressure in a progressive wave. In literature the terms "Eckhardt streaming" or "quartzwind" are found. However there was no significant difference in the acoustic material quality factors measured for pure water and 12%($^{v}/_{v}$) EtOH-water, respectively, thus the hypothesis of damping of the liquid seemed not to provide a sufficient explanation for the breakdown of the spatial arrangement observed in a 12%($^{v}/_{v}$) EtOH-water mixture.

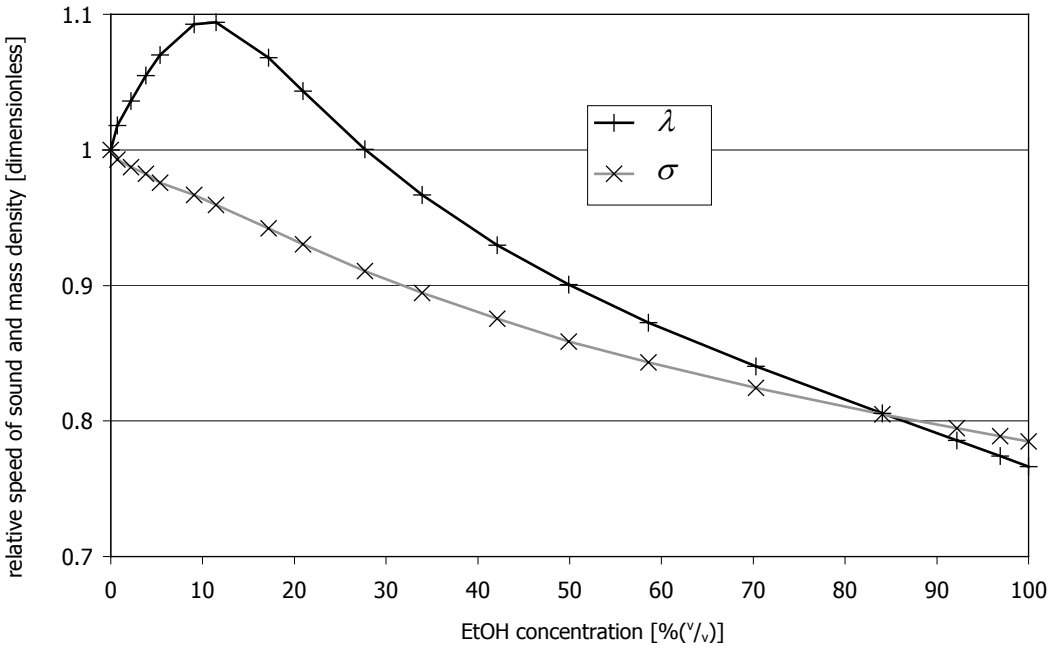

Figure 37 Speed of sound and mass density of water-EtOH mixtures at 25°C in comparison to water (data published by Lara and Desnoyers[70]).

A superficial examination of the speed of sound and mass density of water-EtOH mixtures in comparison to the respective material properties of pure water[70,71] (Figure

37[i]) delivered a deviation of some 10% for the speed of sound and less than that for the mass density at 12%(v/v) EtOH. At first glance, this did not seem to be enough to cause such fundamental changes in behaviour.

A closer look however revealed the precise circumstances to be different. The material properties of the host liquid alone do not yield the whole picture, one has to take the particle into account as well. The comparison of the axial primary radiation forces of a progressive wave F_p and a standing wave F_s yields according to equations **(1)** and **(15)**

$$\frac{\left\langle F_p\left(K_p\right)\right\rangle}{\left\langle F_s\left(x,K_s\right)\right\rangle}=\frac{2\pi\rho\cdot\hat{\Phi}_p^2(ka)^6K_p(\lambda,\sigma)}{4\pi\rho\cdot\hat{\Phi}_s^2(ka)^3K_s(\lambda,\sigma)\sin(2kx)}= \\ =\underbrace{(ka)^3}_{\text{I.}}\cdot\underbrace{\frac{K_p(\lambda,\sigma)}{K_s(\lambda,\sigma)}}_{\text{II.}}\cdot\underbrace{\frac{\hat{\Phi}_p^2}{2\hat{\Phi}_s^2}}_{\text{III.}}\cdot\underbrace{\frac{1}{\sin(2kx)}}_{\text{IV.}}\quad . \tag{53}$$

The ratio as of equation **(53)** consists of four factors expressing the dependencies on various properties of the suspension:

I. describes the influence of the frequency and the particle size; it has already been mentioned that due to the limiting condition $ka\ll 1$ the radiation force of a standing wave in general is much stronger than that of a progressive wave;

II. represents the influence of the speed of sound and the mass density of the particle and the host liquid;

III. describes the amplitude ratio of the progressive and the standing wave and thus is dependent on the effective attenuation, i.e. the viscous damping of the suspension and additional losses as well as the reflection coefficient of the reflector terminating the resonator chamber;

IV. describes the periodic structure of the standing wave's envelope;

The amplitude ratio in term III of equation **(53)** is a general expression valid for arbitrary progressive and standing waves. However, for the quasi-standing wave within the resonator the axial primary radiation forces the progressive and the

[i] In the original work the adiabatic compressibility was used.

standing wave are not independent, i.e. one can not simply add the expressions from equations **(1)** and **(15)**.

Hasegawa[77] calculated the averaged axial primary radiation force of the quasi-standing wave $\langle F_{qs} \rangle$ to be

$$\langle F_{qs}(x) \rangle = \left[1 - \left(\frac{\hat{\Phi}'}{\hat{\Phi}} \right)^2 \right] \langle F_p \rangle + \frac{\hat{\Phi}'}{\hat{\Phi}} \langle F_s(x) \rangle \quad . \qquad \textbf{(54)}$$

The coefficients for the force contributions of the progressive and the standing wave result from the amplitudes of the velocity potential of the quasi-standing wave $\tilde{\Phi}_{qs}$

$$\tilde{\Phi}_{qs} = \hat{\Phi} \cdot e^{i(\omega t - kx)} + \hat{\Phi}' \cdot e^{i(\omega t + kx)} \quad , \qquad \textbf{(55)}$$

comprising of a wave propagating from left to right with amplitude $\hat{\Phi}$ and a wave propagating from right to left with amplitude $\hat{\Phi}'$, respectively. The reflector is assumed at the right-hand side, thus $\hat{\Phi} > \hat{\Phi}'$.

If the coefficients of the force contributions are considered in equation **(53)** the expression for term III in the case of a quasi-standing wave is derived to be

$$\frac{\hat{\Phi}_p^2}{2\hat{\Phi}_s^2} = \frac{\hat{\Phi}^2}{2\hat{\Phi}^2} \cdot \frac{1 - \left(\frac{\hat{\Phi}'}{\hat{\Phi}} \right)^2}{\frac{\hat{\Phi}'}{\hat{\Phi}}} = \frac{1}{2} \frac{\hat{\Phi}^2 - \hat{\Phi}'^2}{\hat{\Phi}\hat{\Phi}'} \quad . \qquad \textbf{(56)}$$

The velocity potential in equation **(55)** does consider losses due to reflection below 100%. If damping effects expressed by the effective attenuation coefficient as of equation **(12)** were to be taken into account, one had to replace the amplitudes by space dependent expressions

$$\hat{\Phi} \rightarrow \hat{\Phi} \cdot e^{-\alpha_{eff} x} \quad \text{and} \quad \hat{\Phi}' \rightarrow \hat{\Phi}' \cdot e^{-\alpha_{eff}(2l - x)} \quad . \qquad \textbf{(57)}$$

However, the acoustic contrast ratio, term II, is the interesting one in equation **(53)**: if the explicit expressions from equations **(3)** and **(16)** were used it turned out that the

acoustic contrast factors of the standing and the progressive wave, respectively, do not both vanish at the same values of the speed of sound ratio σ and the mass density ratio λ. Thus one deals with a *singularity* which lets the radiation force contribution of *any* progressive wave present in the resonator exceed that of the standing wave for certain combinations of the mentioned material properties of particles and host liquid. A progressive wave however can be assumed to be present in any realistic separation system[i].

Figure 38 shows the calculated absolute values[ii] of the acoustic contrast ratio as of term II in equation **(53)**. The ratio is given as height of a data point over a plane the axes of which are λ and. σ The "wall" represents the region where the acoustic contrast factor of the standing wave but not that of the progressive wave is vanishing. The graph was cut-off at values of one which means that the acoustic contrast factors are equal at the top. However the "wall" is of infinite height with the exception of the centre $\lambda = \sigma = 1$, where both contrast factors are zero and therefore II is not defined.

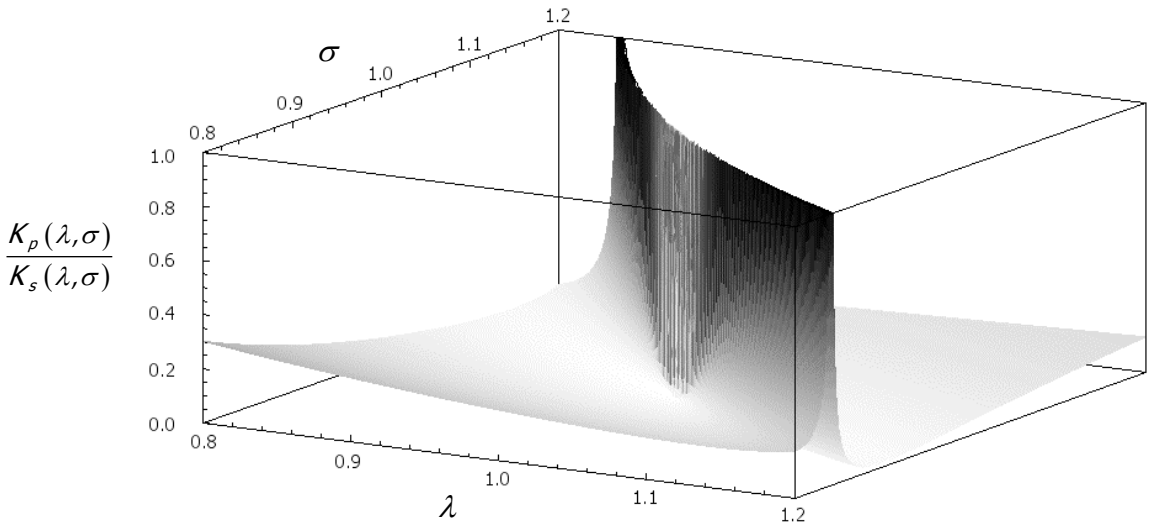

Figure 38 Ratio of the absolute values of the acoustic contrast factors of a progressive wave and a standing. The respective value is shown over a coordinate system of the ratios of mass density λ and speed of sound σ of particle and host liquid. The centre of the graph is modified to disguise confusing artefacts from calculation.

[i] Moreover the progressive wave is necessary to transport the energy replacing the losses within the resonator; a standing wave does not transport energy by definition.

[ii] The direction of the force does not matter here.

Each "point" on the surface in Figure 38 represents a suspension in terms of specific values of the mass density and speed of sound ratio (λ,σ) of the suspended particles and the host liquid, respectively. The evaluation of the acoustic contrast ratio for yeast cells suspended in water-EtOH mixtures was conducted with material properties for the water-EtOH mixtures as presented in Figure 37. For the mass density of yeast $\rho_{yeast} = 1114\ \mathrm{kg\,m^{-3}}$ was used[22], the speed of sound value was estimated from the measured compressibility of erythrocytes[78] to $\upsilon_{yeast} = 1642\ \mathrm{m\,s^{-1}}$.

The resulting values for λ and σ for yeast suspended in water-EtOH mixtures are assigned to the axes of Figure 39. In this illustration the acoustic contrast factor ratio $K_p(\lambda,\sigma)/K_s(\lambda,\sigma)$ is represented by the shading of the (λ,σ) plane, darker regions represent higher values as of Figure 38. With increasing EtOH concentration the "path" approaches the area where the acoustic contrast factor of the standing wave vanishes, however, critical regions are not reached.

As the particles here were yeast cells one may assume changes of their "material properties". The relaxing influence of EtOH on the cell envelope presumably could decrease the speed of sound within the cell. Furthermore mass transfer through the cells wall/membrane occurs, hence the mass density might change too[79]. Therefore the calculation was repeated with modified values of $\rho_{yeast} = 1018\ \mathrm{kg\,m^{-3}}$ and $\upsilon_{yeast} = 1512\ \mathrm{m\,s^{-1}}$, hence $\lambda = \sigma = 1.02$ when suspended in water. Figure 40 shows the acoustic contrast factor ratio $K_p(\lambda,\sigma)/K_s(\lambda,\sigma)$ for suspensions of such particles in water-EtOH mixtures. At EtOH concentrations around 10%($^{v}/_{v}$) the contrast ratio gets very close to those regions where the acoustic contrast factor of the standing wave and hence the cell-ordering effect vanishes.

Discussion

The described phenomenon of the radiation forces exerted by the standing wave on the particle vanishing at certain values of λ and σ has been used for purposes of the analysis of the adiabatic compressibility of liquid droplets and particles before[78,80,81].

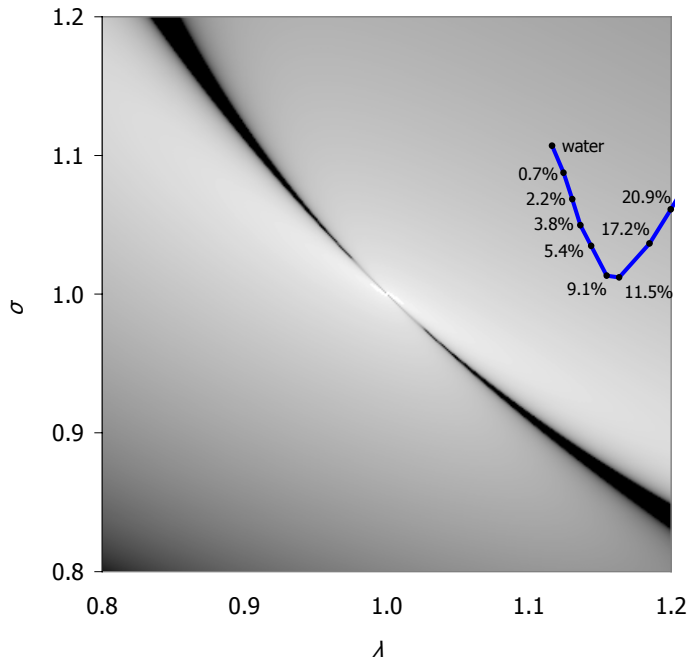

Figure 39 Acoustic contrast factor ratio $K_p(\lambda,\sigma)/K_s(\lambda,\sigma)$ of yeast cells suspended in water-EtOH mixtures. Numbers represent the EtOH concentration.

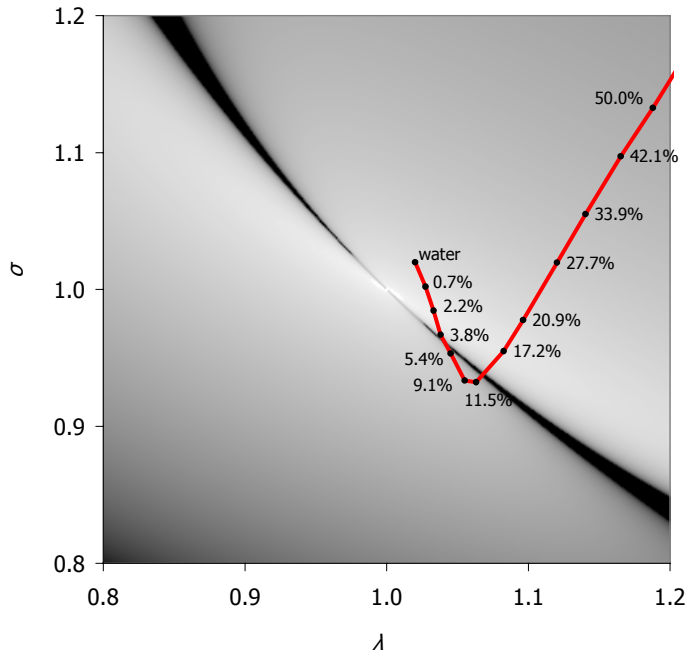

Figure 40 Acoustic contrast factor ratio $K_p(\lambda,\sigma)/K_s(\lambda,\sigma)$ of yeast cells with modified material properties suspended in water-EtOH mixtures. Numbers represent the EtOH concentration.

In this attempt to explain the breakdown of the spatial distribution of yeast cells in an acoustic field when water-EtOH mixtures were used as host liquid the speed of sound and mass density deviations in water-rich EtOH mixtures from the respective values in pure water were found to be a possible reason. This became most evident when certain changes of the respective properties of yeast cells were assumed.

The presented calculations of the acoustic contrast factor ratio, especially with hypothetical yeast cells with modified speed of sound and mass density, shed some light on the unexpected behaviour of turbulence in water-rich EtOH mixtures when subjected to a standing acoustic field.

However this explanation might not be exhaustive. Consideration of viscosity might be necessary, as water-rich EtOH mixtures show a substantial increase of viscosity up to 50%($^{v}/_{v}$) EtOH. At 12%($^{v}/_{v}$) EtOH the viscosity of water-EtOH is more than 1.5 times higher than for pure water.

Higher viscosity could lead to an increase of the radiation force, in particular in a progressive wave[82]. At high frequencies (above 1 MHz) and for particles above 1 μm in diameter the direction of the periodic force may change due to viscosity, particles that in the non-viscous case were driven into the pressure nodes are then concentrated in the displacement nodes[6]. The consideration of viscosity might explain as well the re-establishment of the spatial order at high true electrical power input settings as observed due to some unexpected dependence of the (adiabatic) compressibility of the host liquid on the pressure amplitude or acoustic energy density.

R2.5 Conclusion

The unexpected behaviour of yeast suspensions in the ultrasonic separation system in the presence of EtOH at low concentrations was investigated in detail.

- It was shown that the breakdown of the spatial distribution of cells was followed by complete mixing. The phenomenon was therefore turbulent, no retention/filtration could be measured.
- The breakdown occurred suddenly at a certain EtOH concentration and was reversible, i.e. the addition of water did terminate the streaming and re-established the ultrasonically induced spatial order.

- Heavy decrease of cell viability and an increase of intracellular material in the supernatant was detected after the suspension had been exposed to the turbulent streaming.
- Furthermore the ability of cells to reproduce was severely impaired after sonication, the cells showed alterations to their inner structure, namely the vacuole. All influences showed to increase with sonication time.
- Transmission electron microscopy delivered severe cell damage, especially to the cells' envelopes. Organelles were identified in the suspension.
- As un-sonicated controls exposed to water-EtOH mixtures did show significantly less reaction, the damage was concluded to be mechanical. The yeast cells were cracked open during the ultrasonic exposure very efficiently. There might be some application potential for this effect as well.
- It was shown by the spectra of the true electrical power input that no major differences in respect to the effective attenuation and the presence of a standing wave existed between water and water-EtOH.
- A standing wave was as well present when yeast cells were suspended in a 12%($^{v}/_{v}$) EtOH-water mixture although the separation system displayed the turbulence. However an additional energy consumption was detected by a decrease of the acoustic quality factor at higher settings of input power. This was interpreted due to the drain of kinetic energy by the moving particles within the active volume.
- The material properties speed of sound and mass density of water-rich EtOH mixtures were found to be responsible for the breakdown/turbulence as observed in the ultrasonic separation efficiency. The influences on the acoustic contrast factors between the yeast cells and the host liquid led to acoustic contrast factor ratios which delivered the primary radiation force contribution of the standing wave to be possibly smaller than that of the progressive wave.

R3 Effects of the spatial arrangement: Selective cell immobilisation and alterations of the resonator's acoustic behaviour

R3.1 Introduction

A novel technique was developed for the investigation of the spatial arrangement of the cells in the filter chamber caused by the acoustic forces involved[83,84]. The solid fraction of a suspension (cells or particles) was entrapped in a gel matrix by initiation of polymerisation chemically or thermally *during* the application of the ultrasound (see chapter M4). Thus the particles were "frozen" at their final positions throughout the ultrasonic field in a gel-block.

The novel method will be introduced in chapter R3.2.

The ability of the UES principle to retain particles size-selectively is exploited in chapter R3.3 for a mixture of yeast and the much smaller lactic acid bacteria.

The influence of the arrangement of particles on the acoustic properties of a resonator will be investigated in chapter R3.4. It is the first time this question could be addressed because changes of the acoustic field parameters, e.g. the frequency as it is necessary for a measurement, would instantaneously change the radiation forces exerted on the particles and therefore might change their arrangement. With the gel immobilisation technique the arrangement can be maintained independently of the sound field and therefore an investigation of the acoustic properties of the resonator without the feedback on the spatial arrangement of the particles within becomes possible.

R3.2 Polymerisation of the host "liquid" during sonication – a novel technique

The aim of this study was to evaluate a new technique, which allows to investigate of the effects of the ultrasonic standing wave field on suspended particles. Light microscopy was used to examine the positions of the cell aggregates in the acoustic field in relation to the positions of the field's pressure nodal planes as well as the arrangement of the cells within each nodal plane.

The separation system was filled with a suspension of yeast cells in liquid polyacrylamide and operated in batch mode. After the chemical initiation (see chapter M4.1) of the gelation the ultrasonic field was switched off and the chamber opened, the gel block was retrieved from inside the chamber. This specimen then was sectioned, cells were dyed with toluene blue. The cell distribution was examined by means of light microscopy, cells appear dark in the following figures.

The micrographs in Figure 41 to Figure 42 were taken from thin slices cut out of the gel-blocks in different directions.

Cuts in x,z-direction confirmed the presence of specific regions in the ultrasonic field, the periodical variation of the axial primary radiation force in direction of sound propagation was reflected by the cells' organisation in lines corresponding to the standing waves' pressure nodal planes (Figure 41a).

An aberration of the predicted behaviour was detected (Figure 41b) where cells were concentrated in regions along the direction of sound propagation. This phenomenon is called "dancing" and has been observed as being dynamic, i.e. the cells stream from one nodal plane to the next during sonication.

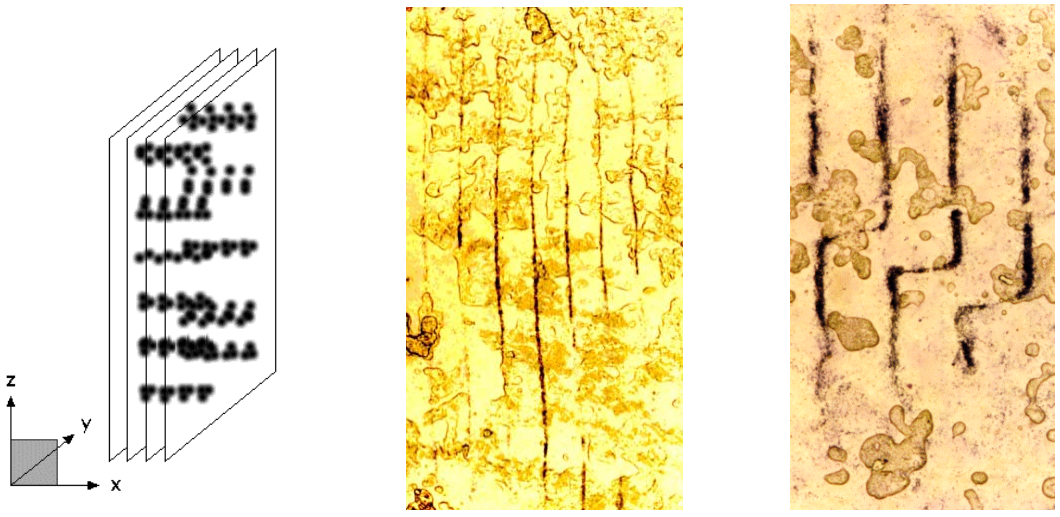

Figure 41 Light micrographs of sections of a polyacrylamide gel-block cut in x,z-direction. The lines (a) reflect the yeast cells which were concentrated in the pressure nodal planes of the standing acoustic field. The "dancing of the cells" (b), i.e. cells streaming from one plane to another is not explained theoretically yet.

Higher magnification of slices cut in x,z-direction however revealed some inner structure of the aggregates (Figure 42). Clearly the width of the bands was greater

than one cell's diameter (Figure 42a). A fine structure like predicted (compare Figure 4) to be brought about by the secondary radiation forces could not be detected. Instead, some kind of stream-like[i] behaviour was suggested by the pictures. However, if the cells in fact have been arranged in a helix as might be concluded from Figure 42b could not be answered due to the two-dimensional nature of the method presented here.

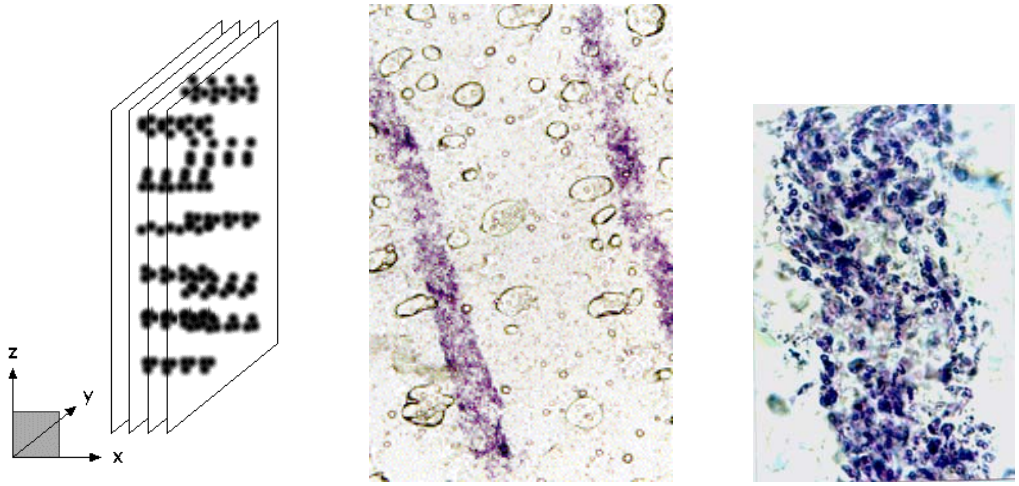

(a) (b)

Figure 42 Increasing magnification of vertical cuts revealed the planes to be several cell diameters thick (a). Instead of the layered structure predicted by theory, an uneven inner structure was found (b).

The cut in y,z-direction in Figure 43 suggested some spatial structure of the aggregates when looked at in direction of sound propagation. A closer look revealed the presence of vertical areas similar to columns, besides an evident characteristic of irregularity of the overall shape. An explanation by secondary acoustic forces failed due to the orientation of these columns. According to theory the layers of the fine structure (compare Figure 4) would appear as such a pattern, however, not in y,z-direction but in x,y- or x,z-direction, as they are parallel to the nodal planes.

The cuts in x,y-direction (Figure 44) showed the influence of the transverse primary radiation force as parallel columns of aggregates were detected. Computer image analysis methods were employed for the determination of the distance between two nodal planes (x_0 = 379.6 $\pm_{s.d.}$ 21.7 μm), which indicates that the speed of sound in

[i] As a term for description; if there was movement involved the imaging method was of course not able to pick up.

polyacrylamide was slightly higher than in water (half-wavelength 337.5 µm at 2.2 MHz, 25°C). The distance between two columns resulting from the concentration within the nodal planes was determined to be $y_0 = 3427.7 \pm_{s.d.} 88.9$ µm. This value is essentially an individual behaviour of the transducer in use and therefore could not be compared to a theoretical counterpart.

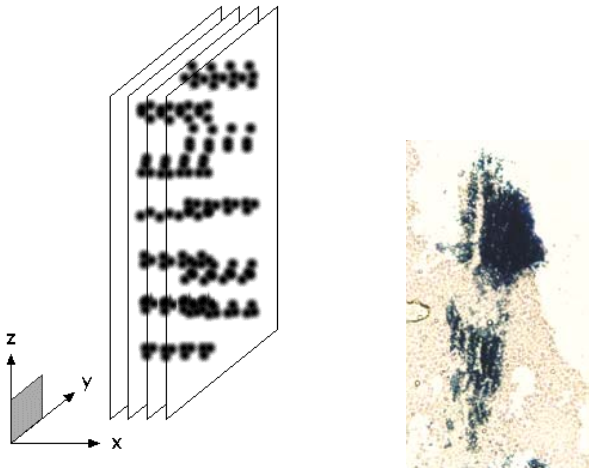

Figure 43 In z,y-direction the overall shape of an aggregate is rather irregular. The fine structure as observed could not be explained by secondary radiation forces.

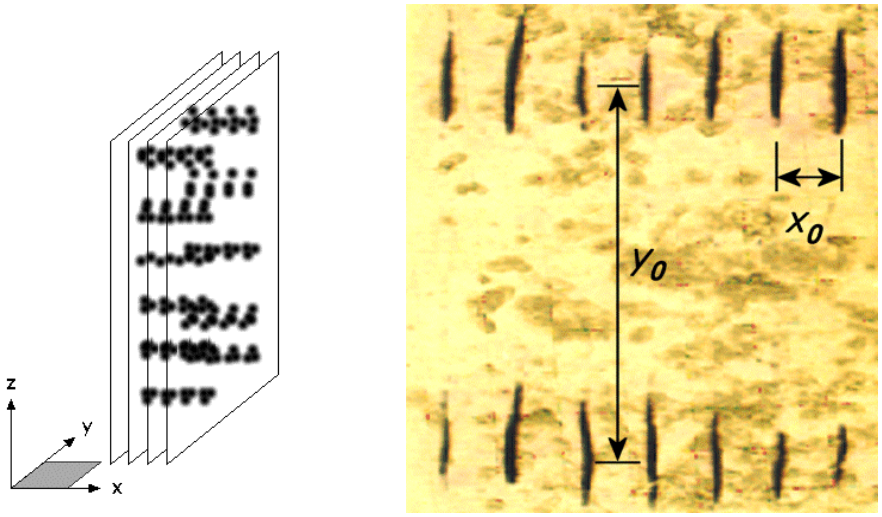

Figure 44 A cut in x,y-direction reflected the influence of the primary radiation forces. The half-wavelength was measured to be $x_0 = 379.6 \pm_{s.d.} 21.7$ µm, the distance between the columns was $y_0 = 3427.7 \pm_{s.d.} 88.9$ µm.

Growth of yeast ultrasonically arranged in gel

While gel entrapment was reported to increase the tolerance of cell cultures to external stress factors[25,26,73], ultrasonic forces have shown to be useful in manipulating and concentrating yeast cells within a gel. The task in the following experiment was to check for the ability to reproduce of gel-entrapped cells after having been arranged by an ultrasonic standing wave field.

Freshly grown yeast cells were suspended in 5%($^{w}/_{v}$) malt extract agar. This growth medium used for cell cultivation is a thermo-gel, i.e. the polymerisation is brought about by decreasing the ambient temperature below some 37°C. Therefore procedures had to be adjusted in that the gelation process could not be initiated untimely, and the sound field had to be present until the filling of the separation system was cooled down throughout the active volume. Subsequently the gel-block was retrieved from the chamber and put into an incubator at 30°C for four days.

Figure 45a shows the cells immediately after arrangement to the standing ultrasound field. It was confirmed that the cells were viable and reproductive, as a significantly higher number of cells were detected in the specimen that has been kept in the incubator (Figure 45b).

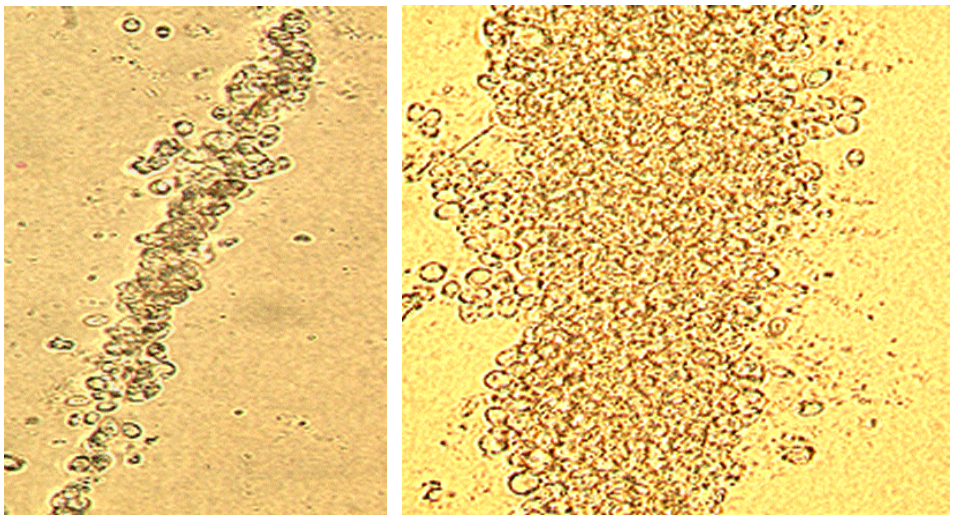

(a) (b)

Figure 45 Growth of yeast cells arranged in malt extract agar by ultrasound. Pictures taken immediately after the manipulation (a) and after four days (b) of incubation.

Discussion

The experimental findings presented here showed the novel technique of gel immobilisation to provide insights to the effects of radiation forces on cell suspensions in an ultrasonic standing wave field.

The axial and transverse primary acoustic radiation forces ordered yeast cells as predicted by theory. However the postulated influence of the secondary radiation force was not found, the aggregates appeared to have a twisted structure.

A cut parallel to the transducer surface revealed an uneven distribution of yeast cells which would allow the perfusion of liquid parallel to the axis of sound propagation. Thus a nutrient medium can reach cells immobilised in an ultrasonic field.

It was shown that yeast cells arranged in a viable gel were replicating.

R3.3 Size selective effects in a yeast/lactic mixture

Lactic acid bacteria are a common contamination in brewing and the question was, if their number can be reduced within a given yeast suspension by UES.

The following experiment was carried out like the separation efficiency measurements for the flow-through set-up in R1.2, however, the suspension used here was a mixture of freshly grown *S.cerevisiae* strain NCYC 1006 at a concentration of $3.9 \cdot 10^7 \pm_{s.d.} 5.4 \cdot 10^6$ cells/mL and the lacto-acid bacteria *L.brevis* (see chapter M2.2) at a concentration of $1.8 \cdot 10^8 \pm_{s.d.} 1.2 \cdot 10^7$ cells/mL. *L.brevis* is rod shaped and smaller (~1 μm in diameter and 2-4 μm in length) than yeast cells. Single cells of *L.brevis* tend to form chains when grown in suspension.

As shown in Figure 46 a significant difference in separation efficiency (*S.E.*) between the two cell types was achieved. While yeast was retained pretty much like in the experiment where no other particles had been present (dashed grey line, compare Figure 14a), the lactic acid bacteria showed a maximum *S.E.* of below 50%. The separation efficiency for yeast cells was therefore significantly higher than for *L.brevis*. The volume that had passed until the main increase was finished was roughly 40-50 mL for both cell types.

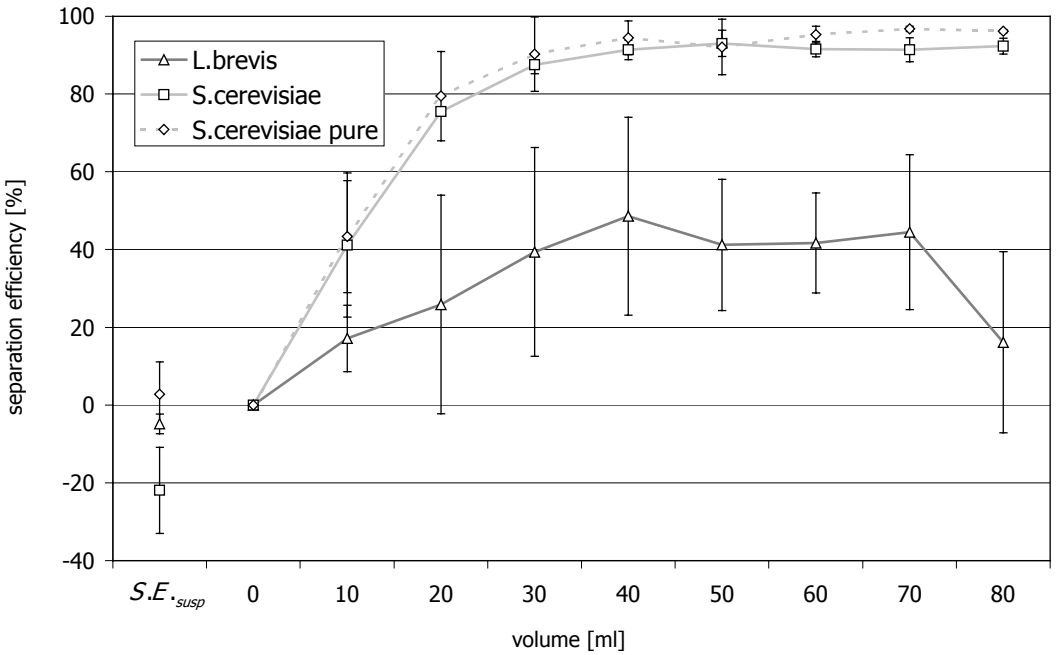

Figure 46 Selective separation efficiency of a yeast/lactic mixture. The Ultrasonically Enhanced Settling showed the predicted size selectivity as the *S.E.* for yeast was significantly higher than for *L.brevis*. Throughput was 5.6 L/d and 8 W true electrical power input was applied. The dashed line represents repeated data from Figure 14a. A settling of yeast cells unrelated to ultrasonic effects was measured as indicated by $S.E._{susp}$.

Figure 47 shows the spatial distribution of yeast and bacteria cells prior to sonication. The cells were dispersed evenly, due to the differences in size and shape both types could be identified easily.

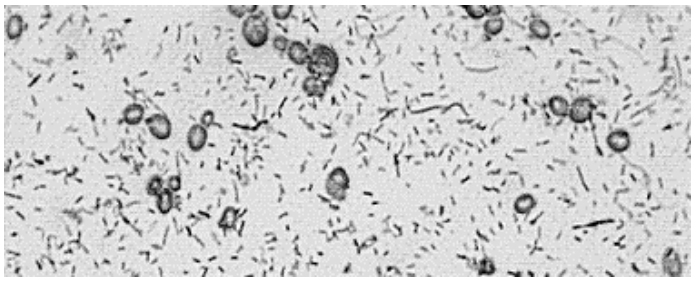

Figure 47 Thin-slice light-micrograph of a mixture of *S.cerevisiae* and *L.brevis* in polyacrylamide gel, both cell types were homogeneously distributed.

The ultrasonic standing wave field was applied during the gelation of the suspension. The micrograph thereof in Figure 48 indicated selective effects on the different cell lines. The yeast cells were driven into the pressure node. The smaller

L.brevis however were concentrated less effectively and detected at some distance from this region.

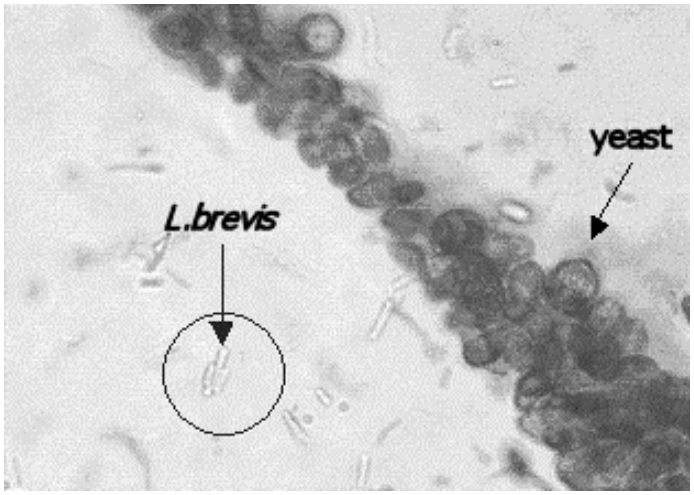

Figure 48 Micrograph taken after sonication. *L.brevis* cells were detected outside the pressure nodal region where the yeast cells were concentrated.

Lower magnification (Figure 49) for the sake of a wider viewing angle revealed some increase in *L.brevis* concentration in the proximity of the pressure node, however *L.brevis* cells were distributed more homogeneously than yeasts.

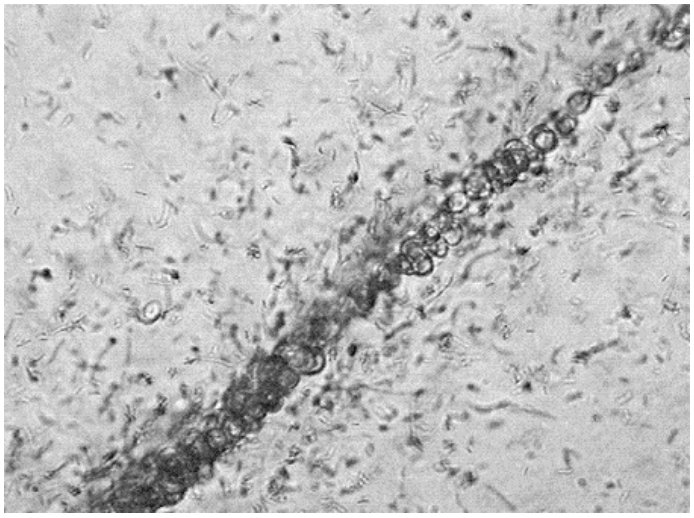

Figure 49 Micrograph taken after sonication with wider field of view than for Figure 48; some increase of concentration of *L.brevis* cells towards the pressure nodal region was detected.

Discussion

The gel-method provided the means to confirm the suspicion that the difference in the radiation forces acting on the two types of particles was responsible for the different *S.E.* The arranging forces exerted on yeast cells were stronger than those acting on the smaller bacteria, the spatial arrangement for the latter therefore was less pronounced. Hence the draft of the liquid carried a higher fraction of the lactic acid bacteria to the outlet.

The comparison with results presented in chapter R1.2 revealed a slight difference between the *S.E.* data for the yeast there and the result just shown. A settling effect not caused by the ultrasound was measured as indicated by the negative separation efficiency of $S.E._{susp}$ in Figure 46. The reason for that may have been the tendency of freshly grown yeast cells to stick to each other which leads to a fraction of compounds of two or three cells. This reduced the cell concentration to $3.2 \cdot 10^7 \pm_{s.d.} 5.6 \cdot 10^6$ cells/mL in the beginning of the run which explains the slight subsequent reduction of *S.E.* due to lower initial bio-mass load (compare Figure 14a).

This result is of practical relevance as it was shown that the ratio of the cell concentrations of yeast and lactic acid bacteria could be positively influenced. An enrichment of yeast in respect to contaminating bacteria by UES is possible.

R3.4 Alterations of the resonator's electrical admittance due to the arrangement of particles

The question if the acoustical behaviour of the resonator changed when the spatial arrangement of particles in the suspension took place was addressed with the gel immobilisation technique for the first time[85].

The scope of the following experiments was to examine the dependence of the resonance quality factor on the spatial arrangement of suspended yeast cells as it can be assessed by measurement of the true electric power input at a given voltage or, at higher accuracy, by the electrical admittance (real and imaginary parts) of the resonator at different frequencies.

In-situ measurement at operational levels of true electric power input

The active volume of the separation system in batch set-up (Figure 9, left) was filled with yeast suspended in liquid 1.2%(w/v) agar technical. The suspension was then sonicated to arrange the cells until cooling had solidified the gel.

On continuing sonication the true electric power input at operating levels was then measured at a fixed output voltage level of the amplifier over a frequency range around the initial driving frequency at which spatial ordering had been brought about. Due to the fixation of the cells' positions by the gel the cells could not be moved anymore by the radiation forces. Figure 50 shows the comparison of this data set expressed as true electrical power input over frequency to a measurement of a sample that had been polymerised with the cells equally distributed in the volume. The resonance quality factor defined by the ratio peak height to peak width, was slightly decreased in the case of ordered cells. The frequencies of the corresponding peaks were slightly shifted due to a change in speed of sound[i].

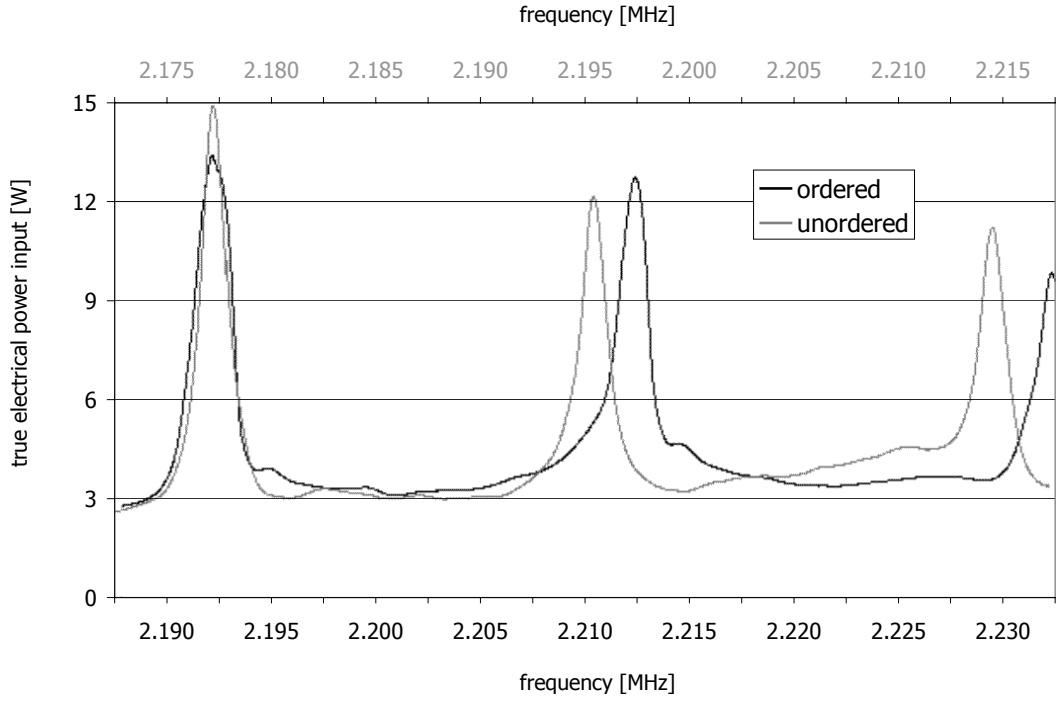

Figure 50 Comparison of the true electrical power input at operation level for the separation system filled with yeast cells 'frozen' in agar technical - freely suspended (grey) and in final arrangement (black).

[i] Besides an explanation by the ordering of the cells this could be a result of temperature differences too.

High-precision measurements employing a special resonator

An experimental system employed for more accurate measurements is shown in Figure 51. Two PZT ceramics glued to either side of a cuvette ensured a symmetrical sound field in respect to the temperature-dependent wavelength as the transducers emit moderate heat into the active volume (AV). Since this volume was also smaller (2 mL) than the UES system used elsewhere in this work, temperature gradients were supposed to be less steep, thus decreasing their influence on the wavelength in direction of sound propagation.

The active volume was filled with a suspension of particles at a solid mass load of 5 g/L in liquid 1.2%(w/v) agar technical. Two types of particles were used: bakery's yeast and latex beads (Bangs Laboratories) which had about the same size distribution as the cells. The volume was then sonicated to arrange the particles until cooling had solidified the gel.

Subsequently, the measurements of the resonator's electric admittance were taken using very low levels of electrical power input, therefore no temperature changes could influence the results. The admittance measurement system was described by Schmid et al.[54].

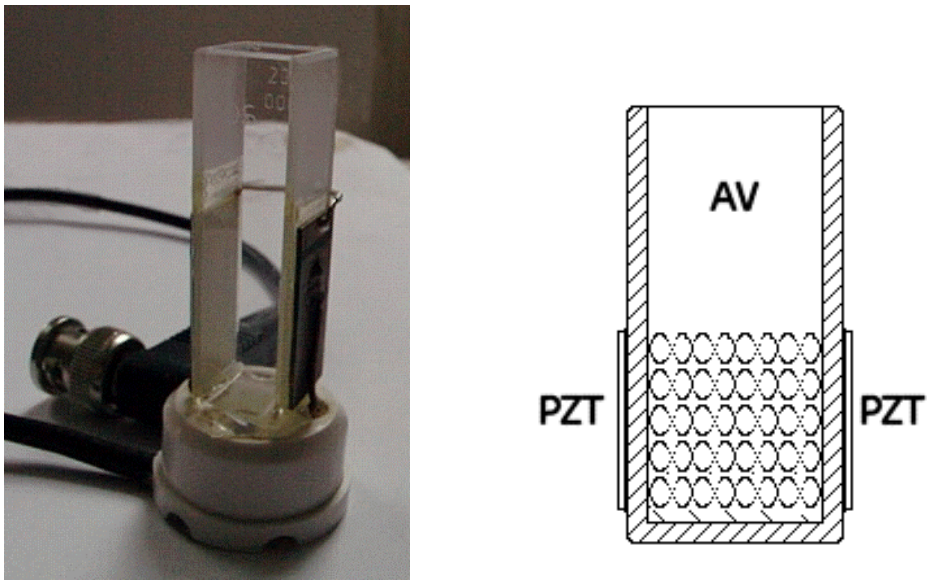

Figure 51 Experimental resonator with two piezoelectric ceramics (PZT) glued to either side of a glass cuvette to deliver a more symmetric acoustic field. The active volume (AV) was holding the suspension.

The results in Figure 52 to Figure 54 consist of locus plots[i] (upper graphs) and of the frequency spectra of the absolute electrical admittance (lower graphs). The smaller circles of the locus plots refer to the corresponding lower resonances, which were as well used for the separation process before. Numbers in the upper graphs are the resonance quality factors, in the lower graphs numbers refer to the peak admittance values.

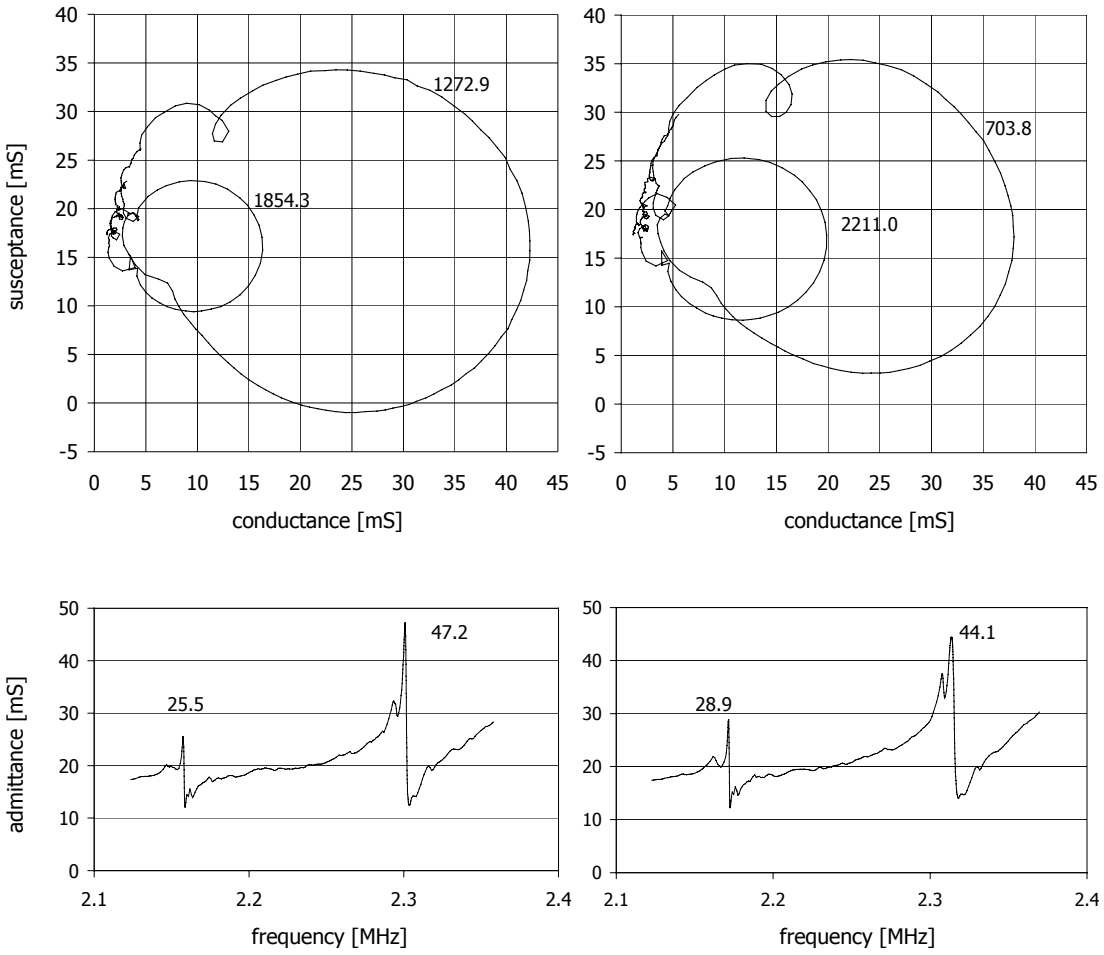

Figure 52 Highly accurate control measurements of the complex electrical admittance of the experimental resonator system filled with water (left) and 1.2%($^{w}/_{v}$) agar technical (right).

[i] A locus plot shows the imaginary and real part of the admittance, respectively, on the complex plane. The frequency is the curve parameter, i.e. changing over the curve.

No significant differences were detected for the control measurements of the pure host media water (Figure 52, left) and gel (Figure 52, right). Addition of 5 g/L yeast cells into the agar did not change the result significantly as well, as long as the solid fraction was freely suspended (Figure 53, left). However, the fixation of the spatial distribution of the cells in the pressure nodal planes during sonication showed remarkable influences on the subsequent high accuracy admittance measurement (Figure 53, right). The separation frequency of about 2.15 MHz showed a significantly lower admittance peak and the height of the second peak was decreased as well.

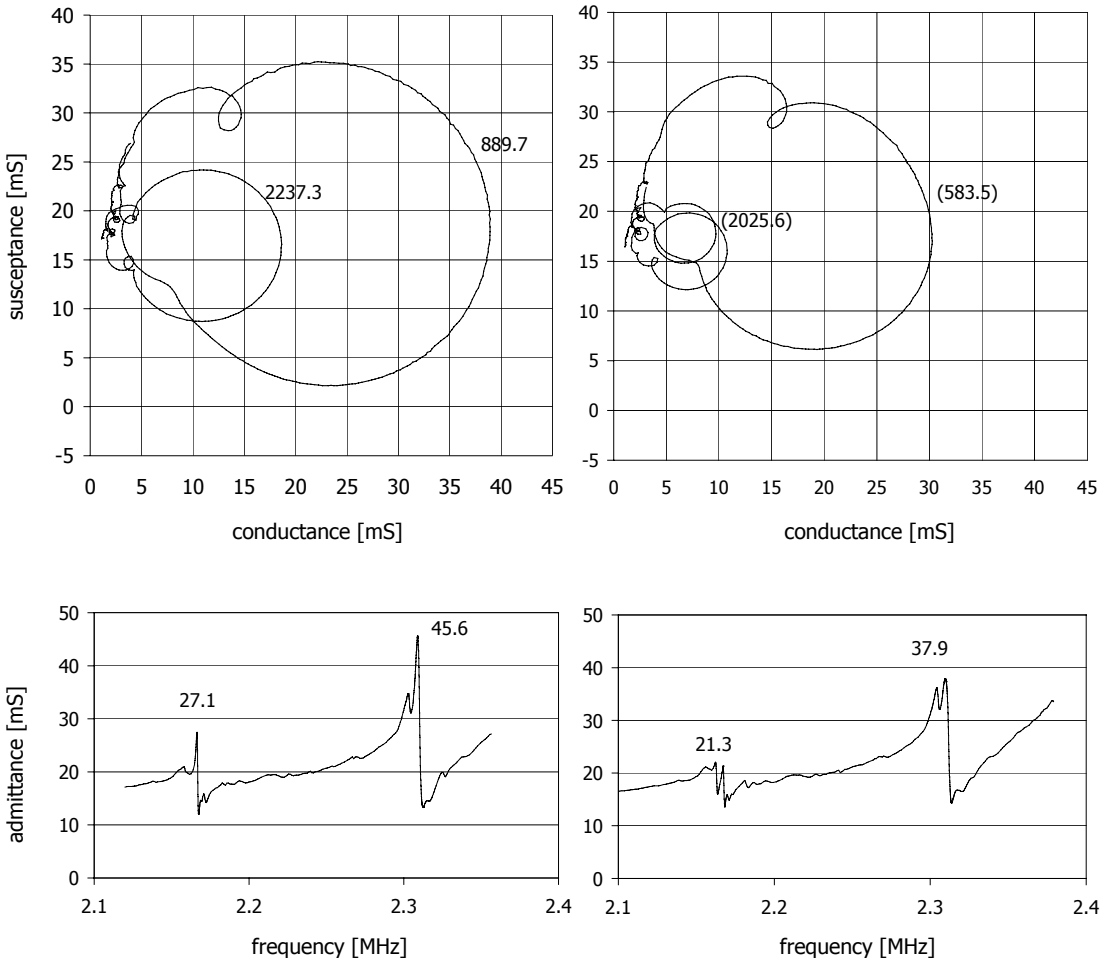

Figure 53 Highly accurate measurements of the complex electrical admittance of the experimental resonator filled with yeast cells (5 g/L) suspended in 1.2%($^{w}/_{v}$) agar technical. A significant decrease of the resonance quality factors or admittance peak heights, respectively, was detected when the cells were arranged due to preceding sonication (right) in comparison to a homogeneous distribution of cells in the gel (left).

Along with this effect a spurious mode was excited as shown in the locus plot by the double circle for the separation frequency of 2.15 MHz. The automatic detection of the quality factors by the measurement system failed for this reason, calculation by hand is denoted by the brackets around the numbers.

Figure 54 shows the results for the latex beads. The changes of the admittance due to the arrangement of the particles was very similar to the result for yeast cells. Again the separation frequency showed a significant lower admittance and the second peak was decreased. The excitement of a spurious mode however, might not have taken place to the same extent for the latex particles as for the yeast cells.

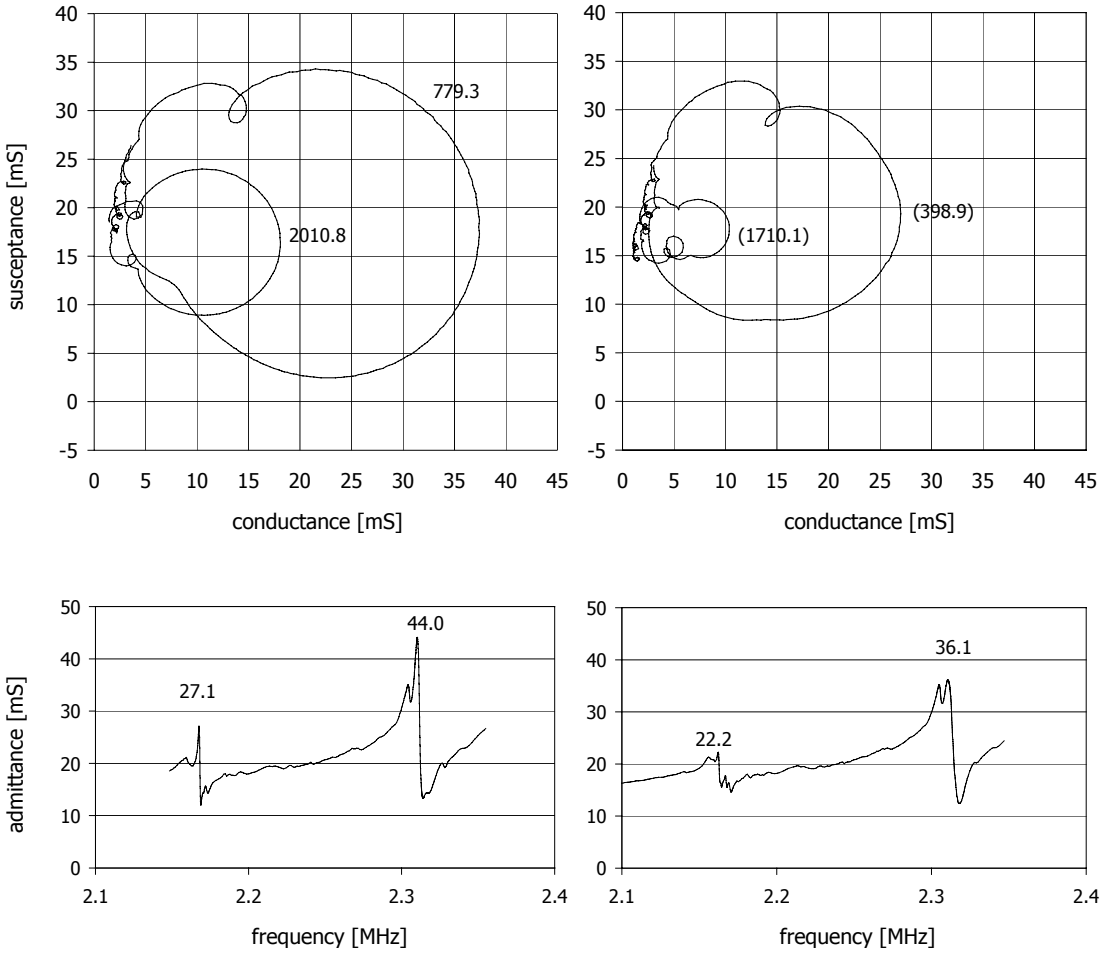

Figure 54 Highly accurate measurements of the complex electrical admittance of the experimental resonator filled with latex beads (5 g/L) of a similar size distribution as yeast suspended in 1.2%($^{w}/_{v}$) agar technical. A significant decrease of the resonance quality factors or admittance peak heights, respectively, was detected when the beads were arranged due to preceding sonication (right) in comparison to a homogeneous distribution of the particels in the gel (left).

Discussion

The comparison of the resonator admittance results between freely suspended and arranged particles delivered a decrease of the resonance quality factors in the latter case. Similar results were achieved with two different types of suspended particles, yeast and latex beads.

That an effect exists was shown and the different acoustic behaviour is plausible if a damping mechanism due to the ordering of the particles is assumed. However, further investigations aiming on the exact nature of this attenuation are necessary, the effect is easily accessible by the electric admittance (or impedance) measurement at the transducer electrodes.

This could be exploited in future separation systems. An on-line measurement system could precisely detect when the arrangement of particles is finished, the acoustic field and the throughput pump could be automatically switched off at this moment to let the aggregates settle. This might increase the performance number – throughput per power input and time – by decreasing the energy consumption.

R3.5 Conclusion

The presented novel gel immobilisation technique was shown to be suitable for the investigation of ultrasonically arranged particles. The following results were obtained:

- The effect of the acoustic radiation forces on different particles was examined employing light microscopy.
- An explanation for different separation efficiencies of a two particle suspension, *S.cerevisiae* and *L.brevis*, was found in the particle-specific spatial distribution in respect to the periodic pattern of the standing wave.
- It could be shown that the arrangement of particles by an ultrasonic field influences the field itself. A decrease of the resonance quality factors of the separation system was detected.

R4 Examination of damage to yeast cells exposed to plane ultrasonic fields

R4.1 Introduction

Ultrasonic systems are used routinely to break up cells, for instance when substances produced inside are of interest. For this purpose, however, much lower frequencies in the ten and hundred kilohertz range are used and completely different transducers called horns irradiate the suspension with a high-energy progressive wave in such ultrasonic disruptors[86]. Yeast cells however are known even in this regime to be resistant, intense sound exposure is necessary for the brakeage[87].

Therefore it was necessary to further investigate the cell damage and decreased viability reported in chapter R2.3 as the separation system used here was tested with various cell lines, however a decrease of viability or cell damage as reported in chapter R2 was not reported when UES or similar ultrasonic particle manipulation was applied.

In chapter R4.2 the results of thorough examinations will be presented, if cells exposed to ultrasound generating the described heterogeneous spatial ordering, i.e. driving the cells in the pressure nodal planes, display alterations to various properties.

Thacker[88] connected the presence of air bubbles in addition to ultrasonic treatment with yeast damage, finding distinct differences between sonication with 20 kHz and 1 MHz. During the experiments presented in chapter R2 gas arising from the process of mixing of EtOH and water has been present. At the same time cell damage was observed. Therefore a sono-chemical test has been applied to check for cavitation as described in chapter R4.3.

A different resonator advantageous from the observation point of view was used to further confirm and enhance these results in chapter R4.4.

Anticipating some results, it was indicated to investigate the response of yeast to the exposure of altered ultrasonic fields. In chapter R4.5 the absence of viability changes due to a standing wave applied to gel immobilised cells will be reported and chapter R4.6 is about the sonication of yeast suspensions in a separation system with a

reduced reflection coefficient thus producing a sound field with a low standing and a significant progressive wave component.

R4.2 Effects on yeast exposed to ultrasound in the pressure nodes of a standing wave field

The UES principle is purely based on gentle, acoustically induced, loose particle aggregation followed by sedimentation. It has been shown that the use of cell filters based on the UES principle is not influencing the viability of yeast and other cell lines[5,7,9,10], methods employed included flow cytometry[20].

However the results of chapter R2.3 showed severe influences on yeast[89]. Thus the investigations in this section will concentrate on the question, to which extent the exposure to ultrasound in the pressure nodes, essentially due to acceleration/vibration, affects the viability, integrity/leakage, the ability to reproduce and also the vacuole of the cells.

Effects on viability, integrity, ability to reproduce and morphology

The study was conducted for *S.cerevisiae* NCYC 1006 in the logarithmic phase (20-24 hours) and the stationary phase (40-60 hours) of the growth cycle separately. Older cells have divided more often and each replication leaves a bud mark in the cell wall. The number of such marks alters the mechanical strength of a cell and furthermore older cells have larger vacuoles. Mechanical damage to the cell envelope and the vacuole was suggested, thus specific effects on these components could surface when results were compared.

Logarithmic phase

The viability was examined using the methylene blue staining technique (see chapter M3.3). The result in Figure 55 showed no influence of the sonication on the ratio of viable/non-viable cells. For all treated samples and controls the average viability was measured to be above 94%, standard deviation was low as indicated by the error bars.

The absorption of UV-light of 280 nm (see chapter M3.4) had been used to establish a statement if yeast cells leak intracellular material into the supernatant when sonicated in water. The means of the optical density (O.D.) readings at 15, 30 and

60 minutes in Figure 56 did not show any increase of leakage over time, the standard deviations were as well low and of equal magnitude.

Plate counts (see chapter M3.5) yielded data about the cells' ability to reproduce on a plate. To increase the precision of the measurement the numbers of colony forming units (CFU) found on the malt agar extract plate were normalised by the cell concentration of the individual samples giving a CFU/cell ratio shown in Figure 57.

The resulting values were decreased in both the sonicated sample and the control to some 50%. The large standard deviations of the means prevented a significant result, whether the exposure to the ultrasound affected the cells' ability to reproduce in comparison to the un-sonicated control. Furthermore no influence of the duration of the sonication was observed due to this instability. Except for the 60 minute measurement, the standard deviations for the controls where higher than for the treated samples.

The integrity of the internal structure of the cells' vacuoles was measured with a fluorescent vacuole membrane stain (see chapter M3.6). No influence of the sonication and very low standard deviations where the result for yeast cells in logarithmic phase (Figure 58).

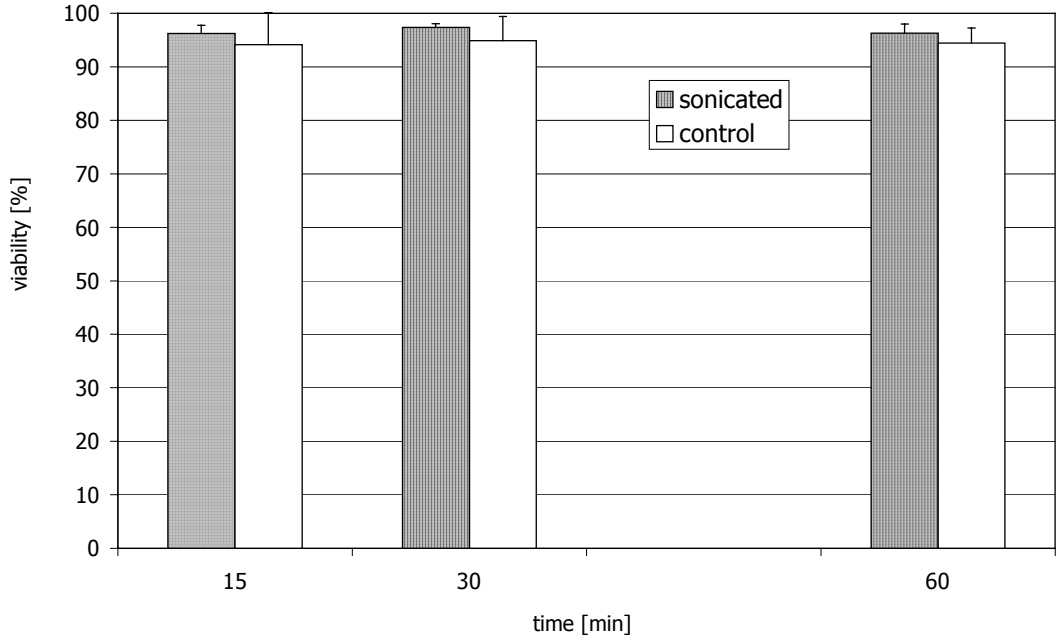

Figure 55 Viability measured by methylene blue counts. Data acquired after 15, 30 and 60 minutes of log-phase yeast cells suspended in water sonicated at 24 W. The cells were kept in the pressure nodal planes in the separation system in batch set-up.

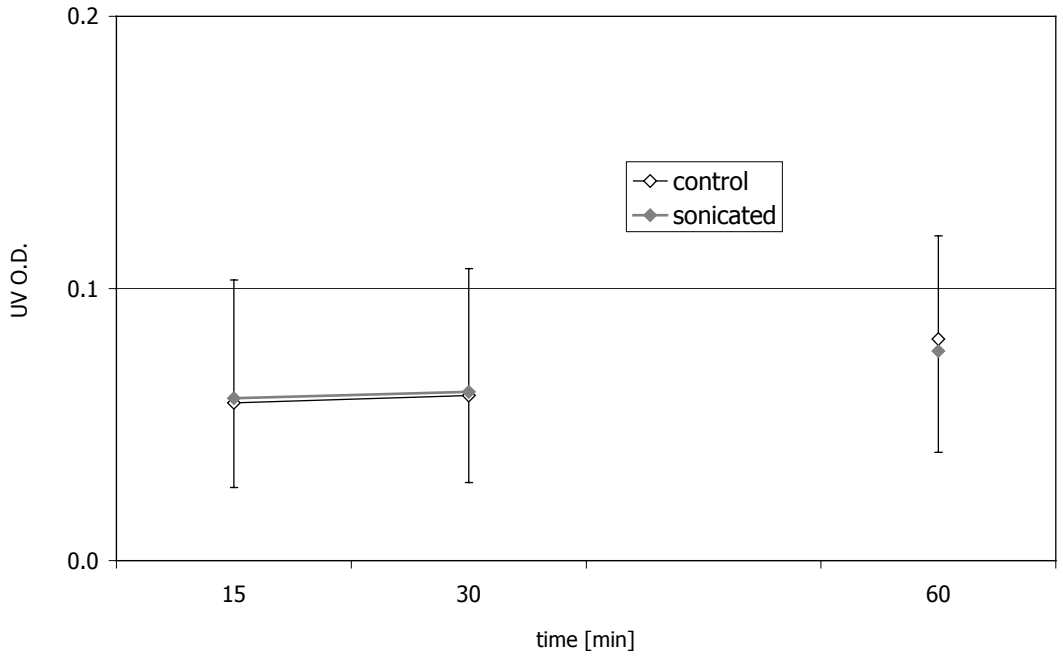

Figure 56 Measurement of the amount of intracellular material in the supernatant by the O.D. of ultraviolet light at 280 nm. Data acquired after 15, 30 and 60 minutes of log-phase yeast cells suspended in water sonicated at 24 W. The cells were kept in the pressure nodal planes in the separation system in batch set-up.

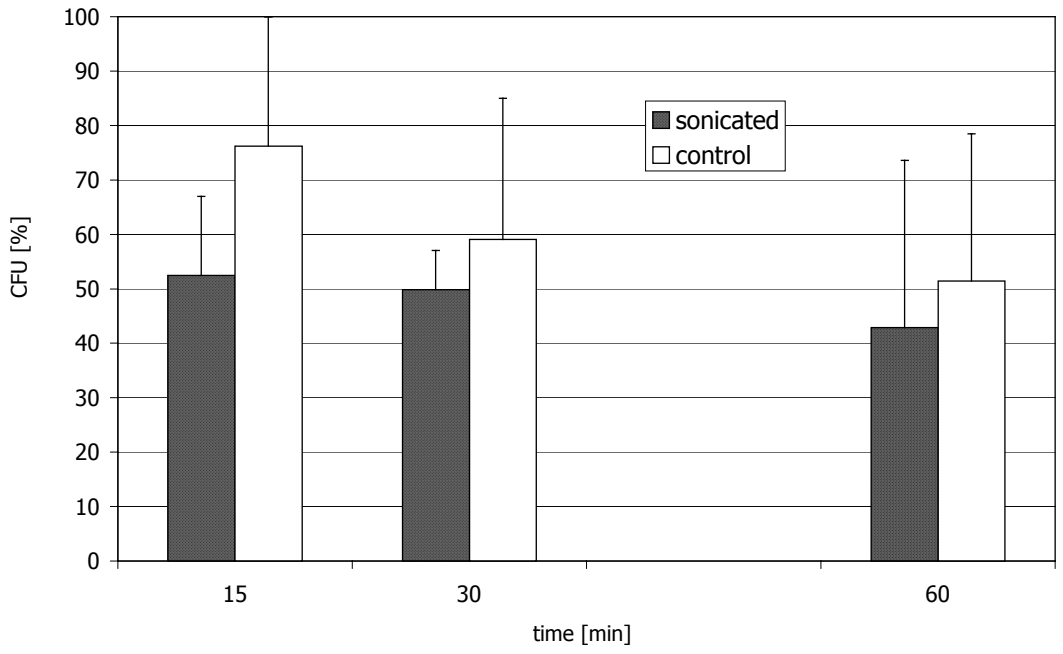

Figure 57 The cells' ability to reproduce as of viable plate counts, result given in percentage CFU. Data acquired after 15, 30 and 60 minutes of log-phase yeast cells suspended in water sonicated at 24 W. The cells were kept in the pressure nodal planes in the separation system in batch set-up.

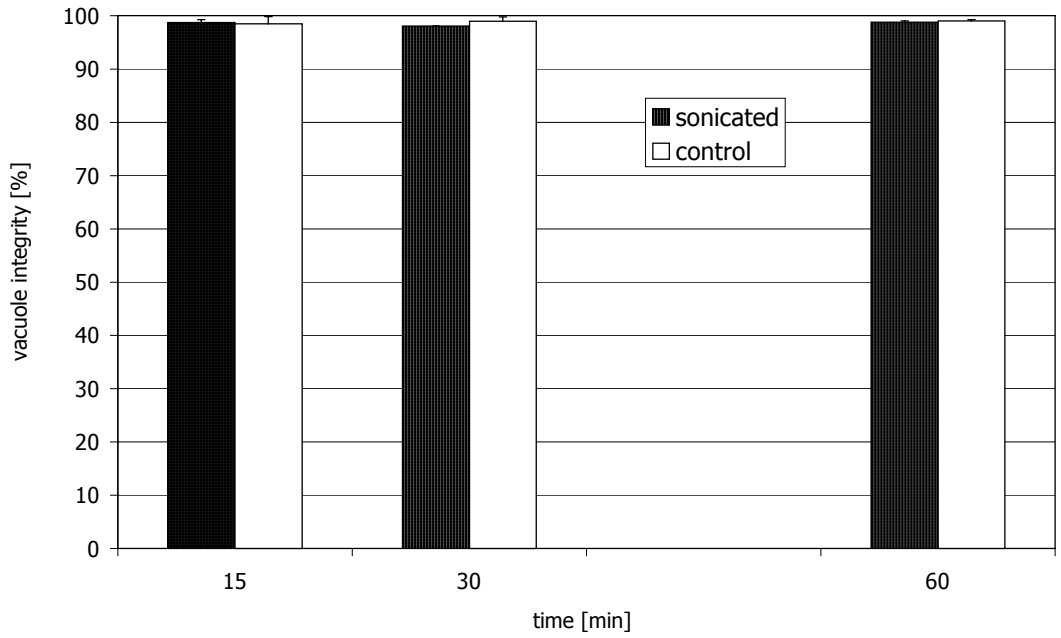

Figure 58 Fluorescent vacuole membrane dye counts to asses the internal integrity of the cells. Data acquired after 15, 30 and 60 minutes of log-phase yeast cells suspended in water sonicated at 24 W. The cells were kept in the pressure nodal planes in the separation system in batch set-up.

Stationary phase

For the same set of experiments as described above, but with suspended yeast cells in the stationary phase of growth, results were as follows.

Methylene blue counts delivered unaffected viability and low standard deviations (Figure 59).

No significant increase in leakage was detected comparing the UV O.D. of sonicated samples and controls (Figure 60).

The results of plate counts for cells in the stationary phase as presented in Figure 61 did not conclusively show a time/dose response or an effect of the sonication due to high standard deviations.

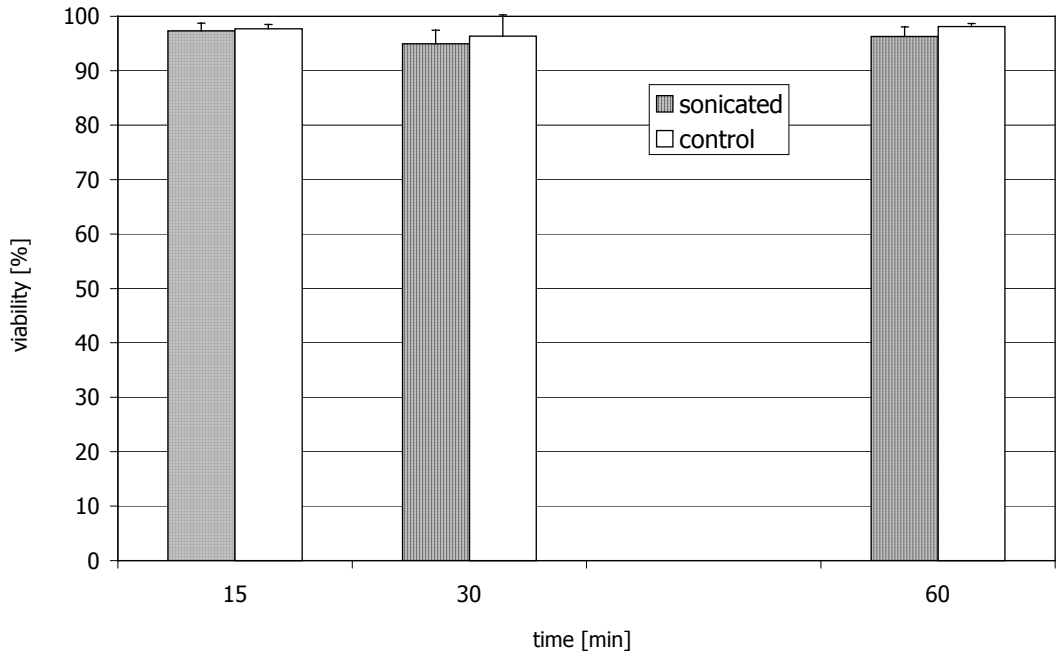

Figure 59 Viability measured by methylene blue counts. Data acquired after 15, 30 and 60 minutes of stat-phase yeast cells suspended in water sonicated at 24 W. The cells were kept in the pressure nodal planes in the separation system in batch set-up.

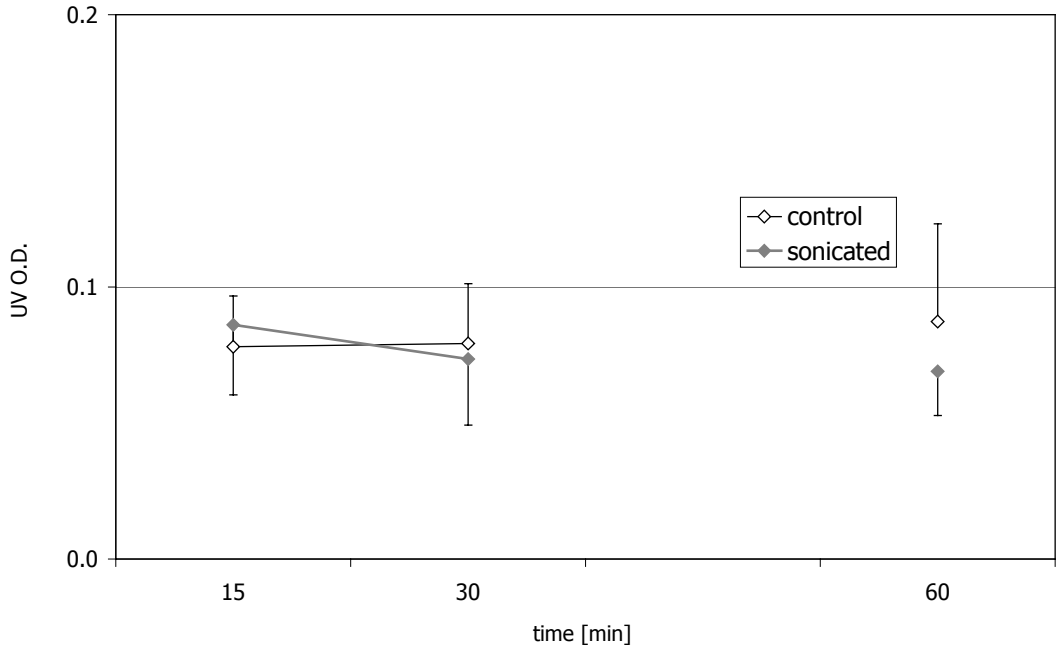

Figure 60 Measurement of the amount of intracellular material in the supernatant by the O.D. of ultraviolet light at 280 nm. Data acquired after 15, 30 and 60 minutes of stat-phase yeast cells suspended in water sonicated at 24 W. The cells were kept in the pressure nodal planes in the separation system in batch set-up.

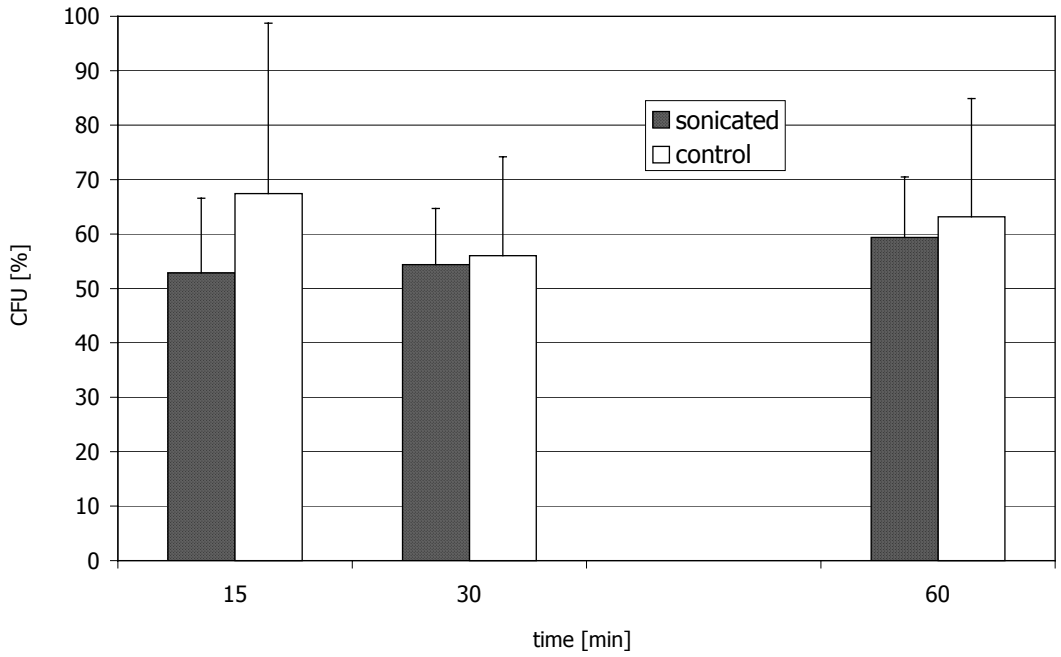

Figure 61 The cells' ability to reproduce as of viable plate counts, result given in percentage CFU. Data acquired after 15, 30 and 60 minutes of log-phase yeast cells suspended in water sonicated at 24 W. The cells were kept in the pressure nodal planes in the separation system in batch set-up.

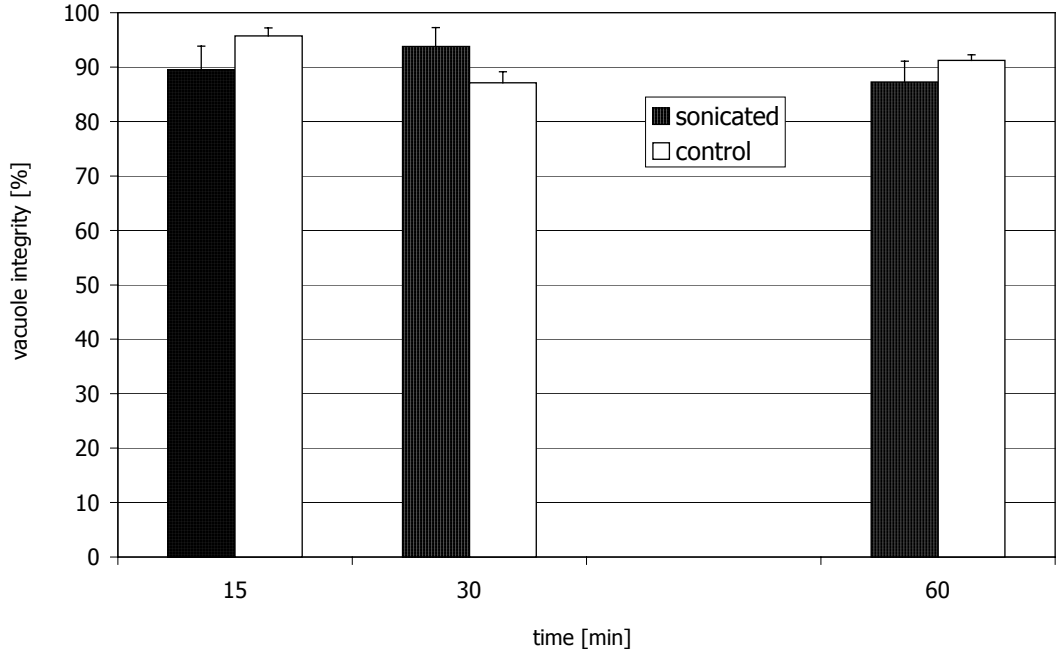

Figure 62 Fluorescent vacuole membrane dye counts to asses the internal integrity of the cells. Data acquired after 15, 30 and 60 minutes of stat-phase yeast cells suspended in water sonicated at 24 W. The cells were kept in the pressure nodal planes in the separation system in batch set-up.

The composition of the cells' vacuoles however was different for stationary phase cells. The standard deviation was slightly higher than for the results in logarithmic phase. Figure 62 shows values around 90% - in comparison to well over 95% for the log-phase cells - for both the controls and the sonicated samples. No trend over time could be detected.

Comparison of fluorescent vacuole membrane staining results

This investigation was set out to establish if significant differences existed between the vacuole states of logarithmic phase and stationary phase cells and whether sonication influenced the vacuoles at any phase of growth.

Sonicated samples where compared to controls for the different stages in the growth cycle, regardless how long the ultrasound was applied. The result (Figure 63) clearly showed, that in respect to this examination there was a difference between logarithmic and stationary phase cells. While for the logarithmic phase no influence of sonication was measured, results for the stationary phase had to undergo a t-test. Some possibility of an effect of the ultrasound existed but below the significance level ($P = 0.11$).

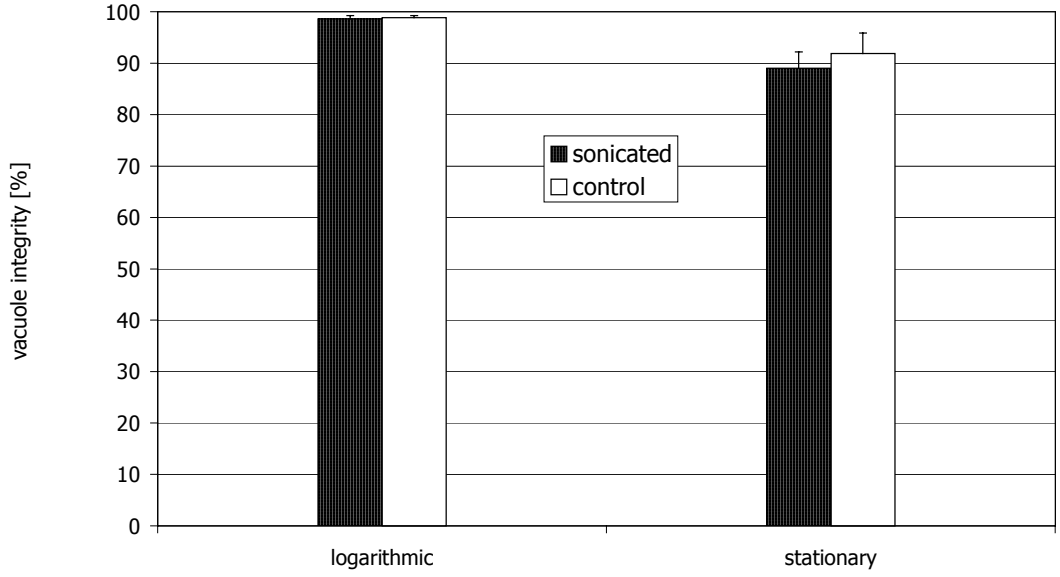

Figure 63 Fluorescent vacuole membrane dye counts for the comparison of the influence of a standing wave on cells of different age. Results showed a trend to a very mild effect on the older cells in stationary phase.

Statistical examination of plate counts

The results of viable plate counts for logarithmic and stationary phase cells were noisy. It was not clear why the standard deviation was increased, the measurements were carried out with much care. However the lack of evidence about an influence of the exposure to sound was unsatisfactory, hence it was tried to improve the limited result by statistical means.

These investigations were not aiming on significant differences between logarithmic phase and stationary phase cells. Thus, to increase the number of samples, the hypothesis that each of the two corresponding samples (15, 30 and 60 min. treatment and control respectively) came from the same populations with the same means has been tested. A two-tailed t-test showed this to be likely (*P*-values 0.39, 0.61, 0.67, 0.53, 0.45, 0.62), but in one case (60 min. treatment) the assumption of the variances being unequal had to be used. The means of both the logarithmic and the stationary results and the standard deviations thereof are shown in Figure 64.

That analysis of variances (ANOVA) was applicable had to be shown by means of a one-tailed F-Test checking for equal variances of treated samples and controls for each time-point. Although the hypothesis of equal variances had to be dropped for the data of 30 min ($P = 0.033$) and almost for 15 min ($P = 0.051$) sonication, it was assumed, that the subsequent ANOVA was stable enough due to the equal number of samples used in all cases[90] for the calculation of the means and thus the.

A one-way ANOVA performed on the sonicated samples showed significantly, that there was no dose response up to one hour as the means confirm to be equal ($P = 0.999$) as they appear in Figure 64.

Finally a two-way ANOVA with replication was carried out. Duration of sonication and the statistical interaction between ultrasonic treatment and exposure time did not show much influence (*P*-values 0.57 and 0.59). The sonication itself ($P = 0.11$) possibly affects the behaviour of the cells when plated out, as suggested by the means, but below the demanded significance level of 95%.

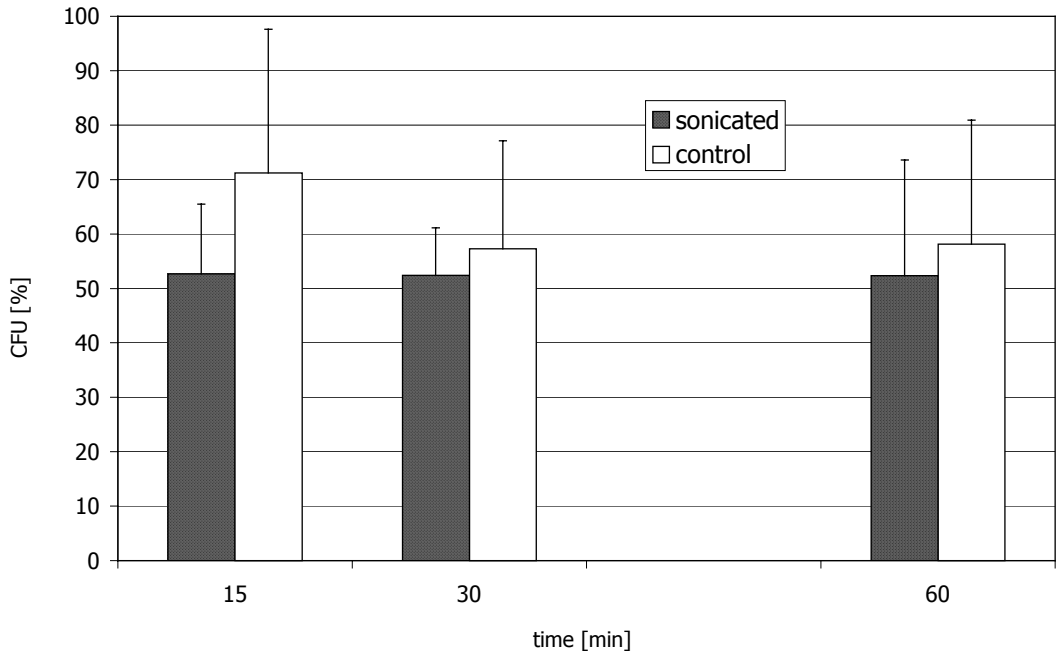

Figure 64 Combined results of viable plate counts for cells in logarithmic and stationary phase of the growth cycle, respectively. Statistics suggest an effect of sonication just below significance but no time dose response was observed.

Transmission electron micrograph

To further confirm these results and for reasons of comparison the internal composition of yeast cells exposed to ultrasound while the spatial arrangement took place was assessed with transmission electron microscopy (see chapter M6). A suspension of yeast cells in broth was sonicated for 30 minutes at a power input of 14 W.

In comparison to the very distinct morphology of the control – cells not exposed to ultrasound, see Figure 33 - in the sonicated sample cells showed a somewhat differently looking internal composition (Figure 65). The vacuole(s) could not be identified, the cells' internal composition looked mingled. The cells' envelopes (E) however stayed intact and no breakage of the membrane-wall complex was detected. The nucleus (N) was identifiable.

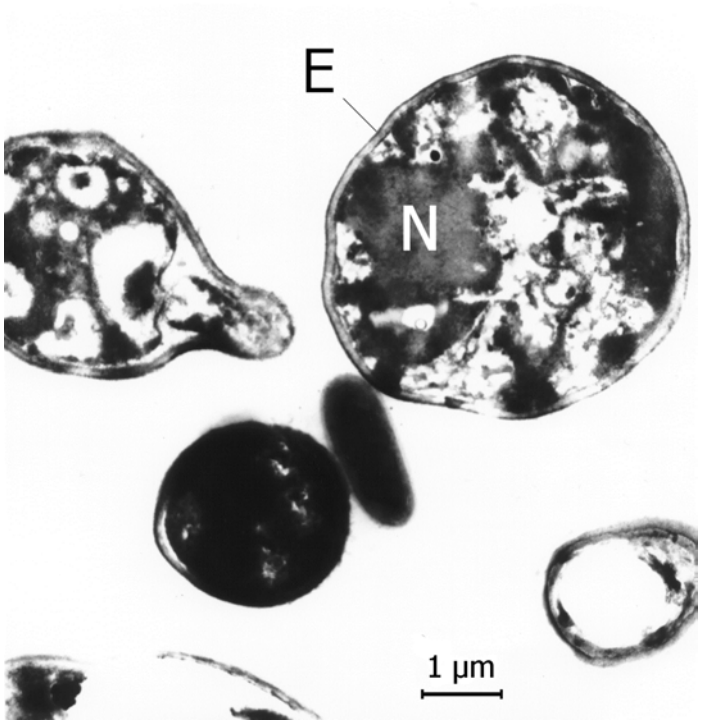

Figure 65 Transmission electron micrograph of yeast cells treated with ultrasound within the pressure nodes of a standing wave sound field. The appearance of the internal components of the cell suggested that the vacuole was damaged. The nucleus (N) was visible and the envelope (E) seemed to remain intact after sonication.

Discussion

Confirming many reports no evidence of a decreased viability of yeast cells was found when exposed to ultrasound in the pressure nodal planes of a standing field at frequency around 2 MHz. Furthermore no leakage was detected for sonication in a properly working separation system for durations up to one hour. This was confirmed by TEM delivering the cell walls to be intact

An effect of the ultrasound on the results of viable plate counts was insignificant and therefore negligible when the spatial arrangement of cells in the sound field took place. The un-sonicated controls did show high standard deviation and a time-dose response was not found. However it could be shown that the exposure to 12%($^{v}/_{v}$) EtOH combined with ultrasound treatment (chapter R2.3, Figure 31) represented an additional stress to the cells in respect to their ability to replicate on a plate.

No alterations to the integrity of the vacuole for cells exposed to sound and controls was measured for cells out in logarithmic phase of the growth cycle. Cells in

the stationary phase showed a small decrease[91] of vacuole integrity, however the an influence of the ultrasonic treatment was insignificant.

The immobilisation of the yeast cells within the pressure nodal planes did minimise damaging effects, however TEM showed morphological changes when compared with a non-treated culture. The ultrasound seemed to alter the integrity of the cell vacuole while the nucleus was not affected. Although the corresponding data on the viability showed that this degree of damage was not lethal, these alterations associated with the heterogeneous spatial ordering of cells in the pressure nodal planes can be regarded to be reversible for a cell culture.

R4.3 Cavitation

Acoustic cavitation is described as the initiation and/or excitation of gas bubbles within a liquid by an acoustic wave or, in more general terms, as "any stimulated bubble activity due to various mechanisms, e.g. a sound wave"[92]. The mechanism is a well known phenomenon[93-96], referring to the behaviour of bubbles within the sound-field one distinguishes between *inertial* cavitation where a phase of rapid growth for a few oscillation cycles is followed by the collapse of the bubble producing shock-waves and high fluid velocities, and the more gentle *non-inertial* cavitation where a bubble oscillates excited by the sound wave over a long period[i]. The size changes of the bubble during one cycle of non-inertial cavitation is rather small[92].

A theoretical value of the threshold of acoustic pressure below which cavitation cannot take place at a given frequency and gas saturation can be derived[96], although the particular circumstances concerning the liquid and the sound field are of substantial importance[97]. EtOH for example might provide non-uniform hydrogen bond networks[98] and thus lower the cavitation threshold for alcohol-rich water-EtOH mixtures in comparison to pure water[15].

Cavitation is held responsible for cell inactivation[99] and cell damage[52,88]. For the ultrasonic separation system used in this work the peak pressure of the standing wave was calculated to be 0.6 MPa at 24 W true electrical input power in the pressure anti-nodes which is an indication that cavitation is unlikely at a frequency of above

[i] These designations have replaced the formerly used terms "transient" and "stable" cavitation.

2 MHz[96,100]. However the following two reasons were decisive to address the occurrence of cavitation experimentally.

Firstly, the consideration of the detected damages presented in chapter R2.3 had clearly indicated a connection between the alterations of the cells and their exposure to ultrasound when suspended in 12%($^{v}/_{v}$) EtOH-water. Secondly, the presence of gas bubbles arising when water and EtOH were mixed were be assumed to decrease the cavitation threshold as gas bubbles represent cavitation nuclei. Moreover recent reports connected bacteria damage by cavitation to the presence of micro-bubbles in a 1 MHz wave field[101].

The method of choice was to detect free radicals produced sono-chemically when cavitation occurred. This method has the advantage to consider the whole volume of irradiated sample and the full duration of sonication. The measurement of radical production is a common method of detecting cavitation[102], others are acoustic imaging, sono-luminescence and the generation of sub-harmonics. The test used here was originally introduced by Weissler[103], later extensively evaluated by Coakley[52] and subsequently developed into the IEEE standard iodine test for (stable) cavitation[104].

The degradation products of water, H^+ and OH^-, ions are produced by the high local energy concentration provided by a cavitating bubble and especially by its implosion. The subsequent interaction with KI delivers free iodine. The starch indicates molecular I_2 by turning blue (see chapter M3.1). This blue colour can be observed[52] and additionally quantified by O.D. at 565 nm.

A preliminary experiment was conducted in an ultrasonic disruptor (IKASONIC U 200 S), a device built for destruction of cells by cavitation. Suspensions of yeast in water and water-EtOH, respectively, were exposed to the ultrasonic wave at approximately 60 W/cm² at a frequency of 24 kHz. Both suspensions showed a similar decrease of methylene blue viability to some 40% after 10 minutes sonication. A repetition with a filling containing the appropriate chemicals delivered colouring of deep blue and violet, thus clearly indicating the presence of cavitation.

The following experiment therefore was aiming on the detection of blue colour occurring while samples were irradiated in the UES system. In addition, the O.D. at 565 nm was measured. The experiment was performed in the ultrasonic separation system as cavitation is influenced by the vessel[105] and its geometry[106]. To increase the chance of so-called Willard events (bubble bursts[107]) the liquids and suspensions used

were exposed to fields at higher true electric power input settings than recommended for separation/filtration purposes. 40 W and 56 W where used in addition to a treatment with 24 W like in the studies of chapters R2.3 and R4.2. The chamber was filled with water and 12%($^{v}/_{v}$) EtOH with and without yeast cells, respectiely. The cell concentration was 10^{7} cells/mL.

After the described ultrasound exposure and subsequent centrifugation of the samples the O.D. at 565 nm was measured. Neither in the case of clear liquids, water or water-EtOH, nor in the presence of yeast any increase of iodine in the starch indicated by a blue colouring was observed, the resulting O.D. in Figure 66 did not show any increase.

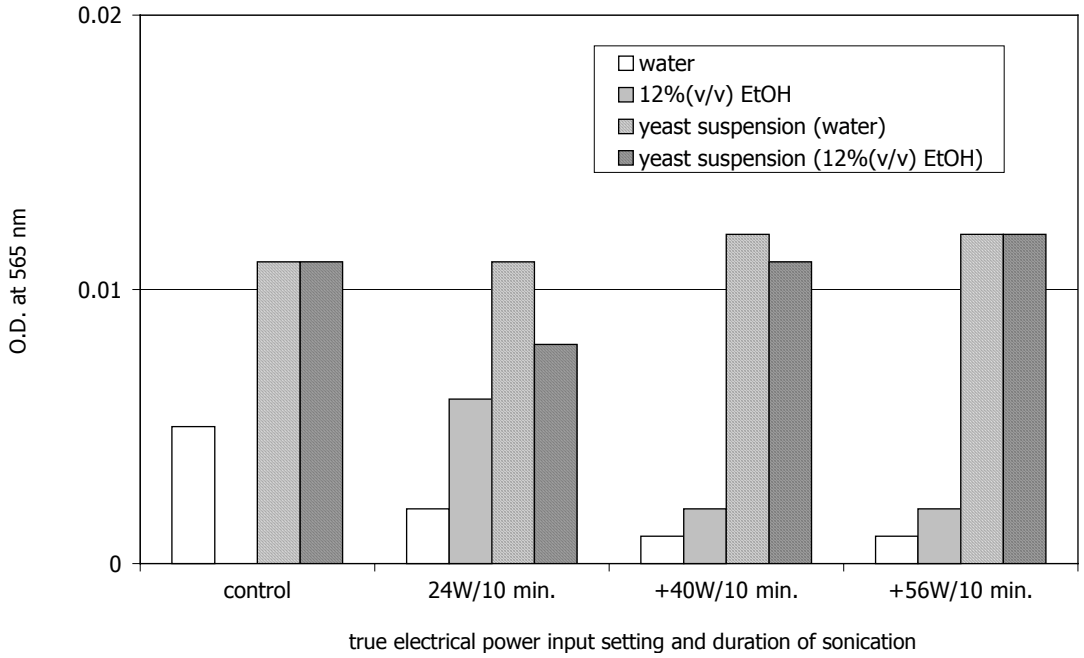

Figure 66 Inertial cavitation in water and water EtOH detected by the free radical-iodine-starch reaction measures as of optical density at 565 nm. Sonications were performed at much higher power inputs than during normal ultrasonic treatment. No blue colour was observed.

Discussion

It was shown that the irradiation in an ultrasonic disruptor led to decreased viability of yeast cells suspended in water or water-EtOH. The degree of decrease was the same for both host liquids which indicated that a physiological effect of EtOH when cells were exposed to ultrasound did not exist. The occurrence of cavitation

during this treatment shown by the production of free radicals therefore was connected to the decreased yeast viability.

In the ultrasonic separation system, however, cavitation as it can be detected by the production of free radicals was not occurring. The power input applied was higher than those levels leading to disruption of the cells.

This result indicates that the cell damage that occurred during experiments in this work was related to other effects. However, evidence of cavitation was not found does not mean that evidence of no cavitation was given.

R4.4 Effects on yeast sonicated in an experimental resonator

The following experiments were carried out in the experimental resonator described in chapter R3.4, a small cuvette resonator with two PZT ceramics glued to either side (compare Figure 51). This system has some advantages for research purposes in comparison to the separation system. It is transparent which allows the inspection of the behaviour of the particles within the resonator chamber. It is small enough to fit completely into the field of view of a light microscope, which enables one to observe the movement of the particles microscopically. It is working at 2.3 MHz.

This system was exploited for tests aiming on the confirmation of the connection between the observed occurrence of turbulence and cell leakage. As cavitation is influenced by the volume of a vessel[108] the respective examinations as describe in chapter R4.3 were repeated with the experimental resonator.

However, a disadvantage of this system has to be mentioned: it was not possible to use the presented one-dimensional model for this system as the available computer programs cannot deal with two transducers yet, although this is not at all a restriction to the model itself. Therefore the results are confined to phenomenological observations, no evaluation of the parameters of the acoustic field could be presented.

Effect of turbulence on cell integrity at different true electrical power inputs

As a preliminary test the resonator was checked for the production of free radicals indicating cavitation (compare chapter M3.1) for true electrical input power (t.e.p.i.) settings of 2 W, 2.5 W and 3 W filled with non-turbulent yeast suspensions of 4%($^{v}/_{v}$) and 5%($^{v}/_{v}$) EtOH-saline and with turbulent suspensions at EtOH concentrations of

6%($^{v}/_{v}$) and 7%($^{v}/_{v}$), respectively[i]. In no case blue colour or an increase of optical density (O.D.) at 565 nm was observed.

In the same liquid samples freshly grown NCYC 1006 yeast at a concentration of $3 \cdot 10^{7}$ cells/mL in mixtures was put in. Sonication experiments were carried out in doublets, duration of sonication was one minute in each case.

Figure 67 shows the resulting leakage of intracellular material. For the non-turbulent sample at 5%($^{v}/_{v}$) EtOH no change of the leakage was detected. However when the cells were turbulently driven through the resonator at 6%($^{v}/_{v}$) EtOH an increase of UV-light absorbance at 280 nm was observed indicating leakage of intracellular material in the supernatant. Furthermore did the results indicate increased leakage at higher settings of the applied t.e.p.i.

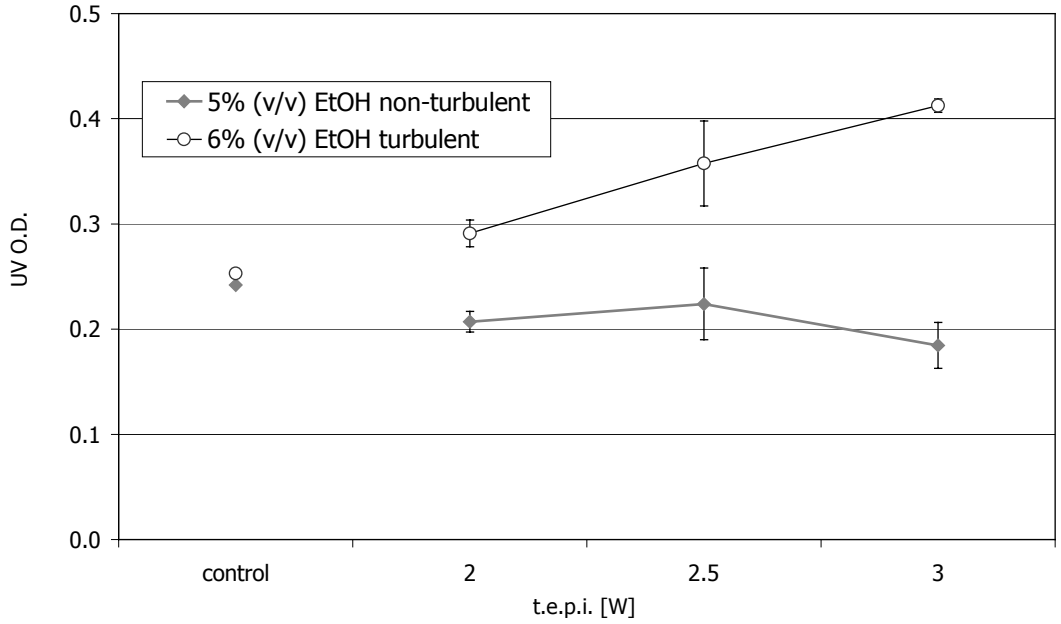

Figure 67 Leakage of yeast in sound fields of 2 W, 2.5 W and 3 W t.e.p.i. suspended in saline-EtOH mixtures at EtOH concentrations of 5%($^{v}/_{v}$) and 6%($^{v}/_{v}$). Turbulence was observed just for 6%($^{v}/_{v}$) EtOH at which leakage was detected too.

Effect of turbulence on cell viability and integrity in the presence of EtOH

The experimental resonator was used for the sonication of suspensions of freshly grown yeast cells at a concentration of $4 \cdot 10^{7}$ cells/mL in 0.9% ($^{w}/_{v}$) physiological saline.

[i] The level of EtOH at which turbulence occurred was lower in this experimental resonator.

Samples containing 4%($^{v}/_{v}$) and 5%($^{v}/_{v}$) EtOH respectively were prepared. Sonication was performed at 2.5 W t.e.p.i. for 3 minutes, turbulence was observed for the lower EtOH concentration only.

Table 13 shows a significant decrease of viability and increase of leakage for the turbulent sample. The experiment during which the normal spatial arrangement of the cells was observed indicated no change in respect to this examinations.

Table 13 Effect of turbulence in the presence of EtOH on viability and leakage of yeast cells sonicated for 3 minutes at 2.5 W t.e.p.i.

Viability [%] and intracellular material in supernatant

EtOH conc. of suspension [%($^{v}/_{v}$)]	turbulent	viability [%]		UV O.D.	
		sonicated	control	sonicated	control
4	no	98.2	95.8	0.054	0.050
5	yes	17.4	97.3	0.682	0.054

Effect of turbulence on cell integrity in absence of gas

During the process of mixing of water or saline and EtOH the generation of a fair amount of gas bubbles was observed. This was not suppressed when both liquids were boiled[i] prior to the preparation of the mixture.

The attempt to eliminate the gas bubbles during sonication was motivated by the additional stress-factor they may represent to the cells. Although cavitation was not observed the surface of the gas bubbles represented obstacles to the moving yeast. Preliminary tests showed that an in case of gas-free liquids a higher concentration of EtOH had to be present to initiate the turbulent behaviour. Therefore the suspension for this experiment was additionally degassed after preparation by exposure to an under-pressure of 20 kPa for 10 minutes.

The suspension used contained 12%($^{v}/_{v}$) EtOH in 0.9%($^{w}/_{v}$) physiological saline at a cell concentration of some $2 \cdot 10^{7}$ cells/mL. Three degassed and three non-degassed samples were sonicated in the experimental resonator at 2.5 W t.e.p.i. for 3 minutes.

[i] and cooled down in a closed bottle filled to the rim

During sonication the behaviour of the cells within the resonator was carefully observed over time. Whereas the non-degassed samples did show turbulent (Eckhardt) streaming for the whole duration of sonication the trials with degassed suspensions displayed a different behaviour because the EtOH concentration was on the threshold of turbulence for this case:

- Trial 1 was turbulent from the beginning.
- Trial 2 was banding from the beginning until 30 seconds before the end of the sonication, from then turbulence was observed.
- Trial 3 was banding for the duration of the experiment, no turbulence occurred.

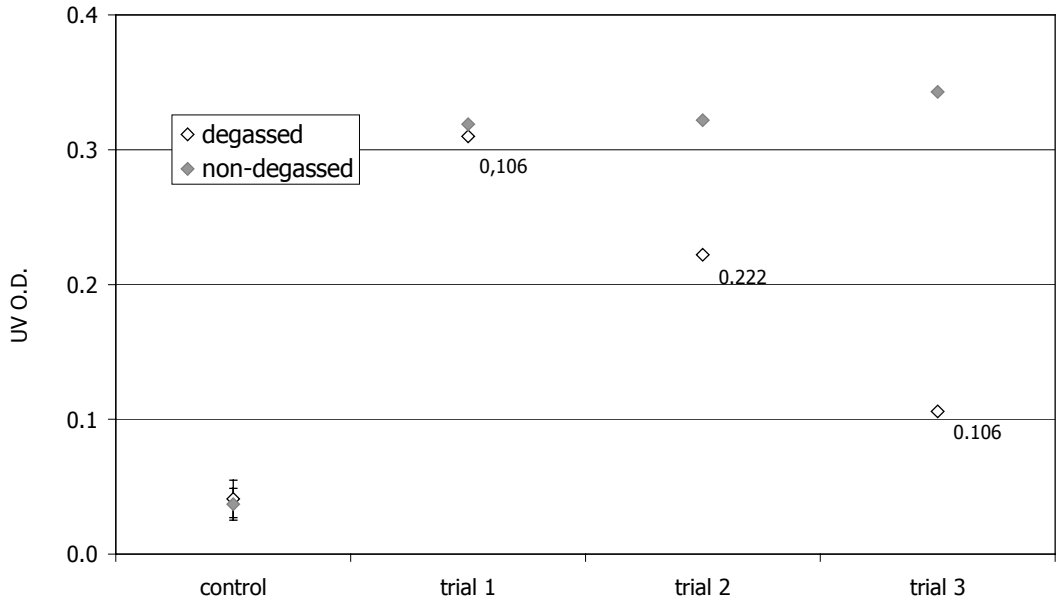

Figure 68 Leakage of intracellular material as delivered by UV O.D. The un-sonicated control was compared to three trials of sonication at 2.5 W t.e.p.i. Turbulence was observed for the whole duration of 3 minutes for non-degassed samples (grey markers), but shorter for degasses samples (open markers, see text for further explanation).

The measurement of light absorbance at 280 nm as shown in Figure 68 reflected this. During the turbulent treatment (grey markers) the cell leakage was increased in respect to the un-sonicated control to the same level for each experiment. The results for the trials which where only partly turbulent (open markers) indicated a connection between the time it took until turbulence set in and the amount of intracellular

material found in the supernatant. The leakage of trial 1 (turbulence during the whole experiment) was not different for degassed and non-degassed samples.

During all experiments the temperature never rose above 34.5°C, no gas bubbles were observed in the degassed trials.

Discussion

Damage to the cells was confirmed also to occur under certain conditions in the experimental resonator, a small ultrasonic cuvette resonator.

No evidence of cavitation was found in this system. In the same samples used for cavitation checks the leakage of intracellular material was detected, hence this decrease of the cells' integrity occurred while no evidence of inertial cavitation was measured.

When yeast cells were arranged in the pressure nodal planes of the sound field although EtOH was present, i.e. the described turbulence did not occur, no leakage and an unaffected viability of yeast cells was measured.

Results indicated that in case of turbulence the amount of protein in the supernatant was increased when higher settings of the electrical power input were used and the ultrasonic field was stronger.

The presence of gas bubbles in the host liquid might increase the probability for cells to be turbulently driven through a standing wave field. However, yeast in carefully degassed suspensions containing 12%($^{v}/_{v}$) EtOH showed this behaviour as well. This further confirms the explanation of the turbulence by the variation of the acoustic contrast (see chapter R2.4).

Furthermore it could be shown that the amount of intracellular material in the supernatant measured by UV O.D. was a function of the duration of turbulence, regardless if gas bubbles were present or not. An increase of the temperature was insignificant.

R4.5 Effects on yeast homogeneously immobilised in a gel-block exposed to an ultrasonic standing wave

One hypothesis regarding the cell damage was that the environment in the inter-nodal regions, i.e. outside the pressure nodes, where the acoustic pressure pulsates with the frequency of the ultrasound was responsible for the cell damages. Therefore decreases in cell viability appeared to be a direct function of the intensity of the sound pressure applied when the cells were displaced from the pressure nodal planes. However in the presence of EtOH this was connected with turbulent movement which exposes the culture to an additional stress of shear[i]. Therefore the following experiments were designed to clarify if viability changes would occur for cells displaced from the pressure nodes if the streaming was eliminated.

Employing the novel method of gel immobilisation introduced in chapter R3.2 yeast cells were suspended in liquid gels and filled into the separation system in different configurations of the batch set-up (compare Figure 9, page 40). Before the ultrasonic field was applied the agar gels were cooled down until gelation was finished resulting in a gel-block with homogeneously distributed cells immobilised by the gel matrix. Therefore the cells were not banded in the pressure nodes by the standing wave but exposed to the sound field at their random positions. Thus cells were distributed over the volume treated with the whole range of pressure environments given by the periodic structure of the standing wave.

Table 14 lists the various configurations, examination methods and sonication "styles" used. In the beginning of the study the growth of the cells was used as examination method. The malt extract agar gel block was kept at 30°C for four days to allow growth of the cells after sonication. The block was finally cut and examined using light microscopy. No differences in growth in respect to the cells' position relative to the standing wave field were detected.

Therefore different dyes were used for cells in agar technical, the result was negative again, no significant dependencies on the location were found. Furthermore no decrease in viability (methylene blue) was observed.

[i] The term shear in the context of this work is used not the strict physical sense but in the meaning of non-symmetric particle-liquid or particle-particle interactions.

EtOH was added to the gel to simulate additional stress, however no influence on the cells was found.

Table 14 List of experiments in which viable yeast cells fixed at random positions in a gel-block were exposed to a standing ultrasonic wave field. None of the examinations did show any influences due to the cells location in respect to the sound field, i.e. nodal versus inter-nodal space.

Experiments aiming on space dependent effects of standing waves on yeast cells.

host medium	t.e.p.i. [W][a]	duration	configuration	examination method
5% malt extract agar	56	15 min.	no foil[b]	4 day growth in incubator
	48	15 min.		
	24	30 min.		
	16	15 min.	35 mm cooling volume, no foil	
	24	5 min.	no foil	
0.6 % agar technical	8	6x1min./ 1min. break	no cooling volume	methylene blue overnight
	24	20 min.	no foil	
	32	20 min.	standard configuration	UV fluorescent DNA dye
	32	20 min.		3 fluorescent dyes[c] in confocal microscope
0.6% agar technical 12%($^{v}/_{v}$) EtOH	32	20 min.		methylene blue overnight

[a] true electrical power input
[b] for the presence of the gel-blocks the separating foil as used in the standard configuration of the UES system was not necessary
[c] vacuole membrane, respiratory mutants, calcium cage

Discussion

It shall be mentioned that, although the experiments were carried out with great care, a lack of control existed. The methodology was not suitable to detect possible in-homogeneity in the spatial distribution of viable cells.

However, no over-all influence of the exposure of cells to the standing wave was picked up. The cells did not show alterations due to their different locations in the sound field throughout all the experiments. This result suggested that in the absence of continuous movement through the field the cells were not damaged. The exposure

to the pressure amplitude of a standing ultrasonic wave in a gel did not change cell viability.

R4.6 Effects on yeast exposed to ultrasound in an anechoic system

A cell moving in direction of sound propagation through the separation system is exposed to the sound not just mainly in the pressure nodes, but occasionally as well in the displacement nodes where the sound pressure amplitude is a maximum. The movement by the radiation pressure induces quick changes between these regions and therefore from the cells' point of view an exposure to interacting pressure and shear.

However, in all experiments showing decreases of viability and increased leakage so far, the combination of ultrasound *and* EtOH were inducing the streaming/shear. The influence of EtOH on the mechanical properties of yeast cells, relaxation and increase permeabilisation of the membrane, motivated further examinations whether an effect on the viability and/or mechanical damages would remain if EtOH was removed.

The following experiment was therefore designed to simulate the cells' stress as seen when moving through a standing wave field, but in absence of EtOH[109].

To accomplish this task the sound field had to be modified in that the axial primary radiation force of the standing wave was reduced to have the corresponding force distribution of the progressive wave drive the cells out of the nodal planes. As the standing wave is the superposition of the incoming wave and its reflection its amplitude can be altered by the reflection coefficient. The separation system was therefore modified (Figure 69), the reflector was replaced by an absorber of sponge (Sp). Open-porous material was used to ensure it was water-immersed and therefore reflection due to a change in the acoustic impedance at the water/sponge interface was minimised. In addition to that the incoming wave was scattered at the spike-shaped surface of the sponge, thus considerably decreasing the amplitude ratio of the standing and the progressive wave to below 0.5%. Thus, despite of the small sample volume, a free field condition was very well approximated, the modified separation system will be referred to as *anechoic system*. To disconnect the active volume from the absorber an additional cooling volume (C2) was connected to the original cooling volume (C1). The AV was terminated by acoustically transparent polyurethane foils on both sides.

However, two differences in comparison to the standard UES system have to be noted. Firstly, the amplitudes of sound pressure and displacement were decreased due to the decrease of resonant amplification and due to an electrical impedance mismatch between the amplifier and the acoustic system. Secondly, the rate of change between maximal pressure and maximal displacement when moving through the field was different from the cells point of view, because the relative velocity between the slow particle and the progressive wave in the anechoic system is in first approximation of course the speed of sound propagation, whereas in the standing wave field in case of turbulences due to EtOH the cells' velocity itself was the relative speed.

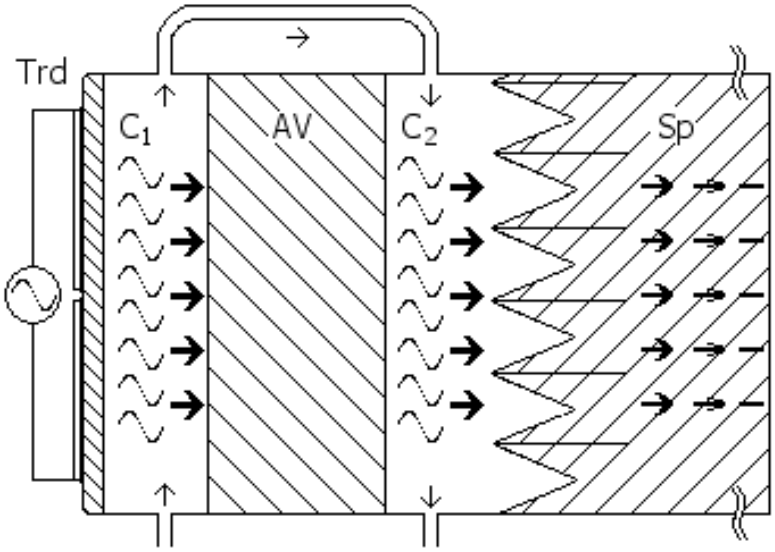

Figure 69 Anechoic sonication system with sound absorbing sponge (Sp). A suspension in the active volume (AV) was exposed to ultrasound at 14 W true electrical power input emitted by the transducer (Trd). Water was pumped through the cooling volumes (C1, C2). The second foil separated the AV from the absorber.

The effort was successful, the cells were driven through the active volume (AV). However due to the different magnitudes of the radiation force contributions of standing and progressive waves due to term I in equation **(53)**, rare occurrences of cell banding were still observed. But the majority of cells was exposed to alternating pressure and displacement and therefore to an environment much like the one experienced in a standing wave due to the presence of EtOH.

Effects on cell viability and integrity

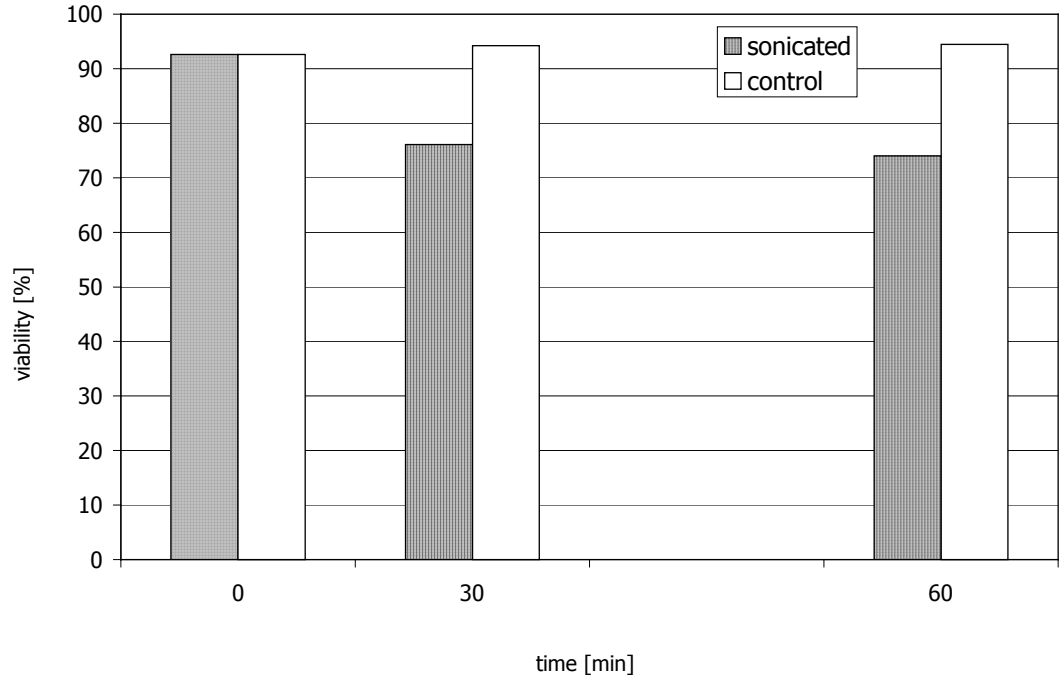

Figure 70 Viability measured by methylene blue counts. Data acquired after 15, 30 and 60 minutes for yeast cells suspended in water and sonicated at 14 W in an anechoic system.

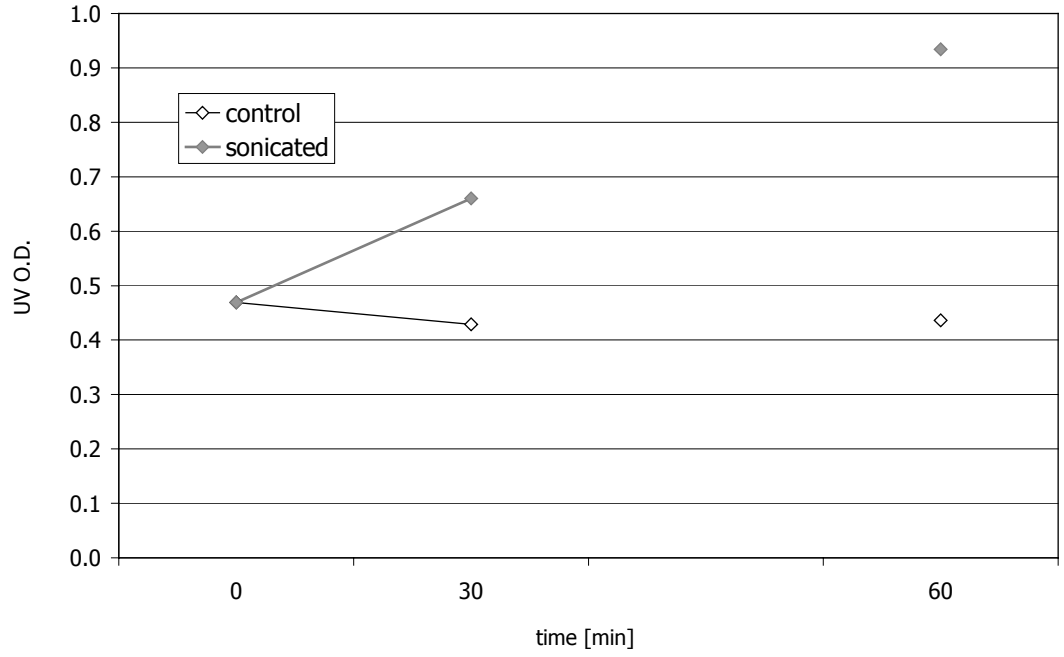

Figure 71 Measurement of the amount of intracellular material in the supernatant by the O.D. of ultraviolet light at 280 nm. Sonication at 14 W for 15, 30 and 60 minutes in an anechoic system.

A subsequent examination of samples sonicated in the anechoic system delivered a decreased viability as measured by methylene blue counts and an increase in absorption of UV light by protein in the supernatant.

The methylene blue count (Figure 70) showed a mild but significant decrease of viable cells. After one hour of sonication only some 75% of the cells were reducing the stain in comparison to a viability of almost 95% in the control.

In addition to that a steady increase of intracellular material was detected by UV optical density (Figure 71).

Transmission electron micrographs

TEM after half an hour treatment at a true electrical power input of 14 W in the anechoic system delivered two types of cell damage. The micrograph in Figure 72 shows a breakage of a cell's envelope. A distinct gap can be identified between cell wall and cell membrane, however the wall seems to be intact.

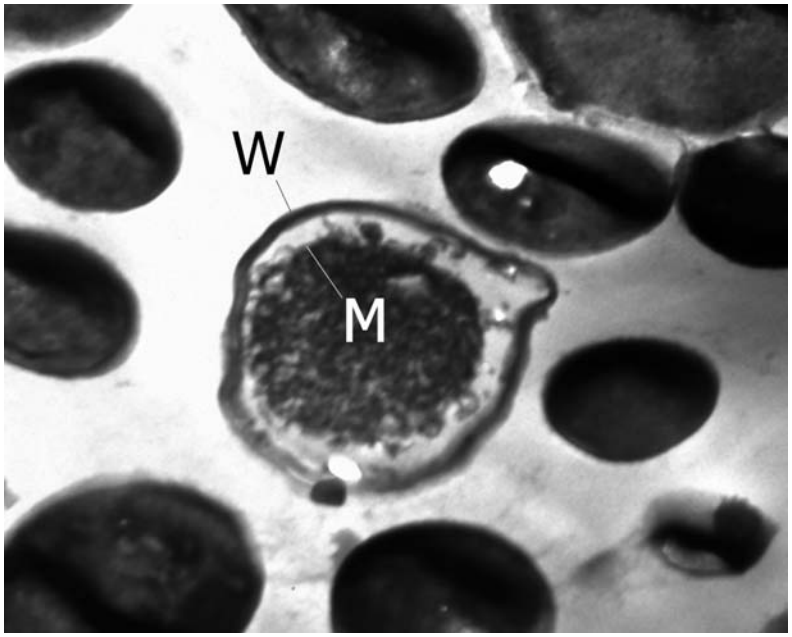

Figure 72 TEM of yeast after 30 minutes of ultrasonic treatment in the anechoic system. The morphology of the cell was altered, a significant gap between the membrane (M) and the wall (W) is visible.

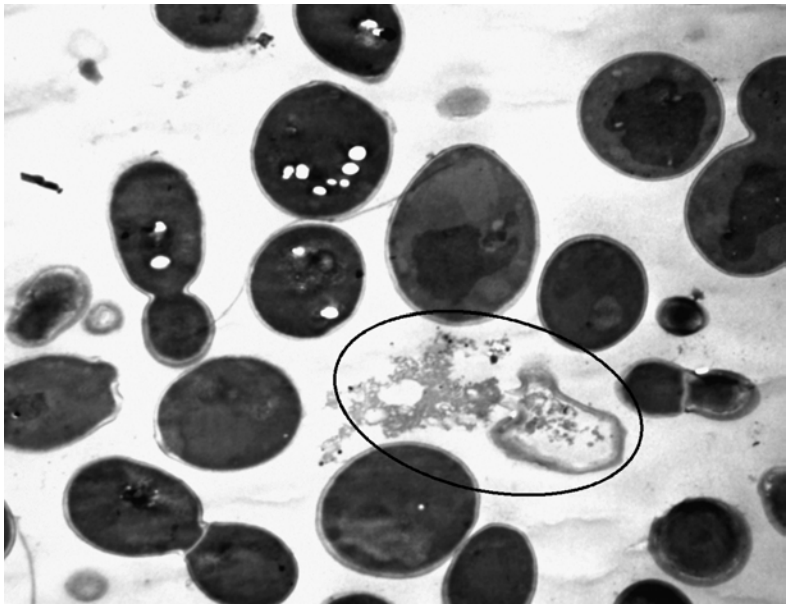

Figure 73 TEM of yeast after 30 minutes of ultrasonic treatment in the anechoic system. The wall of the cell in the circle appears to have just opened and released its content. Surrounding cells do not show significant damage.

Another picture (Figure 73) clearly shows a cell in proximity to its internal compartments. The almost empty hull seems to just have spilled out the intra-cellular material. The surrounding cells do not show alterations.

Discussion

Treatment of cells with progressive ultrasonic waves in the anechoic system confirmed the association between the presence of damage and the displacement of the cells from the pressure nodal planes in combination with shear in absence of EtOH. Following the treatment the cells displayed loss of viability and increasing amount of intracellular material in the extra-cellular space. Both alterations appeared to be directly correlated with the duration of the sonication. In these experiments the pressure amplitude of the wave was essentially constant in space and the cells were homogeneously distributed in the suspension.

However the degree of cell death and leakage was smaller when compared with the same time point values detected in water-EtOH mixtures exposed to standing waves. This might be caused by the fact that due to the lack of resonance the cells treated within the anechoic system experienced a lower pressure than in the standing wave system in presence of EtOH.

TEM confirmed mechanical damage to the cell envelopes at the membrane-wall interface. Furthermore the measured decrease in UV optical density was explained by a micrograph showing an empty cell's hull next to its content.

R4.7 Conclusion

The presented results were aiming on the investigation of alterations that occurred when yeast cultures were exposed to plane ultrasonic fields.

- It was shown that the viability and integrity of yeast cells sonicated in the separation system under normal operation conditions was not affected. An influence of the ultrasound on the ability to replicate and on the integrity of the vacuole was not found when the cells were immobilised in the pressure nodal regions of the standing wave. TEM showed some non-lethal morphological changes.
- Free radicals were not detected, therefore no evidence of cavitation was found. Explicitly this was not interpreted as evidence of no cavitation.
- The use of a different resonator indicated that the occurrence of cell leakage and decreased viability was not connected with the specific system in which the sonication took place.
- It was shown that an increase of the power input increased the leakage and that the leakage coincided with the set in of turbulence in the sonication chamber.
- Degassing of the host liquid was observed to alter the EtOH concentration at which turbulence occurred, however cell leakage as of intracellular material in the supernatant was detected for degassed suspensions as well when cells were turbulently driven through a standing wave field.
- After suppression of the turbulent movement by immobilisation of the cells in a gel matrix no influences on the ability to reproduce, their viability and morphology were detected due to the location of a cell in respect to the applied standing wave field.
- Leakage and decreased viability were found when the sonication took place in an anechoic chamber exposing the cells to the combination of a high

progressive and a low standing wave to simulate the turbulence in absence of EtOH. TEM indicated severe damage to the cells' membrane-wall interfaces and breakage of the hulls. Thus it was shown that EtOH present in a sonicated suspension is not the direct reason for cell damage, but indirectly may cause the damage due to the induced turbulence.

- However the mechanisms responsible for the observed cell alterations were not finally elucidated.

OUTLOOK

The development of separation systems utilising the principle of ultrasonic particle manipulation is ongoing, especially in respect to scale-up. Optimisation of the materials the resonators are built of, their size and the used frequency has reached a very high level[57]. Results presented in R1.2, R1.5 and R3.4 might flow into the design of control logics of the resonator drive unit and pump control to enable further steps of optimisation in respect to the separation efficiency and energy consumption of these systems.

The ultrasonic principle has again shown to be save when applied on suspensions of biological cells. The mingled inner cell structure found with transmission electron microscopy might be connected with results of most recent investigations indicating that lag time (i.e. the time occurring before cells duplicate) observed in sonicated cells is longer than in the control. Further examinations utilising growth curves and fluorescent flow cytometry might be indicated, as these results support earlier observations[74] that the structure of the elements responsible for cell division may be partially damaged or passivated. Such experiments would as well be suitable to answer the question if the observed alterations occur while the cells are kept in the pressure nodal planes, where they are exposed to vibration/acceleration, or prior to that, while the cells are still moving there from their original locations.

From today's point of view the possibility of arranging particles or cells within a gel by ultrasound is very promising. Investigations of the aggregates' structures employing scanning electron microscopy and fluorescent confocal microscopy are already on the way[110]. Further investigations will finally lead into applications utilising this technique, possibly in the regime of bio-encapsulation, e.g. artificial organs or ecological highly competent fermentation capsules.

A clarification of the exact mechanism of the cell damage is desirable. The explanation suggested by the results in this work is either shear or shear/pressure[111] interaction and unlikely but possibly heating. However, in comparison to stresses yeast cells have been reported to *withstand* this might not include the phenomenon in its entirety. Two hypotheses shall be mentioned, that surfaced during the experiments but could not be evaluated.

The first hypothesis is based on rumours, that yeast cells contain gaseous CO_2. Although some effort was put into, a final answer if this is true could not be found even though the question seems to be very old[112]. This could lead to some kind of interaction of the ultrasound with the intracellular gas[113] destroying the inner structure of the cell. An effect like this would have to be called intracellular cavitation. Although no evidence of cavitation was found, it must not be excluded to be responsible as recent reports show how hard it actually is to prove a negative in this regime[114-118].

The measurements indicated, that leakage connected with damage to yeast cells occurred when cells experienced the space between the pressure nodal planes if turbulently driven through the sound field. If the cells were immobilised in a gel-block no damage was found. The second hypothesis that shall be put forward is, that these findings might represent two effects. On one hand the damage is brought about by the cells experiencing the acoustical pressure between the pressure nodal planes in which they are usually retained. Although the reported pressure of 0.6 MPa would be easily endured by a yeast cell[119] if the pressure increased and decreased slowly. But the acoustic pressure changes two million times per second. This could likely be too fast for the cell to adjust its turgor pressure and furthermore a mass transfer into the cell seems possible[120], the cells would be pumped up and finally burst. Reports about decreases of viability in sparged bio-reactors due to liquid jets beneath a bubble bursting at the surface[113,121,122] could well be describing the same phenomenon. On the other hand the entrapment in the gel may protect the cells[25,26]. It is imaginable, that the availability of liquid is decreased at the time scale of ultrasonic excitement and therefore inside the polymer the mass transfer is inhibited. Work was published[84] where scanning electron micrographs show yeast cells tightly packed in the gel's structure within the pressure node, but when the cells where kept in pressure inter-nodal space a void around cells was visible. This void could indicate the size of the cell when the ultrasound was at work.

ACKNOWLEDGEMENTS

M.Gröschl and A.J.McLoughlin are thankfully acknowledged for the supervision of this work and the guidance they gave me. Both were always open for discussions and helpful when necessary, both were willing to take the exertion to read, correct and, by that, substantially improve this work. All errors left are my responsibility.

E.Benes is acknowledged for co-ordinating the TMR programme which provided the scientific environment for this thesis.

W.T.Coakley helped me with his experience and knowledge about the problems that can occur when biological cells and ultrasonic radiation meet.

All researchers of the EUSS project shall be is thanked for the co-operation, for their contributions and help, especially H.Böhm, S.Sielemanns, H.Lawler, C.Cousins, J.Hawkes, and last but not least L.Gherardini, who I really enjoyed to work with.

The staff at the University College Dublin, Department of Industrial Microbiology and at the Vienna University of Technology, Institute of General Physics is acknowledged.

Mr. Tipsy has provided me with the oldest reference in this work.

My friends and partners of 20first.cc are acknowledged for their understanding.

My father Peter, my brothers Mathias and Philipp and Uschi are my family which supported this work in many ways, my dad is thankfully acknowledged for providing me with a quiet room in his house, where most of this pages were written. Uschi helped me out with printer and photocopier in last minute.

But without the loving support and help of my wife Christiane this thesis would not have come into being, thank you so much!

Work supported in part by the European Commission's TMR Programme, Contract No. ERBFMRXCT97-0156, EuroUltraSonoSep.

BIBLIOGRAPHY

[1] R.P. Feynman, R.B. Leighton, and M. Sands, *The Feynman lectures on physics (dt.)*. Vol. 1. 1991, München, Wien: R.Oldenbourg Verlag. 748.

[2] A. Kundt and O. Lehmann, *Longitudinal vibrations and acoustic figures in cylindrical columns of liquids.* Ann Phys Chem, 1874. **153**: p. 1-12.

[3] T.L. Tolt and D.L. Feke, *Separation of dispersed phases from liquids in acoustically driven chambers.* Chem Eng Sci, 1993. **48**(3): p. 527-540.

[4] J.A. Gallego-Juárez, I. González, and E. Riera. *Separation of fine aerosol particles by high power ultrasounds*. in Proc. *137 Meeting of the Acoustical Society of America and the second Convention of the European Acoustic Association: Forum Acusticum*. Berlin, Germany. 1999

[5] M. Gröschl, W. Burger, B. Handl, O. Doblhoff-Dier, T. Gaida, and C. Schmatz, *Ultrasonic separation of suspended particles - Part III: Application in biotechnology.* Acustica - acta acustica, 1998. **84**: p. 815-822.

[6] M. Gröschl, *Ultrasonic separation of suspended particles - Part I: Fundamentals.* Acustica - acta acustica, 1998. **84**: p. 432-447.

[7] J. Zhang, A. Collins, M. Chen, I. Knyazev, and R. Gnetz, *High-density perfusion culture of insect cells with a Biosep ultrasonic filter.* Biotech Bioeng, 1998. **59**(3): p. 351-359.

[8] R.A. Barnes, P. Jenkins, and W.T. Coakley, *Preliminary clinical evaluation of meningococcal disease and bacterial meningitis by ultrasonic enhancement.* Arch Disease Child, 1998. **78**: p. 58.

[9] O. Doblhoff-Dier, T. Gaida, H. Katinger, W. Burger, M. Gröschl, and E. Benes, *A novel ultrasonic resonance field device for the retention of animal cells.* Biotechnol Progr, 1994. **10**: p. 428-432.

[10] T. Gaida, O. Doblhoff-Dier, H. Katinger, M. Gröschl, and E. Benes, *Scale-up of ultrasonic resonance field cell separation devices used in animal cell technology*, in *Animal Cell Technology: Developments towards the 21st Century*, E.C. Beuvery, J.B. Griffiths, and W.P. Zeijlemaker, Editors. 1995, Kluwer: Dordrecht. p. 699-703.

[11] F. Trampler, S.A. Sonderhoff, P.W.S. Pui, D.G. Kilburn, and J.M. Piret, *Acoustic cell filter for high density perfusion culture of hybridoma cells.* Bio/Technology, 1994. **12**: p. 281-284.

[12] P.W.S. Pui, F. Trampler, S.A. Sonderhoff, M. Gröschl, D.G. Kilburn, and J.M. Piret, *Batch and semicontinuous aggregation and sedimentation of hybridoma cells by acoustic resonance fields.* Biotechnol Prog, 1995. **11**: p. 146-152.

[13] H. Bierau, A. Perani, M. Al-Rubeai, and A.N. Emery, *A comparison of intensive cell culture bioreactors operating with Hybridomas modified for inhibited apoptotic response.* J Biotech, 1998. **62**: p. 195.

[14] C.M. Cousins, P. Holownia, J.J. Hawkes, C.P. Price, P. Keay, and W.T. Coakley, *Clarification of plasma from whole human blood using ultrasound.* Ultrasonics, 2000. **38**: p. 654-656.

[15] K. Yasuda, M. Kiyama, S.-I. Umemura, and K. Tekeda, *Deoxyribonucleic acid concentration using acoustic radiation force.* JASA, 1995. **99**(2): p. 1248-1251.

[16] J.J. Hawkes, M.S. Limaye, and W.T. Coakley, *Filtration of bacteria and yeast by ultrasound enhanced sedimentation.* J Appl Microbiol, 1997. **82**: p. 39-47.

[17] J.J. Hawkes, D. Barrow, J. Cefai, and W.T. Coakley, *A laminar flow expansion chamber facilitating downstream manipulation of particles concentrated using an ultrasonic standing wave.* Ultrasonics, 1998. **36**: p. 901-903.

[18] J.J. Hawkes, D. Barrow, and W.T. Coakley, *Microparticle manipulation in millimetre scale ultrasonic standing wave chambers.* Ultrasonics, 1998. **36**: p. 925-931.

[19] J.J. Hawkes and W.T. Coakley, *Force field particle filters, combining ultrasound standing waves and laminar flow.* Sens Actua B, 2001. **75**: p. 213-222.

[20] M.S. Limaye and W.T. Coakley, *Clarification of small volume microbial suspensions in an ultrasonic standing wave.* J Appl Microbiol, 1998. **84**: p. 1035-1042.

[21] J.J. Hawkes, J.J. Cefai, D.A. Barrow, W.T. Coakley, and L.G. Briarty, *Ultrasonic manipulation of particles in microgravity.* J Phys D: Appl Phys, 1998. **31**: p. 1673-1680.

[22] J.J. Hawkes and W.T. Coakley, *A continuous flow ultrasonic cell-filtering method.* Enz Microb Tech, 1996. **19**: p. 57-62.

[23] T.M.P. Keijzer, F. Trampler, A. Oudshoorn, O. Doblhoff-Dier, and H. v/d Berg. *Integrating acoustic perfusion in mammalian cell culture. Scale-up and performance characterisation*. in Proc. *Cell Culture Engineering VII*. Snowmass Village, Colorado, USA: United Engineering Foundation, Inc. 2002

[24] T. D'Amore, *Improving yeast fermentation performance.* J Inst Brew, 1992. **98**: p. 375.

[25] A.J. McLoughlin, *Controlled release of immobilised cells as a strategy to regulate ecological competence of inocula.* Adv Biochem Eng Biotech, 1994. **51**: p. 2-45.

[26] T.R. Mhatzo, A.J. McLoughlin, and E. Benes. *Immobilisation in carrageenan polymer as a strategy to enhance the ecological competence of brewers' yeast inocula*. in Proc. *BRG International Workshop VII*. Maryland USA. 1998

[27] B. Brohan and A.J. McLoughlin, *The influence of yeast metabolism on dispersion in a fluidised yeast bed.* Appl Microbiol Biotechnol, 1984. **20**: p. 146-149.

[28] B. Brohan and A.J. McLoughlin, *Characterization of the physical properties of yeast flocs.* Appl Microbiol Biotechnol, 1984. **20**: p. 16-22.

[29] B. Brohan and A.J. McLoughlin, *The behavior of yeast flocs in hindered settling and fluidized bed regimes.* Appl Microbiol Biotechnol, 1984. **20**: p. 10-15.

[30] Y.-L. Jin and R.A. Speers, *Flocculation of Saccharomyces cerevisiae.* Food Res Int, 1998. **31**: p. 421-440.

[31] G.B. Davies, *Developments in downstream processing: Application of ultrasound to liquid-solid separation.* BRF Int, 1992: p. 169-173.

[32] G.B. Davies. *Application of ultrasonic wave fields to brewing separation processes*. in Proc. *European Brewing Convention*. 1993. p. 701-708.

[33] M. McKechnie, *Advances in separation technologies for the brewer.* BDI, 1993. **July 1993**: p. 27-28.

[34] A.P.J. Middelberg, *Process-scale disruption of microorganisms.* Biotechn Adv, 1995. **13**(3): p. 491-551.

[35] L.D. Landau and E.M. Lifschitz, *Fluid Mechanics*. 1959, New York: Pergamon.

[36] L.V. King. *The acoustic radiation pressure on spheres*. in: Proceedings of the Royal Society London. 1934. p. 212-240.

[37] K. Yosioka and Y. Kawasima, *Acoustic radiation pressure on a compressible sphere.* Acustica, 1955. **5**: p. 167-173.

[38] L.P. Gor'kov, *On the forces acting on a small particle in a sound field.* Sov Phys Acoust, 1962. **6**(9): p. 773-775.

[39] E. Benes, F. Hager, W. Stuckart, and H. Frischherz, *Abscheidung dispergierter Teilchen durch Ultraschall-induzierte Koagulation*, in *Fortschritte der Akustik*. 1989, DPG-GmbH: Bad Honnef. p. 255-258.

[40] W. König, *Hydrodynamisch-akustische Untersuchungen: II. Über die Kräfte zwischen zwei Kugeln in einer schwingenden Flüssigkeit und über die Entstehung der Kundtschen Staubfiguren.* Ann Phys Chem, 1891. **42**(4): p. 549-563.

[41] V.F.K. Bjerknes, *Die Kraftfelder*. 1909, Braunschweig: Vieweg und Sohn.

[42] L.A. Crum, *Acoustic force on a liquid droplet in an acoustic stationary wave.* JASA, 1971. **50**(1): p. 157-163.

[43] M.A.H. Weiser and R.E. Apfel, *Interparticle forces on red cells in a standing wave field.* Acustica - acta acustica, 1984. **56**: p. 114-119.

[44] V.A. Sutilov, *Fundamental physics of ultrasound*. 1988, New York: Gordon and Breach Science Publications.

[45] K.S. van Dyke, *The electric network equivalent of a piezo-electric resonator.* Phys Rev, 1925. **25**: p. 895.

[46] E. Hafner, *Resonator and device measurements*, in *Precision Frequency Control*, A. Ballato, Editor. 1985, Academic: Orlando. p. 1-44.

[47] E.L. Adler, *Matrix methods applied to acoustic waves in multylayers.* IEEE Trans Ultrason Ferroel Frequ Cont, 1990. **37**(6): p. 485-490.

[48] J.T. Stewart and Y.-K. Yong, *Exact analysis of the propagation of acoustic waves in multilayered anisotropic piezoelectric plates.* IEEE Trans Ultrason Ferroel Frequ Cont, 1994. **41**(3): p. 375-390.

[49] M.J.S. Lowe, *Matrix techiques for modeling ultrasonic waves in multilayered media.* IEEE Trans Ultrason Ferroel Frequ Cont, 1995. **42**(4): p. 525-542.

[50] H. Nowotny and E. Benes, *General one-dimensional treatment of the layered piezoelectric resonator with two electrodes.* JASA, 1987. **82**: p. 513-521.

[51] B.A. Auld, *Acoustic fields and waves in solids*. Vol. 1. 1973, New York: John Wiley and Sons.

[52] W.T. Coakley and M.F. Sanders, *Sonochemical yields of caviation centres at 1 MHz.* J Sound Vib, 1973. **28**(1): p. 73-85.

[53] M.T.Z. Spence (ed), *Handbook of Fluorescent Probes and Research Chemicals*. Sixth edition ed. 1996, Leiden, The Netherlands: Molecular probes.

[54] M. Schmid, E. Benes, and R. Sedlaczek, *A computer-controlled system for the measurement of complete admittance spectra of piezoelectric resonators.* Meas Sci Technol, 1990. **1**: p. 970-975.

[55] F. Trampler, E. Benes, W. Burger, and M. Gröschl. *Method for treating a liquid*. European Patent Nr. 633 049 B1, 1999.

[56] B. Handl, T. Binder, and F. Trampler, *PAS PAAR Acoustic separator - instruction handbook (preliminary)*, ed. H. Weiser. 1997, Graz: Anton Paar GmbH. 69.

[57] F. Trampler. *Accumulation of acoustic energy for fluid-particle separation in industrial processes*. Dissertation. Vienna University of Technology, Vienna, Austria, 2000.

[58] H. Netz, *Formeln und Sätze der Physik*, ed. H. Stroppe. 1989, München, Wien: Carl Hanser Verlag.

[59] E. Benes, M. Gröschl, H. Nowotny, F. Trampler, T.M.P. Keijzer, H. Böhm, S. Radel, L. Gherardini, J.J. Hawkes, R. König, and C. Delouvroy. *Ultrasonic separation of suspended particles*. in Proc. *2001 IEEE International Ultrasonics Symposium*. Atlanta, GA, USA. 2001

[60] S. Radel, A.J. McLoughlin, M. Gröschl, and E. Benes. *Ultrasonically Enhanced Settling: Influence of process parameters on separation efficiency of yeast cells at 2.2 MHz*. in Proc. *Forum Acusticum 2002*. Sevilla, Spain. 2002. p. filename: pha01011.pdf (6 pages).

[61] T. Gaida, O. Doblhoff-Dier, K. Struzenberger, H. Katinger, W. Burger, M. Gröschl, B. Handl, and E. Benes, *Selective Retention of Viable Cells in Ultrasonic Resonance Field Devices.* Biotechnol Prog, 1996. **12**: p. 73-76.

[62] R.B. Gilliland. *The flocculation characteristics of brewing yeast during fermentation*. in Proc. *European Brewery Convention Congress*. Brighton. 1951. p. 35-58.

[63] C.A. Miles, M.J. Morley, W.R. Hudson, and B.M. Mackey, *Principles of separating micro-organisms from supensions using ultrasound.* J Appl Bacter, 1995. **78**: p. 47-54.

[64] S. Radel, A.J. McLoughlin, L. Gherardini, O. Doblhoff-Dier, and E. Benes, *Breakdown of immobilisation/separation and morphology changes of yeast suspended in water-rich ethanol mixtures exposed to ultrasonic plane standing waves.* Bioseparation, 2000. **9**(6): p. 369-377.

[65] S.A. Parke and G.G. Birch, *Solution properties of ethanol in water.* Food Chem, 1999. **67**(3): p. 241-246.

[66] J. Antosiewicz and D. Shugar, *Hydration of alcohols by ultrasonic velocity measurements in ternary systems.* J Sol Chem, 1984. **13**(7): p. 493-503.

[67] A. Laaksonen, P.G. Kusalik, and I.M. Svishchev, *Three-dimensional structure in water-methanol mixtures.* J Phys Chem A, 1997. **101**: p. 5910-5918.

[68] M. D'Angelo, G. Onori, and A. Santucci, *Self-association of monohydric alcohols in water: Compressibility and infrared absorption measurements.* J Chem Phys, 1994. **100**(4): p. 3107-3113.

[69] G. Onori and A. Santucci, *Dynamical and structural properties of water/alcohol mixtures.* J Mol Liqu, 1996. **69**: p. 161-181.

[70] J. Lara and J.E. Desnoyers, *Isentropic compressibilities of alcohol-water mixtures at 25°C.* J Sol Chem, 1981. **10**: p. 465-477.

[71] T.F. Hueter and R.H. Bolt, *Sonics*. 1955, New York: John Wiley&Sons, Inc. 436-438.

[72] S. Norton, K. Watson, and T. D'Amore, *Ethanol tolerance of immobilized brewers' yeast cells.* Appl Microbiol Biot, 1995. **43**: p. 18-24.

[73] P.G. Walsh and A.J. McLoughlin. *Enhancing the ecological competence of brewers' yeast inocula in biotechnological processes*. in Proc. *VI. International Workshop on Bioencapsulation*. Barcelona, Spain: Bioencaspulation Research Group. 1997

[74] H. Kobori, M. Sato, A. Tameike, K. Hamada, S. Shimada, and M. Osumi, *Ultrastructural effects of pressure stress to the nucleus in Saccharomyces cerevisiae: A study by immunoelectron microscopy using frozen thin sections.* FEMS Microbiol letters, 1995. **132**: p. 235.

[75] M. Sato, H. Kobori, S. Shimada, and M. Osumi, *Pressure-stress effects on the ultrastructure of cells of the dimorphic yeast Candida tropicalis.* FEMS Microbiol letters, 1995. **131**: p. 11.

[76] S. Radel, A.J. McLoughlin, M. Gröschl, and E. Benes. *An attempt to explain turbulence occurring when yeast cells suspended in water-rich ethanol mixtures are irradiated in a quasistanding ultrasonic plane wave at 2.2 MHz*. in Proc. *140th Meeting of the Acoustical Society of America and the Noise-Con 2000*. Newport Beach, CA, USA: Acoustical Society of America. 2000. p. 2547.

[77] T. Hasegawa, *Acoustic radiation force on a sphere in a quasistationary wave field - theory.* JASA, 1979. **65**(1): p. 32-40.

[78] M.A.H. Weiser and R.E. Apfel, *Extension of acoustic levitation to include the study of micron-sized particles in a more compressible host liquid.* JASA, 1982. **71**: p. 1261-1268.

[79] H.E. Kubitschek, *Bouyant density variation during cells cycle in microorganism.* CRC Crit Rev Microbiol, 1987. **14**: p. 73-97.

[80] R.E. Apfel, *Technique for measuring the adiabatic compressibility, density, and sound speed of submicroliter liquid samples.* JASA, 1976. **59**(2): p. 339-343.

[81] M.A.H. Weiser and R.E. Apfel, *Extension of acoustic levitation to the measurement of the properties of micron-size particles.* JASA, 1981. **69**: p. S5.

[82] A.A. Doinikov, *Acoustic radiation pressure on a compressible sphere in a viscous fluid.* J Fluid Mech, 1994. **267**: p. 1-21.

[83] S. Radel, A.J. McLoughlin, P. Walsh, L. Gherardini, O. Doblhoff-Dier, and E. Benes, *Application of low intensity ultrasonic wave fields in bioencapsulation: arrangement and immobilisation of yeast cells within gels.* Ir J Agri Food, 2000. **40**(1): p. 118.

[84] L. Gherardini, S. Radel, S. Sielemann, O. Doblhoff-Dier, M. Gröschl, E. Benes, and A.J. McLoughlin, *A study of the spatial organisation of microbial cells in a gel matrix subjected to treatment with ultrasound standing waves.* Bioseparation, 2002. **10**: p. 153-162.

[85] S. Radel, W.T. Coakley, A.J. McLoughlin, F. Trampler, M. Gröschl, and E. Benes. *Alterations in the acoustic quality factor of ultrasonic resonators for particle separation due to re-arrangement of particles by primary radiation forces*. in Proc. *17th International Congress on Acoustics*. Rome, Italy. 2001. p. 10-11, 2_08.pdf.

[86] D.E. Hughes and W.L. Nyborg, *Cell disruption by ultrasound.* Science, 1962. **138**: p. 108-114.

[87] H. Alliger, *Ultrasonic disruption*. 1975: American Laboratory. 8.

[88] J. Thacker, *An approach to the mechanism of killing cells in suspension by ultrasound.* Biochem Biophys Acta, 1973. **304**: p. 240.

[89] S. Radel, A.J. McLoughlin, and E. Benes. *Viability of yeast cells in propagating ultrasonic waves*. in Proc. *137th Meeting of the Acoustical Society of America and the 2nd Conventionof the European Acoustics Association: Forum Acusticum integrating the 25th German Acoustics DAGA Conference*. Berlin, Germany: TU Berlin. 1999. p. filename \files\pdf\2p\2ppac__4.pdf.

[90] M.J. Norušis, *SPSS Introductory guide: Basic statistics and sperations*. 1982, New York: McGraw-Hill.

[91] C.D. Powell, S.M.v. Zandycke, D.E. Quain, and K.A. Smart, *Replicative ageing and senescence in Saccharomyces cerevisae and the impact of brewing fermentations.* Microbiol, 2000. **146**: p. 1023-1034.

[92] R.E. Apfel, *Sonic effervescence: A tutorial on acoustic cavitation.* JASA, 1997. **101**(3): p. 1227-1237.

[93] E.A. Neppiras, *Acoustic cavitation series: part one - Acoustic cavitation: an introduction.* Ultrasonics, 1984. **22**(1): p. 25-28.

[94] A. Prosperetti, *Acoustic cavitation series: part two - Bubble phenomena in sound fields: part one.* Ultrasonics, 1984. **22**(2): p. 69-77.

[95] A. Prosperetti, *Acoustic cavitation series: part three - Bubble phenomena in sound fields: part two.* Ultrasonics, 1984. **22**(3): p. 115-124.

[96] R.E. Apfel, *Acoustic cavitation prediction.* JASA, 1981. **69**(6): p. 1624-1633.

[97] R.E. Apfel, *Acoustic cavitation series: part four - Acoustic cavitation inception.* Ultrasonics, 1984. **July 1984**: p. 167-173.

[98] D. Bertolini, M. Casseliari, and G. Salvetti, *The dielectric properties of alcohols-water solutions: 1.The alcohol rich region.* J Chem Phys, 1983. **78**: p. 365-372.

[99] S. Dakubu, *Cell inactivation by ultrasound.* Biotech Bioeng, 1976. **18**: p. 465-471.

[100] R.K. Gould, W.T. Coakley, and M.A. Grundy, *Upper sound pressure limits on particle concentration in fields of ultrasonic standing-wave at megahertz frequencies.* Ultrasonics, 1992. **4**: p. 239-244.

[101] A.C. Vollmer, S. Kwakye, M. Halpern, and E.C. Everbach, *Bacterial stress response to 1-Megahertz pulsed ultrasound in the presence of microbubbles.* Appl Environ Microbiol, 1998. **64**(10): p. 3927-3931.

[102] G.J. Price, F.A. Duck, M. Digy, W. Holland, and T. Berryman, *Measurement of radical production as a result of cavitation in medical ultrasound fields.* Ultrason Sonochem, 1997. **4**: p. 165-171.

[103] A. Weissler, H.W. Cooper, and S. Snyder, *Chemical effects of ultrasonic waves oxidation of potassium iodide solution by carbon tetrachloride.* JACS, 1950. **72**: p. 1769-1775.

[104] IEEE, *Appendix A - Acoustic cavitation*, in *IEEE Guide for Medical Ultrasound Field Parameter Measurements*, W.T. Coakley, Editor. 1990, Institute of Electrical and Electronics Engineers: New York. p. 79-80.

[105] W. Lauterborn and H. Bolle, *Experimental investigations of cavitation-bubble collapse in the neighbourhood of a solid boundary.* J Fluid Mech, 1975. **72**: p. 391-399.

[106] H.N. Oguz and A. Prospetti, *The natural frequency of oscillation of gas bubbles in tubes.* JASA, 1998. **103**(6): p. 3301-3308.

[107] G.W. Willard, *Ultrasonically induced cavitation in water, a step-by-step process.* JASA, 1953. **25**: p. 669-686.

[108] G. Iernetti, *Cavitation threshold dependence on volume.* Acustica - acta acustica, 1971. **24**: p. 191-196.

[109] S. Radel, A.J. McLoughlin, L. Gherardini, O. Doblhoff-Dier, and E. Benes, *Viability of yeast cells in well controlled propagating and standing ultrasonic plane waves.* Ultrasonics, 2000. **38**(1-8): p. 633-637.

[110] L. Gherardini, J.J. Hawkes, S. Radel, D. McLoughlin, W.T. Coakley, M. Gröschl, and A.J. McLoughlin. *Micro-manipulation of particles in gel suspension by a cylindrical ultrasonic field*. in Proc. *IX. International Workshop on Bioencapsulation: Bioencapsulation in Biomedical, Biotechnological and Industrial Applications*. Warsaw, Poland: Bioencapsulation Research Group. 2001. p. P3.

[111] P.M. Kieran, D.M. Malone, and P.F. MacLoughlin, *Effects of hydrodynamic and interfacial forces on plant cell suspension systems.* Adv Biochem Eng Biotech, 2000. **67**: p. 139-177.

[112] F. Wöhler and J. Liebig, *Solution to the secret of alcoholic fermentation.* Ann Chem, 1839. **29**.

[113] M.R. Bailey, D. Dalecki, S.Z. Child, C.H. Raeman, D.P. Penney, D.T. Blackstock, and E.L. Carstensen, *Bioeffects of positive and negative acoustic pressure in vivo.* JASA, 1996. **100**(6): p. 3941-3946.

[114] W.D.J. O'Brien and L.A. Frizzell, *Ultrasound-induced lung hemorrhage is not caused by inertial cavitation.* JASA, 2000. **108**(3): p. 1290-1297.

[115] R.E. Apfel, *Comment on ''Ultrasound-induced lung hemorrhage is not caused by inertial cavitation'' [J. Acoust. Soc. Am. 108, 1290–1297 (2000)].* JASA, 2001. **110**(4): p. 1737.

[116] L.A. Frizzell, J.M. Kramer, J.F. Zachary, and W.D.J. O'Brien, *Response to ''Comment on 'Ultrasound-induced lung hemorrhage is not caused by inertial cavitation''' [J. Acoust. Soc. Am. 110, 1737 (2001)].* JASA, 2001. **110**(4): p. 1738-1739.

[117] R.E. Apfel, *Reply to Frizzell et al.'s comment to our comment.* JASA, 2001. **110**(4): p. 1740-1741.

[118] L.A. Frizzell, J.M. Kramer, J.F. Zachary, and W.D.J. O'Brien, *Comment on Apfel's second comment.* JASA, 2001. **110**(4): p. 1742.

[119] P.M.B. Fernandes, M. Farina, and E. Kurtenbach, *Effect of hydrostatic pressure on the morphology and ultrastructure of wild-type and trehalose synthase mutant cells of Saccharomyces cerevisiae.* Lett Appl Microbiol, 2001. **32**.

[120] J.-M. Perrier-Cornet, M. Hayert, and P. Gervais, *Yeast cell mortality related to a high-pressure shift: occurrence of cell membrane permeabilization.* 1999. **87**: p. 1-7.

[121] Y. Christi, *Animal-cell damage in sparged bioreactors.* Trends Biotechnol, 2000. **18**(10): p. 420-432.

[122] J.J. Chalmers, *Gas bubbles and their influence on microorganisms.* Appl Mech Rev, 1998. **51**(1): p. 113-120.

CURRICULUM VITAE

Person

Name:	Stefan Radel
Academic degree:	Diplom Ingenieur
Date of birth:	February 26th, 1967
Citizenship:	Austria
Status:	married to Mag. Christiane Radel, one child
Contact:	Felbigergasse 60/10 1140 Wien Austria radel@iap.tuwien.ac.at

Education

1973 - 77	Elementary school, Vienna
1977 - 85	Secondary school, Vienna
1985 - 86	Military service, Vienna
1986 - 88	Vienna University of Technology: Computer science
1986 - 98	Vienna University of Technology: Technical Physics*
1998	Graduation at the Institute of General Physics Thesis: „Contactless Strain Measurement - based on a Laser-Speckle Interferometer“
1998 - 2001	EC's TMR Programme, EuroUltraSonoSep (Post)Doc at UCD, Ireland and University of Wales, U.K.

Experience

1984	Siemens, practical work during holidays
1986 - 94	IBM, contracted work, different projects BMfJ, BMfLV (S/36, PC, RS/6000)
1994-97	consultant/system administrator to E&P, CBM
since 1997	20first.cc, Senior engineer

Main publications

S. Radel, L. Gherardini, A.J. McLoughlin, O. Doblhoff-Dier, E. Benes, *Breakdown of immobilisation/separation and morphology changes of yeast suspended in water-rich ethanol mixtures exposed to ultrasonic plane standing waves*, Bioseparation, 2001. **9**: p. 369-377.

S. Radel, A.J. McLoughlin, L. Gherardini, O. Doblhoff-Dier, E. Benes, *Viability of yeast cells in well controlled propagating and standing ultrasonic plane waves*, Ultrasonics, 2000. **38**: p. 633-637.

S. Radel, A.J. McLoughlin, M. Gröschl, E. Benes, *Ultrasonically Enhanced Settling: Influence of process parameters on separation efficiency of yeast cells at 2.2 MHz*, Official Publication of the Forum Acusticum 2002, Sevilla, Spain (16.-20.9.2002), CD-Rom: File pha01011.pdf, 6 pages (ISBN 84-87985-06-8).

S. Radel, A.J. McLoughlin, P. Walsh, L. Gherardini, O. Doblhoff-Dier, E. Benes, *Breakdown of immobilisation/separation and morphology changes of yeast suspended in water-rich ethanol mixtures exposed to ultrasonic plane standing waves*, Ir. J. Agric. & Food Research, 2001. **40**: p. 118.

C. Exner, M. Gröschl, S. Radel, C. Focke, E. Benes, G. Pavic, *In-plane Laser-Doppler-velocimeter sensor head for the measurement of surface structural intensity*, Acustica - acta acustica, 1998. **84**: p. 1055-1065.

L. Gherardini, S. Radel, S. Sielemann, O. Doblhoff-Dier, M. Gröschl, E. Benes, A.J. McLoughlin, *A study of the spatial organisation of microbial cells in a gel matrix subjected to treatment with ultrasound standing waves*, Bioseparation, 2002. **10**: p. 153-162.

Main International Conferences

137th Meeting of the Acoustical Society of America and Forum Acusticum, Mar 1999, Berlin, Germany.

8th Int. Workshop on Bioencapsulation, Sep 1999, Trondheim, Norway.

Joint Meeting COST Action 840 and EUSS TMR Network, May 2000, Vienna, Austria.

Biotechnology 2000, Sep 2000, Berlin, Germany.

140th Meeting of the Acoustical Society of America, Dec 2000, Newport Beach, CA, U.S.A.

17th International Congress on Acoustics, Sep 2001, Rome, Italy.

Forum Acusticum Sep 2002, Sevilla, Spain.